CHAPTER VI.E

Calibration and validation of the two-step nitrification model

Part of this chapter is in preparation for submission to Biotechnology and Bioengineering

ABSTRACT

In this chapter the two-step nitrification model detailed in Chapter VI.A is calibrated and validated with different experiments which involved several measurements. Only some of the forty model parameters are estimated in the calibration process according to the identifiability analysis developed in Chapter VI.B. Hence, this chapter is particularly focused in calibrating the model and analysing the importance of the different measurement outputs: OUR, HPR, ammonia, nitrite and CO_2 by means of numerical tools such as the Fisher Information Matrix (FIM) or the sensitivity functions. The model used could describe accurately the experimental data obtained and was successfully calibrated and validated using two different sets of experiments. The carbon evolution rate (CER) measurement did not provide any extra information, though CO_2 is substrate of the process. Finally, the evaluation of maximum nitrification rate at different pH values showed an optimum pH value around 7.6.

VI.E.1 Estimation of the measurement error weighting matrix

The procedure used in this thesis for the parameter estimation error assessment is based on the Fisher Information Matrix (FIM), as detailed in Chapter IV. This matrix summarises the quantity and quality of information obtained in each experiment because it gathers the output sensitivity functions and the measurement accuracy (Mehra, 1974). If Q_K is the covariance matrix of the measurement noise, the FIM is defined as equation VI.E1.

$$FIM = \sum_{k=1}^{N} Y_{\chi}^{T}(k) Q_K Y_{\chi}(k) \qquad \text{(VI.E1)}$$

where Y_{χ} stands for the so called output sensitivity function, which are a numerical approach to the derivate of the output variable with respect to one parameter.

Parameter estimation requires the measurement error weighting matrix (Q_K) assessment for the experimental inputs used. Each experimental set-up had its own Q_K matrix value and it had to be estimated separately. Q_K is usually chosen as the inverse of the measurement error covariance matrix, and it is a square matrix with the same number of files and columns as output measurements.

Q_K was estimated following the method described in Petersen (2000). The Petersen's method used data from a time period where the value of the output variable was perfectly known. If possible, a period with constant variables was preferred. For example, Q_{OUR} was estimated before the pulse of substrate was added (i.e. endogenous respiration phase) in which OUR was supposed to be constant. The average of the data and the resulting residuals were calculated in this period of constant OUR. The measurement error (s^2) was calculated as equation VI.E2:

$$s^2 = \frac{SSE}{N - p} \qquad \text{(VI.E2)}$$

where SSE = Sum Squared Errors
N = Number of measurements
p = Number of parameters

Figure VI.E1-left and VI.E2-left show the endogenous period used for Q_{OUR} estimation in the LFS respirometer and in the BIOSTAT B fermenter respectively. The calculated s^2 [eq. VI.E2] for OUR in the LFS respirometer was $2.307e\text{-}^5$ and for the BIOSTAT B fermenter was $8.496e^{-6}$. The values obtained were quite different between equipments since s^2 depends on a lot of factors from the probe precision to the reactor homogenization

degree. These values were in the range of the literature values. As an example, Petersen (2000) obtained a value of $1.385e^{-5}$ for the oxygen measurement.

On the other hand, HPR is only constant for a certain period of time under well-defined conditions (i.e. high carbon dioxide concentration and low k_La_{CO2}). The experimental data used for Q_{HPR} estimation was collected just after the addition of Na_2CO_3 to the system, so that the conditions were the closer possible to the mentioned conditions when HPR should be constant. Figure VI.E1-right and figure VI.E2-right show the HPR period used for Q_{HPR} estimation in the LFS respirometer and in the BIOSTAT B fermenter respectively. The calculated s^2 for HPR in the LFS respirometer was $5.778e^{-6}$ and $1.712e^{-4}$ for the BIOSTAT B fermenter.

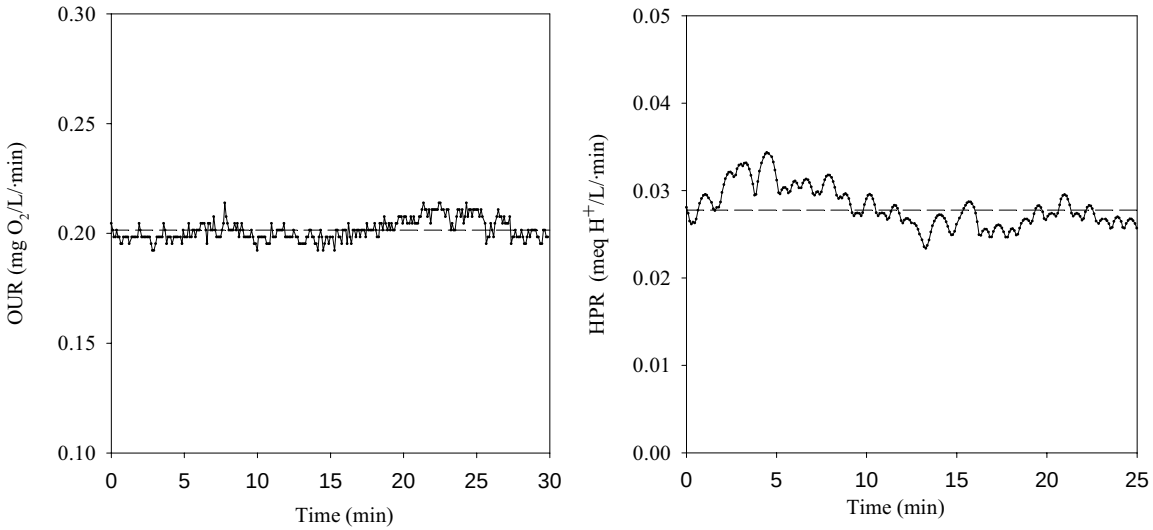

Figure VI.E1 Q_{OUR} and Q_{HPR} estimation for the LFS respirometer (Experimental value- solid line, mean –dashed line)

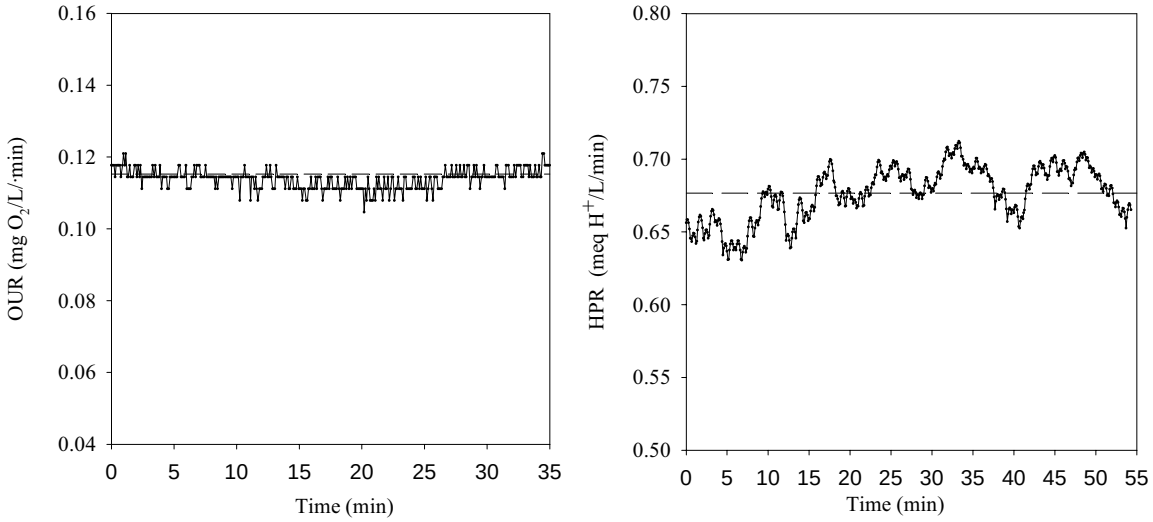

Figure VI.E2 Q_{OUR} and Q_{HPR} estimation for the BIOSTAT fermenter (Experimental value- solid line, mean –dashed line)

As can be observed, this method is going to predict too optimistic confidence intervals since the measurement error is only associated with the probe variability around the mean value, assuming that this mean value is the correct. However, this value ought to have an error, which is not considered.

For example for the LFS respirometer Q_{LFS} was calculated considering OUR as the first measurement and HPR as the second measurement [eq. VI.E3]. This choice of Q_k implies that the more a measurement error is noise corrupted, the less it will count in the FIM.

$$s^2_{LFS} \mid \begin{pmatrix} 2.04e^{45} & 0 \\ 0 & 5.78e^{46} \end{pmatrix} \longrightarrow Q_{LFS} \mid \begin{pmatrix} 4.33e^{4} & 0 \\ 0 & 1.74e^{6} \end{pmatrix} \qquad \text{(VI.E3)}$$

VI.E.2 Model calibration with OUR and HPR

VI.E.2.1 EXPERIMENTAL MEASUREMENTS

Experiment VI.E1 (Table V1.E1) was conducted to calibrate the two-step nitrification model. This experiment consisted of two sequential pulses of ammonium chloride and sodium nitrite of 15 mg N each. The monitored variables are depicted on figure VI.E3 and the calculated variables (OUR, HP and HPR) are depicted in figure VI.E4. A pulse of sodium bicarbonate was added at the start of the experiment to avoid any inorganic carbon limitation.

Table VI.E1 Experiment VI.E1

EXPERIMENT VI.E1	Two-step nitrification model calibration
Equipment	LFS respirometer (V_0 = 0.8 L)
pH	7.5
Temperature	25 ºC
Acid used	HCl = 0.25 M
Base used	NaOH = 0.25 M
Pulses	0.6 g $NaHCO_3$ (t = 0 min)
	15 mg N-NH_4^+ (t = 50 min) -> 18.75 mg N-NH_4^+/L
	15 mg N-NO_2^- (t= 130 min) -> 18.75 mg N-NO_2^- /L

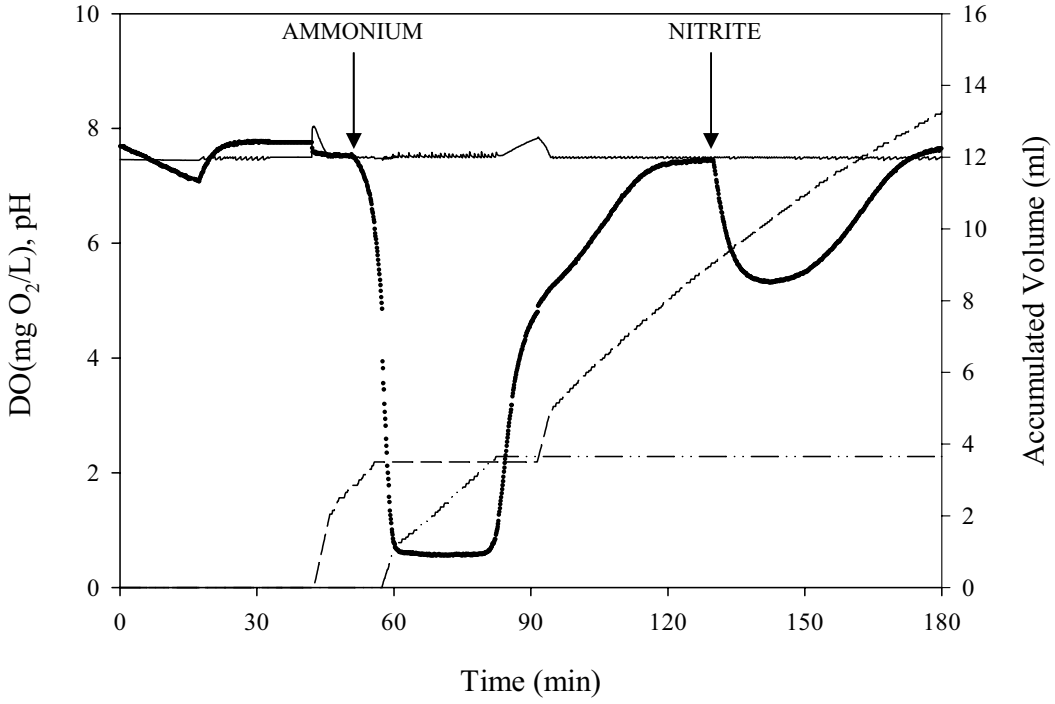

Figure VI.E3 Monitored variables in the respirometer: DO (dotted), pH (solid), accumulated acid (dashed) and accumulated base (dash-dotted) of experiment VI.E1.

The experimental measured DO profile was a classical two-pulse respirogram. The DO level reached at maximum OUR was very low and the system became oxygen limited. The reason was that k_La_{O2} was forced to a low value for a reliable OUR calculation. In any case, this effect could be easily taken into account since the values of both K_O for this system were already properly estimated (Chapter VI.C). The oxygen limitation effect was clearly seen in the OUR and HPR profiles (Figure VI.E4), since both parameters are proportional to the process rate (oxygen is a substrate and OUR indicates the consumption rate and H^+ is a product and HPR indicates the product formation rate). Both profiles showed an initial increase and a subsequent rate reduction which derived in the sharp-pointed peaks experimentally observed. The nitrification process tended to its maximum rate after the ammonia pulse addition, but as the oxygen was decreasing, both the nitritation and nitritation processes became oxygen limited.

HPR measurements started approximately at minute 40 when pH control was turned on and it was only proportional to the nitritation rate since no proton is consumed or produced in the nitratation process. As can be observed, the HPR was negative under endogenous conditions since the system was “proton consuming” due to the stripping process. When the pulse of ammonia was added and the nitritation process started, the system became “proton producing” and HPR became positive. The sharp-peak observed in the HPR indicated the oxygen limitation effect on the nitritation process. Moreover, the HPR is not constant along the experiment because of the length of the experiment and the dynamic CO_2 system had to be taken into account for a proper modelling of the experimental results (see Section V.B.2.5). HP measurement gave similar information to HPR since it indicated the accumulated proton production /consumption on the system.

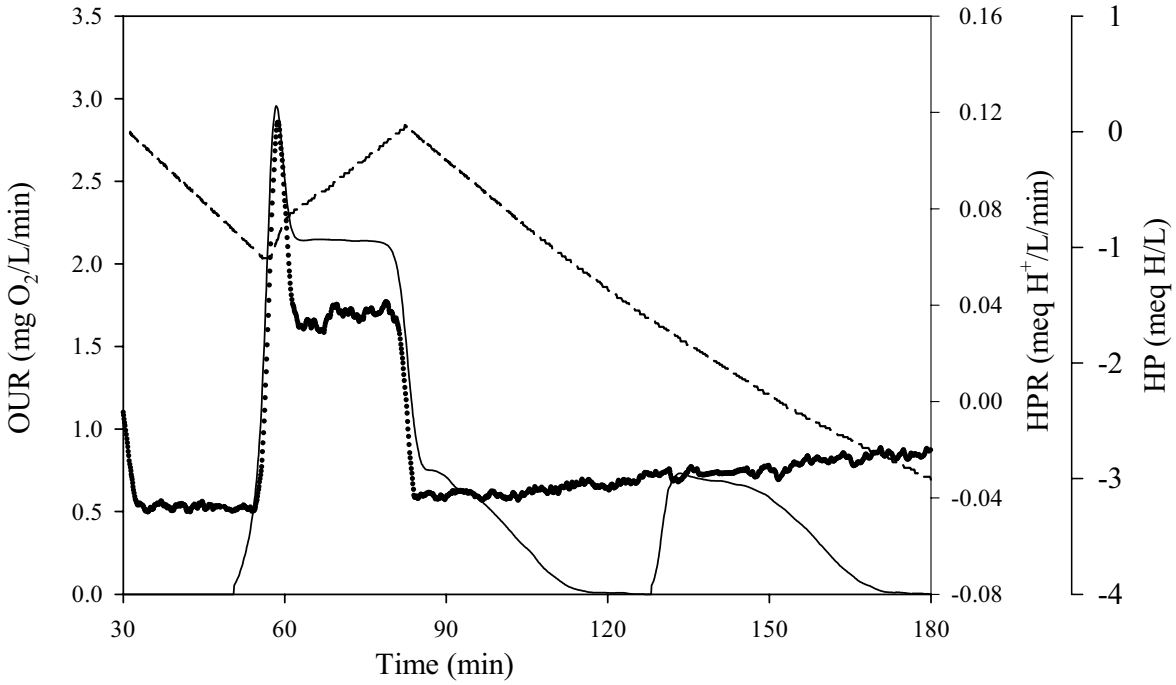

Figure VI.E4 Estimated variables for experiment VI.E1: OUR(solid), HPR(dotted) and HP (dashed).

As described in Chapter VI.B, nine parameters had to be estimated among all the model parameters based on identifiability criteria:

- $\sigma_{MAXA}\cdot f_A$ and $\sigma_{MAXN}\cdot f_N$: The active fraction and the maximum growth rate were estimated as a unique factor since they could not be reliable estimated separately with short-term batch experiments due to correlation.
- $K_{NH,A}$ and K_{NO}: half-saturation constants for the substrate of each process.
- pK_1: bicarbonate-carbonic acid equilibrium constant.
- ϑ: The start-up constant for the nitrite pulse.
- η and#.#: ammonium pulse constants, to describe the acceleration phase.
- TIC (0): total inorganic carbon concentration at the start of the pulse

VI.E.2.2 PARAMETER ESTIMATION RESULTS AND DISCUSSION

Figure VI.E5 shows the model fittings versus the experimental OUR and HPR measurements. As can be seen, these fittings were reasonably good and describe accurately the experimental data. Table VI.E2 shows the most significant model parameters. Only the parameters which have the parameter estimation error in brackets were estimated. The cost function (CF) was calculated as indicated in equation VI.E4.

$$CF = \sum_{i=1}^{n} \frac{\sum_{j}^{m} \left(y_{i,j}^{MODEL} - y_{i,j}^{EXP} \right)^2}{\zeta_i} \qquad \text{(VI.E4)}$$

where y = output measurement
n = number of output measurements (i)
m = number of samples (j)
ζ = weighting correction factor according to the absolute values of each measurement.

Table VI.E2 Parameter estimation for experiment VI.E1

Fitted parameters	Value*	Other parameters	Value
$\sigma_{MAXA} \cdot f_A$ (1/d)	0.27 (0.07 %)	K_{OA} (mg O_2/L)	0.74
$\sigma_{MAXN} \cdot f_N$ (1/d)	0.082 (0.08 %)	K_{ON} (mg O_2/L)	1.75
$K_{NH,A}$ (mg N-NH_4^+/L)	0.92 (0.27%)	k_La_{O2} (1/min)	0.32
K_{NO} (mg N-NO_2^-/L)	2.84 (0.27 %)	k_La_{CO2} (1/min)	0.29
ϑ# (min)	1.58 (0.07 %)	Y_A (g COD_X/g N)	0.21
η#	60.1 (0.007 %)	Y_N (g COD_X/g N)	0.08
..#	16.5 (0.15 %)	#	
pK_1	5.95 (0.03%)		
TIC(0) (mM CO_2)	13.2 (0.23 %)		
		COST FUNCTION	2.10

* Confidence intervals are presented as absolute relative percentage of the parameter estimates, i.e. (confidence interval/parameter)*100.

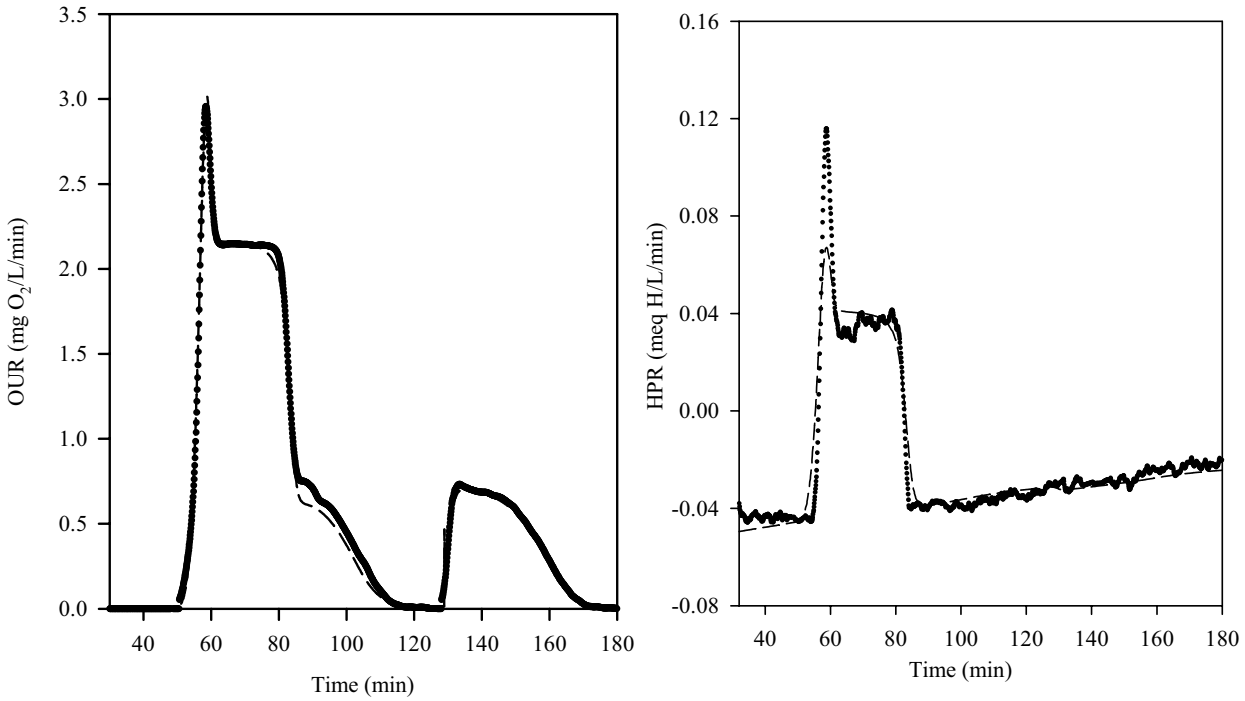

Figure VI.E5 Model fitting (dashed line) versus experimental results (black dotted) for experiment VI.E1.

Although neither HP nor DO profiles provide additional information when compared to OUR and HPR, it is interesting to realise that these measurements could be accurately described with the parameter estimation values obtained (Figure VI.E6).

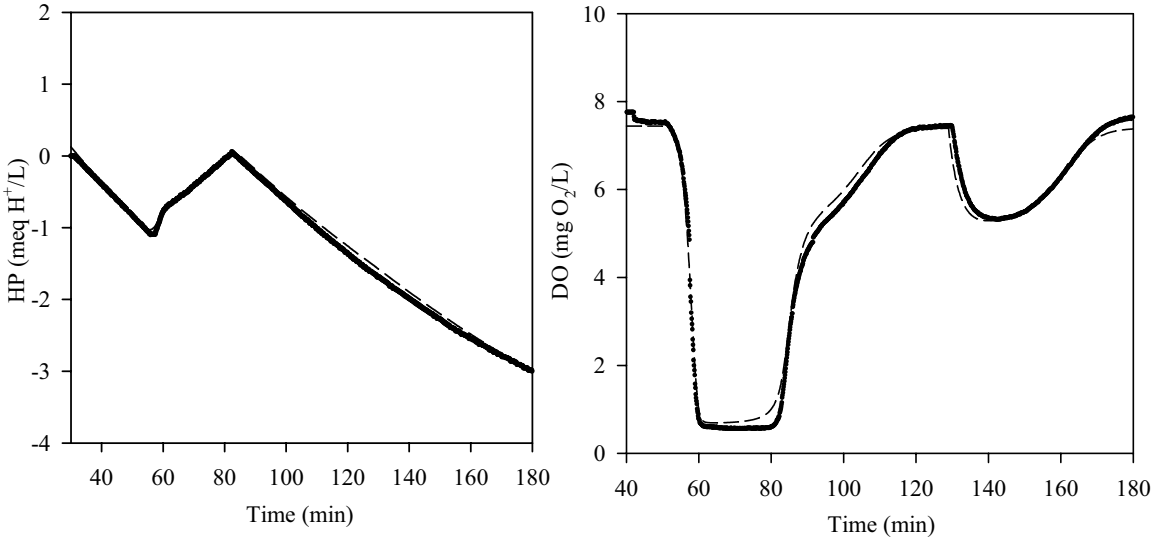

Figure VI.E6 Model fitting (dashed line) versus experimental results (black dotted) for experiment VI.E1.

As described in Chapter VI.B, the values of the maximum growth rate constants could not be correctly estimated separately from the active fraction value using short-term batch experiments. Longer experiments where biomass growth and decay is taken into account are required to estimate the active fractions (Ubisi *et al.*, 1997; Gabriel, 2000). In this thesis, the active fractions were roughly calculated using the endogenous OUR value (equation VI.E5) for σ_{MAXA} and σ_{MAXN} estimation. This approximation is detailed in section VI.B.3.4

$$OUR_{END} = (1 - f_{XI}) \cdot b_A \cdot X \cdot f_A + (1 - f_{XI}) \cdot b_N \cdot X \cdot f_N \qquad \text{(VI.E5)}$$

where f_{XI} = fraction of inerts of the lysis products (g COD/g COD)
b_i = decay rate (1/d)
X = biomass – VSS (mg COD_X/L)
f_i = active fraction

The ASM2 (Henze *et al.*, 2000) default value for the lysis fraction of inerts was used (f_{XI}=0.2). The value of the decay rates came from Jubany *et al.* (2004) calculated for the biomass used in this study (b_i = 0.14 1/d). The ratio of f_A to f_N was assumed to be equal to the ratio between the two yields (Y_A/Y_N) (Gee *et al.*, 1990a). In the experiments of this thesis, the ratio between yields was 2.62; hence, f_A/f_N=2.62. The calculated OUR_{END} and VSS were 0.0372 mg O_2/L/min and 1300 mg VSS/L (~1950 mg COD_X/L), respectively. The resulting active fractions are:

$$\mathbf{f_A} = 0.18 \text{ and } \mathbf{f_N} = 0.07$$

If these were the real values, then σ_A and σ_N would respectively be:

$$\boldsymbol{\sigma_A} = 1.52 \text{ 1/d and } \boldsymbol{\sigma_N} = 1.22 \text{ 1/d}$$

Table VI.E3 compares the maximum growth rate values obtained with some of the values in the literature. The existing range in the literature is very broad probably because these values have been estimated without considering the active fraction value. The nitrification activity is often measured as the rate of ammonium oxidised per gram of biomass (as VSS). However, only part of this VSS corresponds to nitrifying biomass. Hence, these growth rate values are underestimated.

Table VI.E3 Comparison of the σ_{MAX} values with literature values

Reference	T (ºC)	σ_A (1/d)	σ_N (1/d)
Nowak *et al.* (1995)	25	2.2	2.5
Sheintuch *et al.* (1995)	25	0.24	0.144
Hellinga *et al.* (1999)	25	2.1	1.05
Henze *et al. (*2000)	20	1	
Wett *et al.* (2001)	25	1.55	1.79
Copp *et al.* (1995)	20		0.33
EPA (1993)	20	0.84-1.62	
This work	25	1.52	1.22

The values of the pulse obtained (η and ..) could not be compared with other works since this expression has never been applied before in these systems. The difference between the time pulse (~50 min) and the value of η corresponded to the duration of the acceleration phase. In experiment VI.E1, the difference was around 10 minutes which indicated that this phenomenon is important enough to be taken into account.

The value of the total inorganic concentration obtained was a bit higher than the amount of the initial bicarbonate pulse (9 mM), which was logical since the bicarbonate in the system can not be totally depleted even with an overnight aeration (see Chapter VI.D). The pulse was added only to ensure bicarbonate excess during the whole experiment.

The value of the pK_1 obtained is rather lower than the default value for pure water (6.36). However, as mentioned in Chapter VI.B, this value is highly influenced by the ionic strength present in the media (particularly because of nitrate, chloride and sodium ions). This fact could be negligible with the other equilibrium constants of the model, but not for pK_1 since it was one of the most sensible parameters for HPR measurement. Sin (2004) already examined the importance and sensitivity of this value and showed its effect on parameter estimation when using HPR as a measured value.

The thermodynamic equilibrium constant (K_T) is strictly constant and independent of the activity factors (ν) of the present species. However, the equilibrium constant (K) depends on these factors and it is linked to K_T through the activity factors of the equilibrium species. For example, a certain reaction such as:

$$aA + bB \acute{z} cC + dD$$

K and K_T are related through expression VI.E6:

$$K_T = \frac{\nu_C^c \cdot \nu_D^d}{\nu_A^a \cdot \nu_B^b} \cdot K \qquad \text{(VI.E6)}$$

When ionic species are included in the equilibrium this factor may acquire importance and should be taken into account. The law of Debie-Hückel [eq. VI.E7] quantitatively links the activity factor with the ion and solution characteristics. This law appeared as a result of many assumptions (e.g. the ions are punctual masses without size).

$$-\log \nu_i = A \cdot z_i^2 \cdot \sqrt{\sigma} \qquad \text{(VI.E7)}$$

where z_i stands for the ion charge

σ for ionic strength of the solution

A gathers some constants taking into account different effects such as the temperature.

The concentrations of these ions (C_i) were used to estimate the value of the ionic strength of the solution (eq. VI.E8).

$$\sigma = 0.5 \cdot \sum C_i \cdot z_i^2 \qquad \text{(VI.E9)}$$

This law was extended with the expression VI.E8 (Davies equation) since it was proved to fail in some cases (Burriel *et al.*, 1989).

$$\log \gamma_i = -0.512 \cdot z_i^2 \cdot \left(\frac{\sqrt{\sigma}}{1 + \sqrt{\sigma}} - 0.2 \cdot \sigma \right) \qquad \text{(VI.E9)}$$

The amount of nitrate present in the pilot plant where the biomass was withdrawn from ranged around 1 g/L. It has to be noted that the pilot plant was designed to enrich the sludge with nitrifying population and the inflow was high nitrogen loaded. The amount of sodium in the reactor was approximated with the nitrate ion concentration considering that a mol of ammonium was oxidised for each mol of nitrate present in the reactor and, hence, two moles of protons were formed. These moles were balanced with the addition of sodium bicarbonate. Hence, two moles of sodium were added in the reactor for each mole of nitrate present. The range of chloride concentration in the reactor was around 1-1.5 g/L as the ammonium in the pilot plant was fed as NH_4Cl. Na^+, Cl^- and NO_3^- were considered the major ionic contribution for the ionic strength calculation despite the whole feed was more complex and more ionic substances were present in the reactor.

Table VI.E4 shows the estimated values of pK_1 in the range of ionic concentrations found in the reactor. As can be observed, the estimated pK_1 agrees with the theoretical values according to the concentrations of Na^+, Cl^- and NO_3^- listed above. The concentration of Na^+ was calculated as a function of the NO_3^- as described above.

Table VI.E4 pK_1 estimation as a function of the ionic strength of the medium

$N\text{-}NO_3^-$ (g/l) / Cl^- (g/l)	0	0.4	0.8	1.2	1.6
0	6.36	6.13	6.04	5.98	5.94
0.4	6.20	6.09	6.02	5.96	5.92
0.8	6.14	6.05	5.99	5.94	5.90
1.2	6.10	6.03	5.97	5.92	5.89
1.6	6.07	6.00	5.95	5.91	5.87
2	6.04	5.98	5.93	5.89	5.86

Another remarkable issue is the optimistic parameter estimation error (PEE) values obtained. The method used seemed clearly to underestimate these values, probably because a large amount of OUR and HPR data points were used (measuring interval: 5 seconds), the measurement error values estimated were very low (see section VI.E1) and because of OUR data autocorrelation (Sin, 2004). In any case, the real PEE values should also be low, since a previous identifiability work was conducted to ensure parameter estimation reliability. For instance, there was a large period where DO was constant because the biomass was consuming at its maximum rate. Each of these DO measurements provided valuable estimation for the σ_{MAX}, once the growth yield was already known. Table VI.E5 shows how PEE would have increased if yields were include in the estimation process. This increase is particularly high with parameter estimation error of the maximum growth rate due to the existing correlation among them.

Table VI.E5 Ratio of PEE values with and without Y_A and Y_N

Parameter	Ratio	Parameter	Ratio
$\sigma_{MAXA} \cdot f_A$ (d^{-1})	13.07	$\vartheta_{\#}$(min)	1.35
$\sigma_{MAXN} \cdot f_N$ (d^{-1})	1.55	$\eta_{\#}$	1.08
K_{NH} (mg $N\text{-}NH_4$/L)	1.21	..#	0.96
K_{NO} (mg $N\text{-}NO_2$/L)	1.44	$C_T(0)$ (mM CO_2)	1.59
		pK1	1.42

VI.E.2.3 MODEL VALIDATION

Experiment VI.E2 was conducted to validate the parameter estimation values of the previous experiment using different load pulses. The parameters estimated in the validation experiment were those related to the pulses (i.e. ϑ, η and ..) and also the initial inorganic carbon concentration (TIC).

Table VI.E6 Experiment VI.E2

EXPERIMENT VI.E2	Two-step nitrification model validation
Equipment	LFS respirometer (V_0 = 0.8 L)
pH	7.5
Temperature	25 ºC
Acid used	HCl = 0.25 M
Base used	NaOH = 0.25 M
Pulses	30 mg N-NH_4^+ (t = 6.9 min) -> 37.5 mg N-NH_4^+/L
	30 mg N-NO_2^- (t= 110 min) -> 37.5 mg N-NO_2^-/L

Figure VI.E8 and Table VI.E7 show the experimental results versus the model prediction. As can be observed, the predicted profiles agree reasonably well with the experimental ones, which indicate that the parameter estimation values were close to the real ones. The amount of initial inorganic carbonate TIC (0) was lower than the calibration case, since no initial carbonate pulse was added. In any case, the initial value was high enough to prevent carbon limitations from occurring.

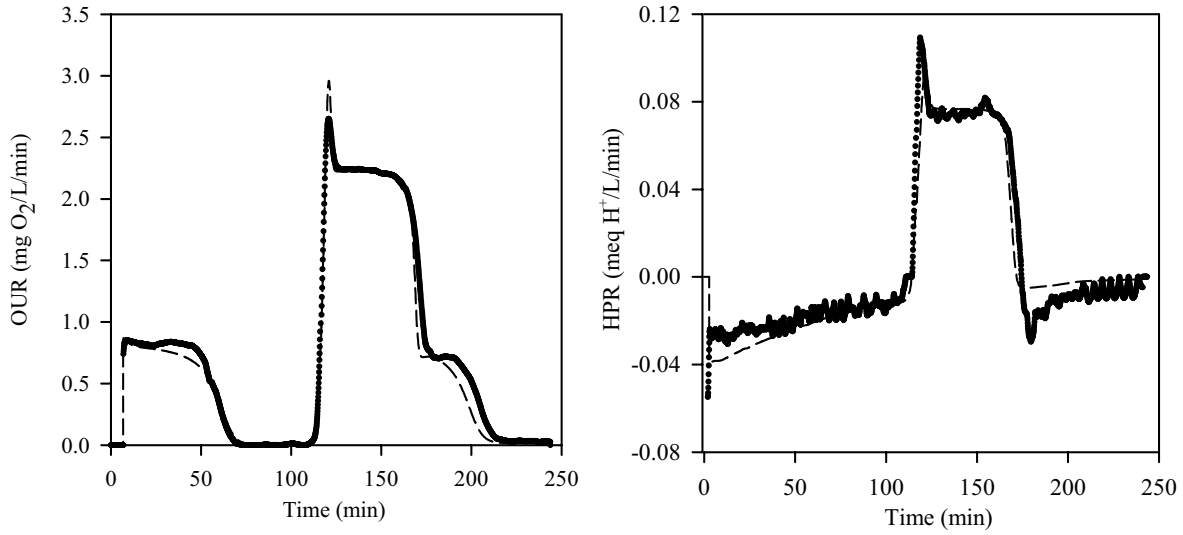

Figure VI.E8 Model fitting (dashed line) versus experimental results (black dotted) for experiment VI.E2.

Table VI.E7 Parameter estimation for experiment VI.E2.

Parameter	Value	Parameter	Value
$\sigma_{MAXA}\cdot f_A$ (1/d)	0.27	pK_1	5.95
$\sigma_{MAXN}\cdot f_N$ (1/d)	0.082	k_La (1/min)	0.31
$K_{NH,A}$ (mg N-NH_4^+/L)	0.92	k_La_{CO2} (1/min)	0.282
K_{NO} (mg N-NO_2^-/L)	2.84	ϑ# (min)	0.018 (13.2%)
Y_A (g COD_X/g N)	0.21	η#	122.9 (0.002 %)
Y_N (g COD_X/g N)	0.08	..#	25.4 (0.11 %)
K_{OA} (mg O_2/L)	0.74	TIC(0) (mM CO_2)	3.92 (0.05 %)
K_{ON} (mg O_2/L)	1.75		
		COST FUNCTION	5.32

VI.E.3 Significance of the CER measurement on the nitrification process

The objective of this section is to evaluate if the measurement of the carbon evolution rate (CER) provides extra information for more reliable parameter estimation. Theoretically, CER should be a very interesting measurement since CO_2 is a substrate of both process and CER could be an indirect measurement of the process evolution likewise OUR. However, the amount of CO_2 consumed for growth is much lower than oxygen in molar terms and the CER measurement is not as straightforward as oxygen.

The analysis of the CER measurement was performed in the BIOSTAT B fermenter, where off-line CO_2 was measured in addition to OUR and HPR. Experiment VI.E3 (Table VI.E8) examines the response of the CER measurement when ammonium was added to an enriched nitrifying biomass. Figure VI.E9 shows the experimental OUR and CER outlet profiles obtained. These profiles are the typical profiles obtained in all of the experiments performed in the BIOSTAT B fermenter. The CER profile had a linear dependence on the outlet CO_2 profile since both the molar flow and the inlet molar fraction of CO_2 were kept constant. CER was calculated as described in equation VI.E10

$$CER = \frac{F_{OUT} \cdot x_{CO2}^{OUT} - F_{IN} \cdot x_{CO2}^{IN}}{V} \cdot MW_{CO2} \qquad \text{(VI.E10)}$$

where F = molar flow (mol/min)
x = molar fraction
V = Reactor volume
MW = molecular weight

Table VI.E8 Experiment VI.E3

EXPERIMENT VI.E3	Analysis of the CER response
Equipment	BIOSTAT B fermenter (V_0 = 5.5 L)
pH	8
Temperature	25 ºC
Acid used	HCl = 0.467 M
Base used	NaOH = 0.472 M
Pulses	2.3 g $NaHCO_3$ (t = 0 min)
	200 mg $N\text{-}NH_4^+$ (t = 30 min) -> 36.4 mg $N\text{-}NH_4^+$/L
	200 mg $N\text{-}NH_4$ (t = 250 min) -> 36.4 mg $N\text{-}NH_4^+$/L

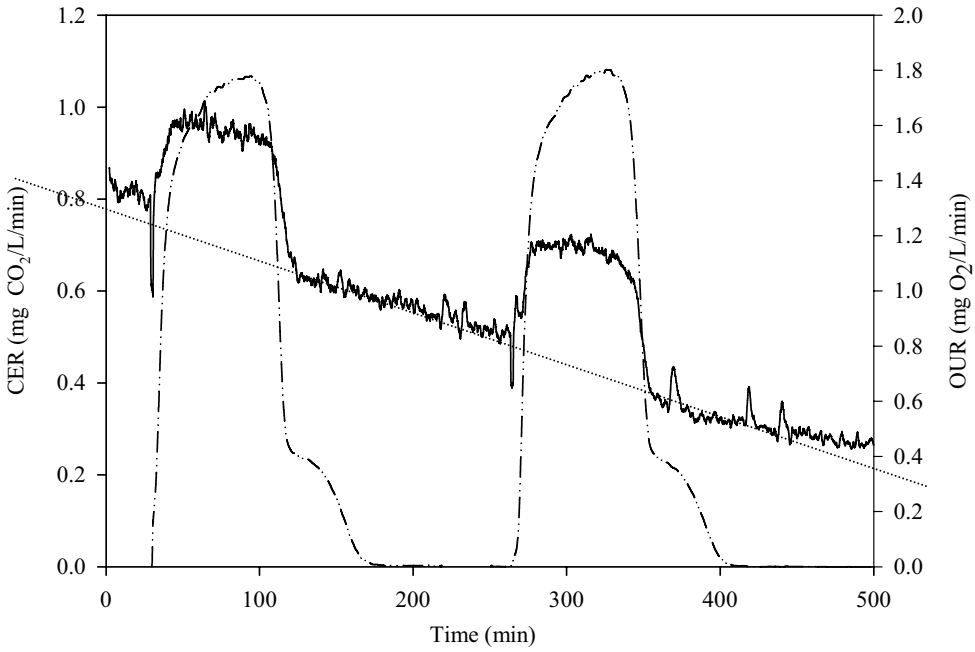

Figure VI.E9 CER (solid) and OUR (dash-dotted) profiles for experiment VI.E3

As a general trend (i.e. dotted line), CER decreases along the experiment because of CO_2 stripping. These experimental measures showed that the assumption of constant background proton rate (i.e. constant CO_2 stripping) proposed by Gernaey *et al.*, (2002a, b) could be successfully sustained in one pulse but not in the whole experiment. For example the CO_2 stripping linearity is lost from minute 400. Sin (2004) already pointed out the experimental constraints required for this assumption to be reliable (i.e. short-term and low k_La_{O2} experiment). This hypothesis has already been deeply examined in the previous chapter (section V.B.5.2).

When a pulse of substrate was added into the system, CER behaviour was surprisingly analogous to the OUR behaviour (i.e. the CER increased with a substrate pulse). At first glance, this increase was in total disagreement with the model predictions since CO_2 consumption due to autotrophic biomass growth should be occurring and the CER should decrease with a pulse of ammonia. The set of equations VI.E11a-f describe the theoretical CER behaviour (i.e. CO_2 consumption for growth and stripping and CO_2 production due to lysis as well as the equilibrium).

$$CPR_{GROWTH_A} = -\frac{i_{NB}}{14 \cdot Y} \cdot \sigma_{MAX_A} \cdot \frac{S_{NH4}}{K_{NH} + S_{NH4}} \cdot \frac{S_O}{K_O + S_O} \cdot X_A \quad \text{(VI.E11a)}$$

$$CPR_{GROWTH_N} = -\frac{i_{NB}}{14 \cdot Y} \cdot \sigma_{MAX_N} \cdot \frac{S_{NO}}{K_{NO} + S_{NO}} \cdot \frac{S_O}{K_O + S_O} \cdot X_N \quad \text{(VI.E11b)}$$

$$CPR_{LYSIS} = \frac{i_{NB}}{14 \cdot Y} \cdot (1 - f_{XI}) \cdot b_A \cdot X_A + \frac{i_{NB}}{14 \cdot Y} \cdot (1 - f_{XI}) \cdot b_N \cdot X_N \quad \text{(VI.E11c)}$$

$$CPR_{EQUILIBRIUM} = k_1 \cdot 10^{pK_1 - pH} + \frac{k_2}{10^{-pK_2}} \cdot S_{HCO3} - (k_1 + k_2 \cdot 10^{pH-14}) \cdot S_{CO2} \quad \text{(VI.E11d)}$$

$$CER_{STRIPPING} = k_L aCO_2 \cdot (S^*_{CO2} - S_{CO2}) \quad \text{(VI.E11e)}$$

$$CER_{TOTAL} = CPR_{TOTAL} + 2CER_{STRIPPING} \quad \text{(VI.E11f)}$$

The CER behaviour was simulated with the previous set of equations under different scenarios varying the initial TIC concentration and the k_La_{CO2}. Figure VI.E10 depicts two boundary examples of these simulations. The figure on the left shows how the simulation results with low initial bicarbonate concentration and k_La_{CO2} values were clearly in contrast to the experimental CER measured where CO_2 production is observed. However, the fact that CO_2 consumption was observable was only predicted under these conditions because the figure on the right shows the simulated CER profile with high amount of bicarbonate and the effect of CO_2 stripping under these conditions is much more important than the CO_2 consumption due to growth which becomes totally masked.

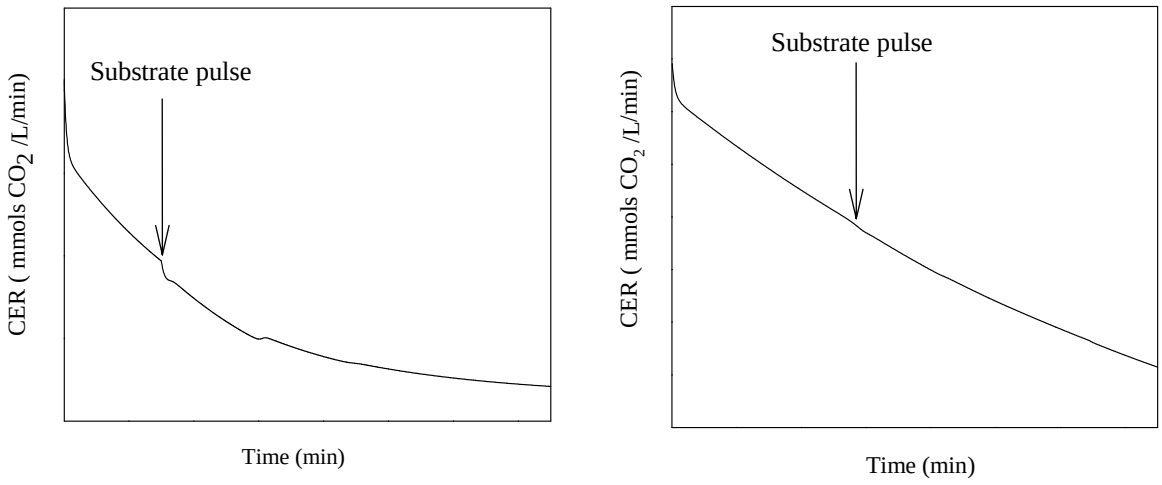

Figure V1.E10. CER simulations under different conditions: low k_La_{CO2} and low initial bicarbonate concentration (LEFT) and high k_La_{CO2} and high initial bicarbonate concentration (RIGHT)

The pH control is the cause of observing CO_2 production instead of CO_2 consumption. The CO_2 equilibrium is so dependent on the pH that low pH variations due to the controller were much more important than the CO_2 consumption due to growth. Under endogenous conditions the system became "proton consuming" due to CO_2 stripping and the pH controller maintained the pH at the setpoint value with acid addition. Under these circumstances, the pH value was equal or slightly higher than the setpoint value.

By the same token, when ammonium was consumed and the system became "proton producing", the pH controller added base to maintain the pH at the setpoint value. In this period, the pH level was lower or equal than the pH setpoint. Hence, in the non-nitritation periods the pH was ranging from setpoint and 0.01 more and in the nitritation periods, the pH was ranging form setpoint and 0.02 units less. These low variations were more influent to the CER response than the CO_2 consumption due to autotrophic growth. In this sense, experiment VI.E4 was conducted to assess the effect of a pH change on the CER measurement and to confirm the hypothesis described above. Two identical pulses of ammonium were added under different pH conditions. Figure V1.E11 shows the experimental results.

Table VI.E9 –Experiment VI.E4

EXPERIMENT VI.E4	Effect of pH on CER response
Equipment	BIOSTAT B fermenter (V_0 = 5.5 L)
pH	7.8 & 7.5
Temperature	25 ºC
Acid used	HCl = 0.467 M
Base used	NaOH = 0.472 M
Pulses	2.1 g $NaHCO_3$ (t = 0 min)
	200 mg $N\text{-}NH_4^+$ (t = 76 min) Ą 36.4 mg $N\text{-}NH_4^+$/L
	200 mg $N\text{-}NH_4^-$ (t = 380 min) Ą 36.4 mg $N\text{-}NH_4^+$/L

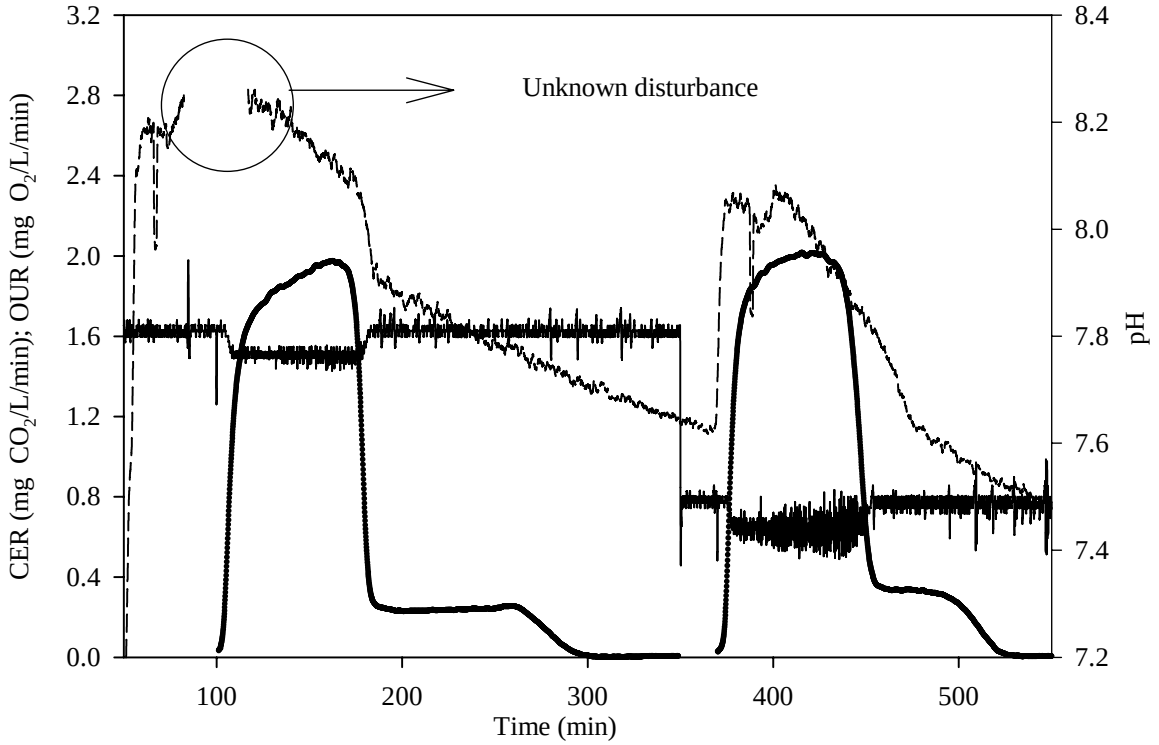

Figure VI.E11 CER (dashed), OUR (dotted) and pH (solid) profiles for experiment VI.E4.

As can be observed, the measured CER increased when pH was decreased from 7.8 to 7.5, confirming the huge influence of pH on CO_2 measurements. Moreover, the pH profile showed the positive and negative offsets obtained depending whether the control was with acid or base. In the first pulse the amount of pH variation for a small acid/base

addition was lower than in the second pulse. The reason was that in the second pulse a higher amount of CO_2 had already been stripped and the buffer effect had decreased. The increase in the measured CER coincided with the nitritation step and the change in the pH control.

Figure VI.E12 shows a simulation of the previous experiment in order to detect whether the model could predict this pH effect on CO_2 measurements. Hence, pH was fixed 0.01 units higher than the setpoint in the non-nitritation period and 0.02 units lower when ammonium was present. The simulated results agreed with the experimental profiles and clearly showed that minor changes in the pH were much more influent in the CER measurement than the CO_2 consumption linked to the nitrification.

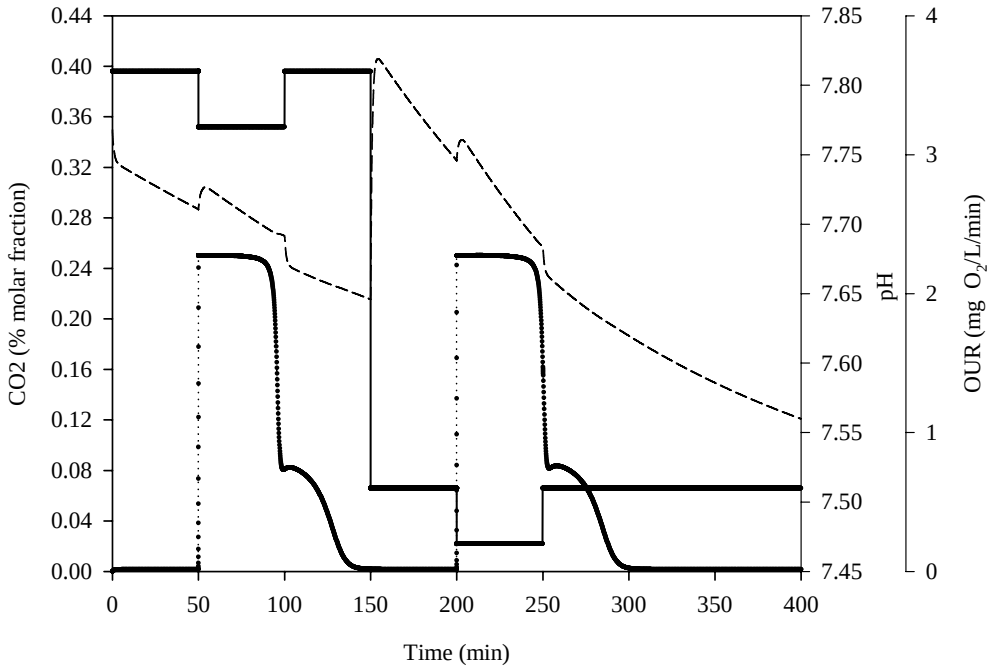

Figure VI.E12 Simulation of the CO_2 outflow molar fraction(dashed), pH (solid) and OUR (dotted) profiles for the addition of two pulses of 35 mg N-NH_4/L at two pH setpoints (7.8 and 7.5).

This result may somehow invalidate the use of the CO_2 measurement for parameter estimation. CO_2 measurement is not a straightforward issue since it requires new equipments such as a mass spectrophotometer and if this measurement does not provide essential information as demonstrated above, the inversion required may not be worth. In the literature, Gapes et al. (2003) used the CO_2 measurement for the examination the two-stage nitrification process in the Titrimetric Off-line Gas Analysis (TOGA) sensor. This sensor is similar to the fermenter used in this thesis and has the same on-line measurements discussed in this chapter: OUR, HPR and CO_2. Although they obtained interesting results with the measured OUR and HPR, they did not use the CO_2 neither for parameter estimation nor validation.

VI.E.4 Effect of different measurements on parameter estimation

The aim of this section is to evaluate whether the parameter estimation values obtained with OUR and HPR as measured variables are reliable or not. For this aim, parameter estimation was performed with extra measurement outputs such as ammonium or nitrite. If OUR and HPR contained enough information for a reliable estimation of these parameters, the parameter estimation values obtained with only these two measurements should be very similar to the ones obtained with OUR, HPR, ammonium and nitrite together.

VI.E.4.1. EXPERIMENTAL RESULTS

Experiment VI.E5 was conducted to study the effect of the different measurements on the parameter estimation for the two-step nitrification model. The measured variables were OUR, HPR, CER, ammonium and nitrite. Figure VI.E13 and VI.E14 show the experimental and calculated profiles obtained in this experiment. The two steps of the nitrification could not be clearly distinguished as in the experiments of section VI.E.2 though the biomass was withdrawn from the same pilot plant. The main cause could be that these experiments were conducted within more a month of difference and the biomass could somehow have changed. In any case, the two steps were occurring almost simultaneously and the model could be fitted to the experimental results.

The DO level did not reach low values despite the low airflow (0.14 vvm) due to the efficient stirring capacity of the fermenter. Hence, high k_La_{O2} values were obtained (0.53 vs 0.31 1/min in LFS respirometer). The oxygen limitation effect was not observed at these DO levels. One major improvement of this thesis is to operate the fermenter as a LFS respirometer, since the OUR values obtained with the off-line oxygen measurements were extremely noisy (see equipments - chapter III.1.2).The DO profile demonstrated that the fermenter could be used as a LFS respirometer since a constant DO level was measured when biomass was aerated under endogenous conditions. The aeration was stopped for approximately 15 minutes to calculate the OUR_{END} and k_La_{O2} (from the subsequent reaeration profile). Obviously, when the air inlet was turned off to measure the endogenous value the CO_2 measurement lost reliability since no air was entering to the mass spectrophotometer. On the other hand, a pulse of sodium bicarbonate was added at the start of the experiment to avoid carbon limitations.

Table VI.E10 –Experiment VI.E5

EXPERIMENT VI.E5	Effect of different measurements on parameter estimation
Equipment	BIOSTAT B fermenter (V_0 = 5.6 L)
pH	7.5
Temperature	25 ºC
Acid used	HCl = 0.5 M
Base used	NaOH = 0.25 M
Pulses	2g $NaHCO_3$ (t = 0 min)
	200 mg $N\text{-}NH_4$ (t = 76 min) Ą 35.7 mg $N\text{-}NH_4^+$/L

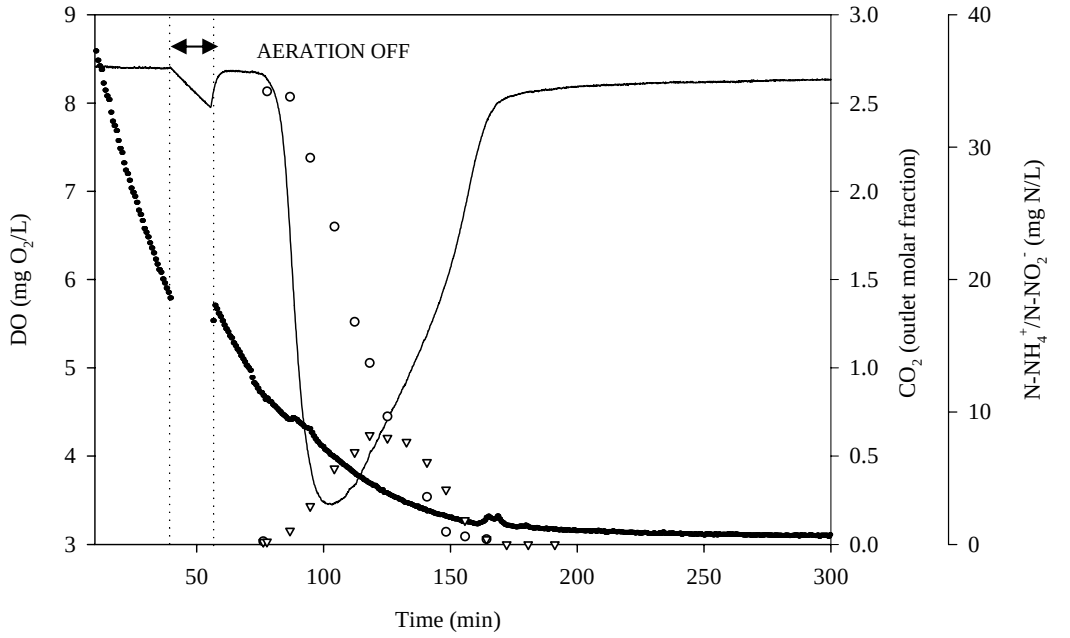

Figure VI.E13 DO (solid), CO_2 (dotted), $N\text{-}NH_4^+$(circle) and $N\text{-}NO_2^-$ (triangle) for experiment VI.E5

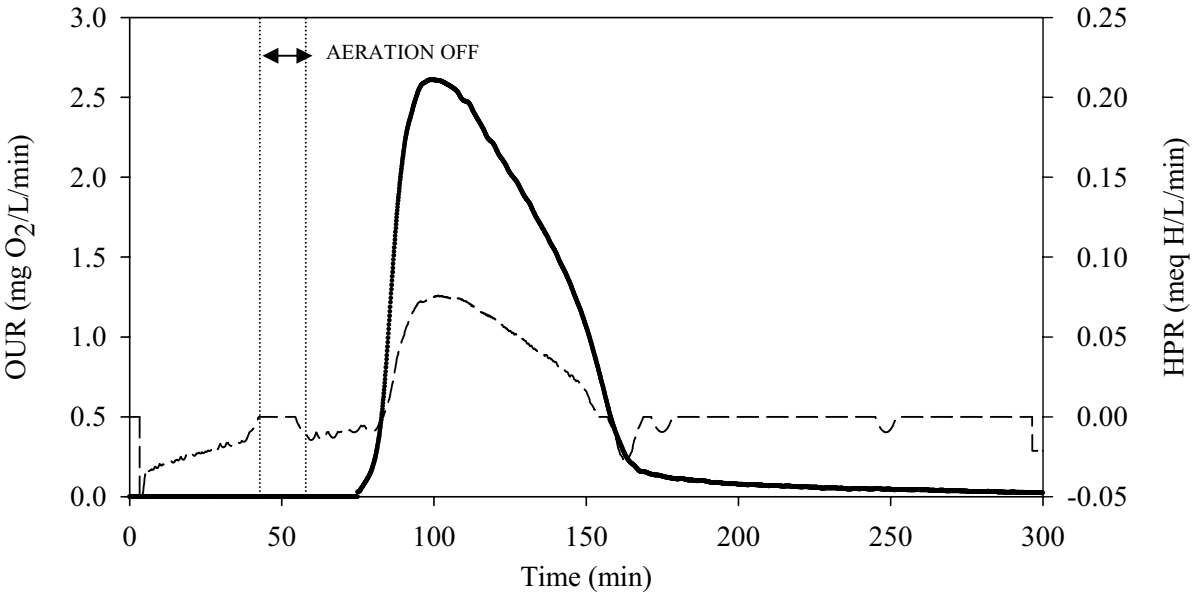

Figure VI.E14. Calculated OUR (solid) and HPR (dashed) profiles in experiment VI.D5

Both the ammonium and the OUR profile showed an acceleration phase since the ammonium consumption (and nitrite production) started at a low velocity after the pulse addition and then it speeded up after some ammonium consumption. The pH controller was manually tuned to obtain lower offset values around the pH setpoint. Hence, the CO_2 measurement in the outlet would be less influenced by pH changes around the setpoint and more influenced by the nitrification process (see previous section). This tuning improved the measurement since some CO_2 consumption could be detected linked to the ammonium pulse. Nevertheless, a high proportional gain was required to reduce the offset, which caused high disturbances and sudden pH changes at the start/end of the nitrification process. At this point, the controller needed to change from acid addition (i.e. CO_2 stripping) to base addition (i.e. nitritation) and inverse (figure VI.E15). These punctual disturbances were also reflected in the CER measurements at the start and the end of the nitritation process. In any case, the CER could not be used as an output variable for parameter estimation, despite the system was conditioned to obtain optimum measurements (low initial CO_2). Thus, it can be concluded that CER measurement is useless for parameter estimation for a nitrification model.

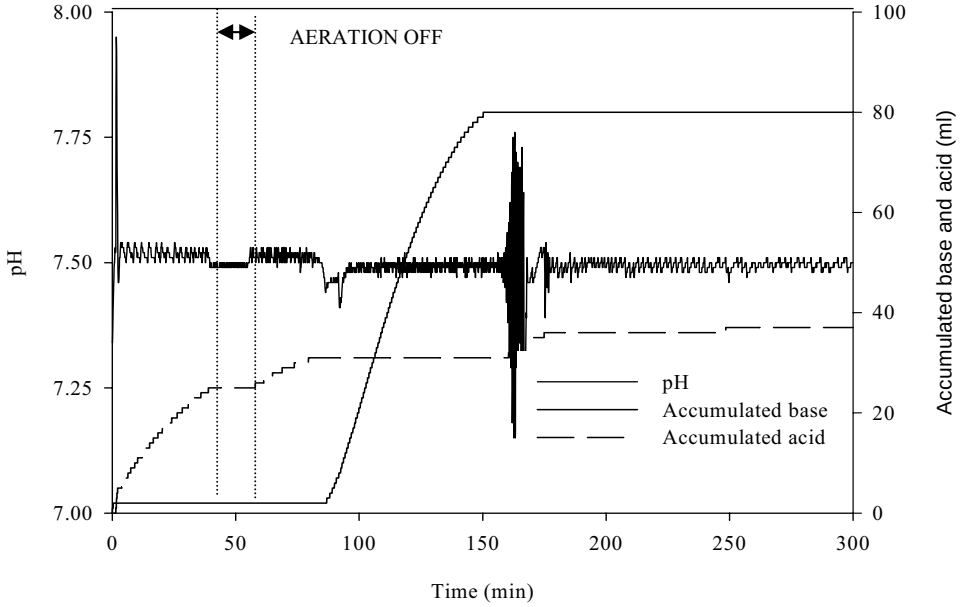

Figure VI.E15. Accumulated acid, base and pH profiles of experiment VI.D5

VI.E.4.2 PARAMETER ESTIMATION RESULTS

Parameter estimation was conducted 5 times using different output variables in the cost function to assess the effect of the different measured variables. The parameter estimation results are depicted in Table VI.E11 (the values in brackets are the percentage of error of the parameter). The cost function shown in the last row, corresponds to the cost function considering the four measurements and a weighting factor [eq VI.E4]. Then, these values are not comparable in each FIT since different experimental measurements are considered.

Table VI.E11 – Parameter estimation of experiment VI.D5 using OUR, HPR, ammonium and nitrite measurements

Output variables / Parameter	FIT 1 OUR	FIT 2 HPR	FIT 3 NO_2+NH_4	FIT 4 OUR+HPR	FIT 5 OUR+HPR $+NH_4$ + NO_2
$\sigma_{MAXA}\cdot f_A$ (1/d)	0.244 (0.08)	0.210 (0.01)	0.229 (1.04)	0.224 (0.06)	0.236 (0.4)
$\sigma_{MAXN}\cdot f_N$ (1/d)	0.059 (0.06)	0.059	0.087 (14.88)	0.096 (0.4)	0.083 (5.4)
K_{NH} (mg N-NH_4/L)	12.8 (0.16)	7.17 (0.002)	7.84 (1.23)	10.36 (0.26)	9.35 (0.47)
K_{NO} (mg N-NO_2/L)	0.48 (0.40)	0.48	3.78 (19.28)	4.51 (1.1)	3.33 (6.6)
Y_A (g COD_X·g N)	0.207	0.207	0.207	0.207	0.207
Y_N (g COD_X·g N)	0.079	0.079	0.079	0.079	0.079
K_{OA} (mg O_2/L)	0.74	0.74	0.74	0.74	0.74
K_{ON} (mg O_2/L)	1.75	1.75	1.75	1.75	1.75
k_La (1/min)	0.53	0.53	0.53	0.53	0.53
TIC (0) (mM CO_2)	-	4.01 (2.78)	-	4.00 (2.1)	4.09 (2.24)
$\eta_{\#}$	96.2 (0.15)	97.1 (0.07)	97.7 (0.9)	92.6 (0.18)	95.7 (0.37)
…	95.7 (0.008)	134.1 (0.002)	300.9 (0.12)	94.8 (0.01)	120.8 (0.036)
pK1	-	6.16()	-	6.19 (0.5)	6.18 (0.29)
COST $FUNCTION^{GLOB}$	3.59	2.5	2.95	2.65	1.78

∉ FIT 1, OUR as the sole output variable

FIT 1 was an interesting case since respirometric batch profiles are commonly used as sole output measurement for parameter estimation. Likewise experiment VI.E1, the parameter estimation errors obtained were underestimated due to the high sampling frequency. The measurement error covariance matrix was estimated considering a 3 % error in each sample. As it was a higher value than the Q_K for OUR and HPR, the confidence intervals obtained were higher. As can be observed, the values related to the nitratation process ($\sigma_{MAXN}\cdot f_N$ and K_{NO}) of FIT 1 differed significantly with the same parameters obtained with more measurements (i.e. FITS 4 and 5), which could be considered the closest to the real. This fact is supported with Figure VI.E16-left, where the experimental results are with the simulated profiles using the parameter estimation values of FIT1. According to this figure, the nitratation process is not correctly described despite the accurate OUR fitting, since nitrite measurements are underestimated. This parameter estimation inaccuracy maybe caused by the fact that the two steps of nitrification were simultaneous in this experiment and could not be distinguished with only OUR. Hence, with experiments such as VI.E1 (i.e. two-step OUR profiles), OUR might be enough for a reliable parameter estimation, but not in the case of this (i.e one-step OUR profiles). Another measurement specific for one process (such as nitrite) is necessary to distinguish between the two processes in a reliable way.

In addition, Figure VI.E16-right shows the contour plot of the cost function with OUR as the sole output variable for small variations of σ_{MAXN} and K_{NO} around the optimum. This figure shows the huge correlation existing between both parameters, particularly because of the lack of sensitivity of OUR on the K_{NO} parameter. This lack of sensitivity could be deduced evaluating the direction on the plane of the correlation. As mentioned above, this huge correlation could be successfully solved with an extra measurement.

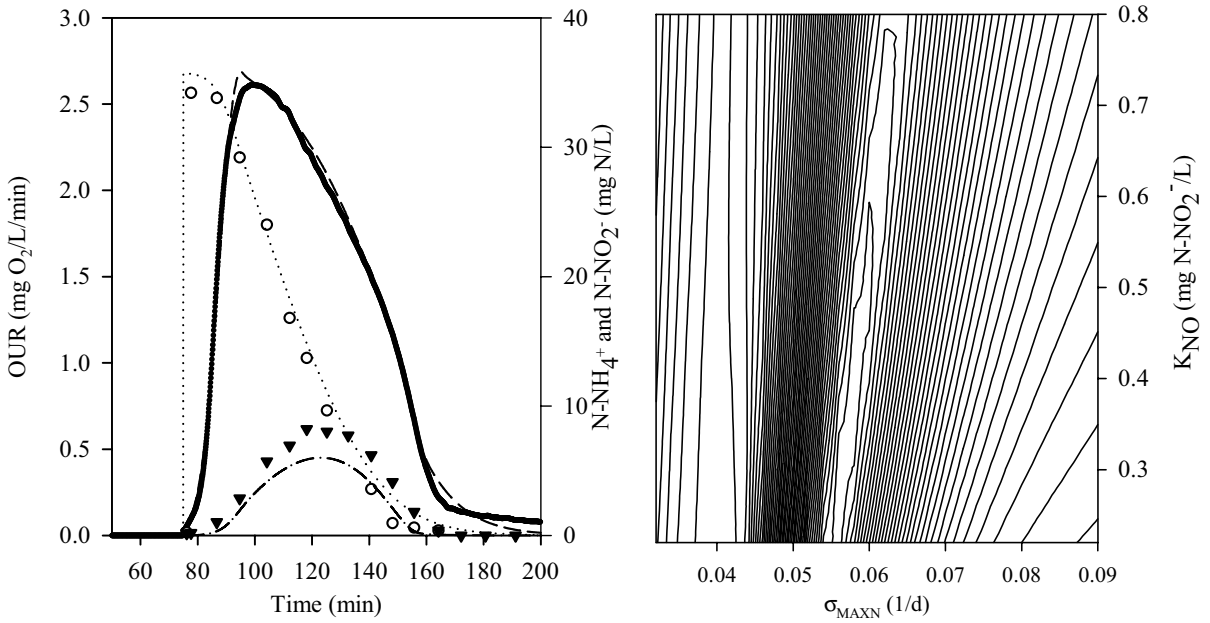

Figure VI.E16. LEFT Experimental versus simulated profiles for FIT 1: experimental OUR (solid line), simulated OUR (dashed line), experimental N-NH_4^+ (white circle), simulated N-NH_4^+ (dotted line), experimental N-NO_2^- (black triangle), simulated N-NO_2^- (dash-dotted line).
RIGHT Contour plot of the cost function with OUR as an output variable for small variations of σ_{MAXN} and K_{NO} around the optimum

∉ FIT 2, HPR as the sole output variable

The HPR profile for experiment VI.E5 (Figure VI.E14) was again proportional to the OUR measurement for the nitritation part of the experiment. Hence, only the parameters related to his process ($\sigma_{MAXA} \cdot f_A$ and $K_{NH,A}$) could be estimated with this measurement. The values obtained for these two parameters were closer to the values obtained in FIT 5. Thus, HPR could be a useful tool for nitritation parameter estimation. Moreover, pK_1 and TIC needed to be estimated for a proper description of the system. The estimated values of both parameters were practically the same in all the fits where HPR was used for parameter estimation, which may indicate that these values (i.e pK_1 ~ 6.18 and TIC (0) ~ 4 mM CO_2) are quite reliable.

The value of pK_1 was lower than the one calculated for pure water (6.36) likewise experiment VI.E1. The reason for this decrease could be again the high ionic strength of the medium, as detailed in section VI.E.2.2. The value of TIC(0) agrees with the initial amount of bicarbonate added at the start of the pulse: 4.25 mM of $NaHCO_3$ (2g). The initial CO_2 amount was very low to increase the influence of the nitrification process on the CO2 measurement. Hence, the CO_2 stripping process was faster than expected because of the high k_La.

∉ FIT 3, ammonium and nitrite measurements

The nitrification models are not usually calibrated using only these measurements. The values of pK1 and TIC(0) were not estimated with these measurements since they had no influence. The values obtained of the rest of the parameters are in the range found in the other FITS. Figure VI.E17 compares the experimental results with the simulated model (FIT 3). As can be observed, OUR is not accurately described though the ammonium and nitrite measurements fits are very good.

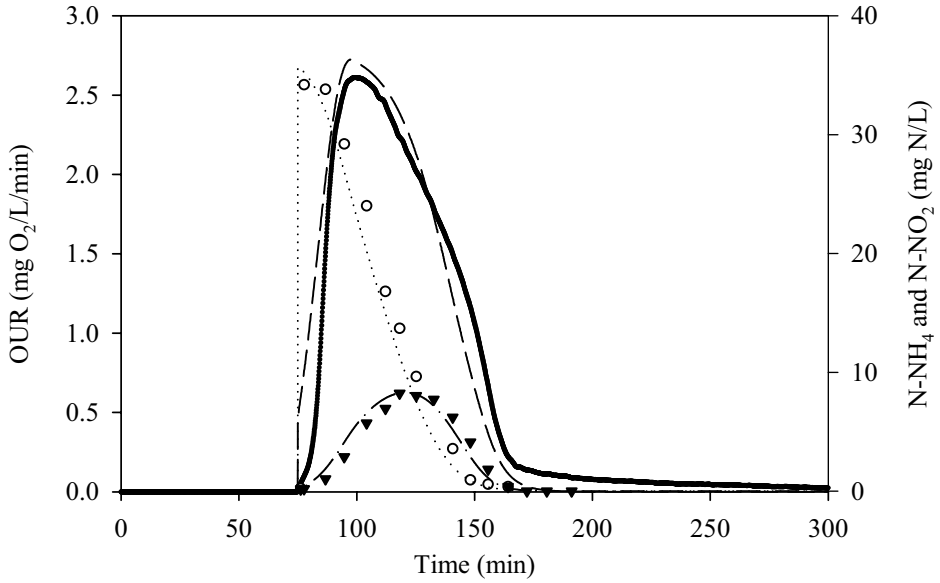

Figure VI.E17. Experimental versus simulated profiles for FIT 3: experimental OUR (solid line), simulated OUR (dashed line), experimental $N\text{-}NH_4^+$ (white circle), simulated $N\text{-}NH_4^+$ (dotted line), experimental $N\text{-}NO_2^-$ (black triangle), simulated $N\text{-}NO_2^-$ (dash-dotted line).

∉ FIT 4, OUR and HPR measurements as output variables

The values obtained in this FIT are very similar to the ones obtained in FIT 5. Again, the parameters related to the nitratation process are the most different between FIT 4 and FIT 5. As abovementioned, the main reason is that OUR is a one single shoulder where the two processes are masked, and the process which has less influence on both measurements (in this case nitratation) is masked. It is important to see that in the nitratation has practically no influence on HPR and the oxygen consumed is lower than in nitritation. Figure VI.E18 compares the experimental profiles with the simulated profiles of FIT4. As can be observed, the description of OUR and ammonium is very accurate and the description of nitrite is quite plausible. Thus, these two measurements seemed to contain enough information for a reliable description of the system without neither ammonia nor nitrite measurements.

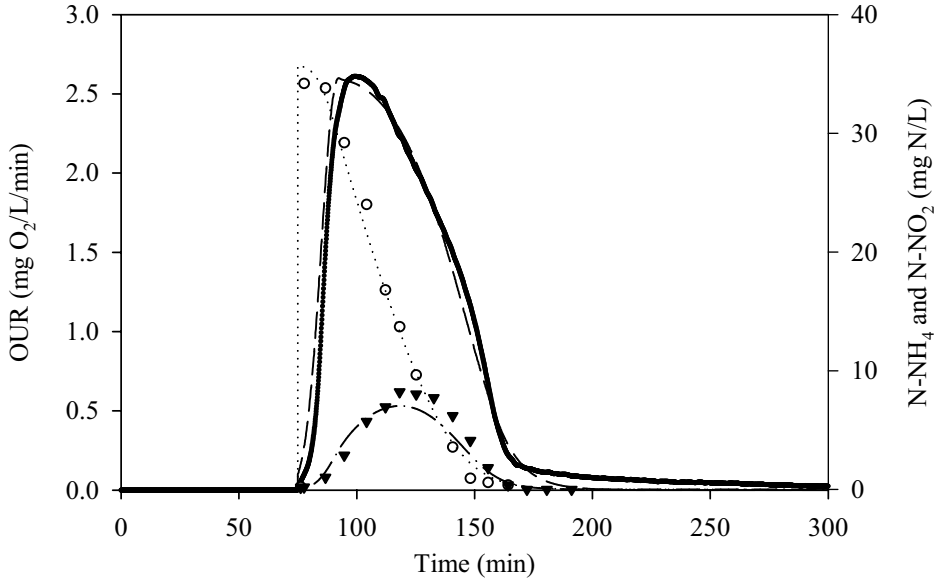

Figure VI.E18. Experimental versus simulated profiles for FIT 4: experimental OUR (solid line), simulated OUR (dashed line), experimental $N\text{-}NH_4^+$ (white circle), simulated $N\text{-}NH_4^+$ (dotted line), experimental $N\text{-}NO_2^-$ (black triangle), simulated $N\text{-}NO_2^-$ (dash-dotted line).

FIT 5, OUR, HPR, ammonium and nitrite measurements as output variables

Finally, the parameter estimation of FIT 5 should be the most close to the reality since the maximum amount of information was used. Figures VI.E19 and VI.E20 compare the experimental profiles with the simulated profiles of FIT 5. FIT 5 provides the best fitting possible to the experimental data.

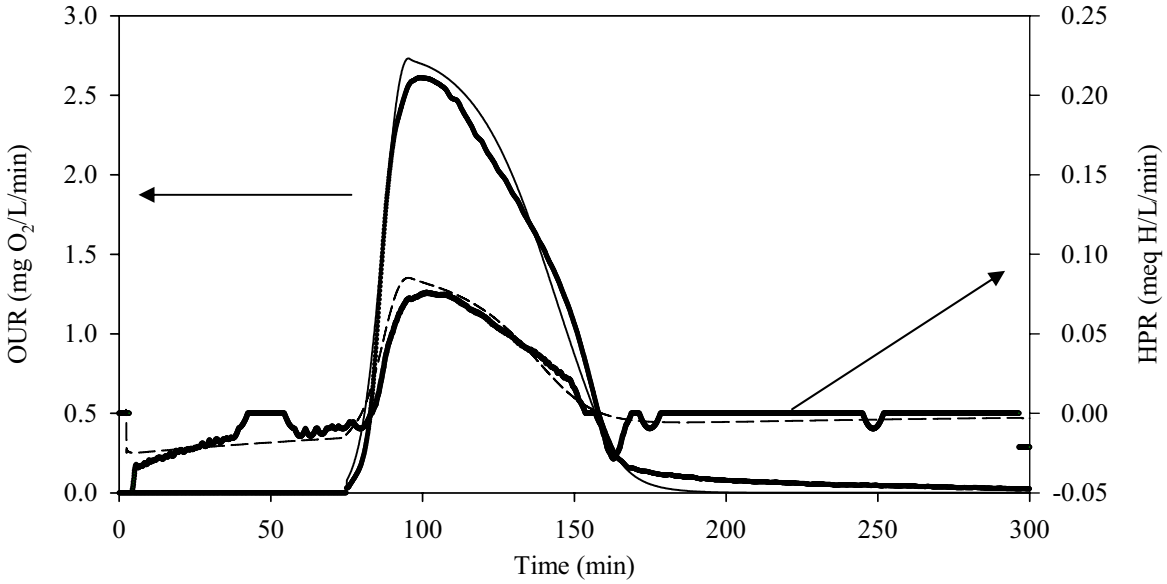

Figure VI.E19. Experimental versus simulated profiles for FIT 5: experimental OUR, HPR (thick lines), simulated OUR, HPR (thin lines)

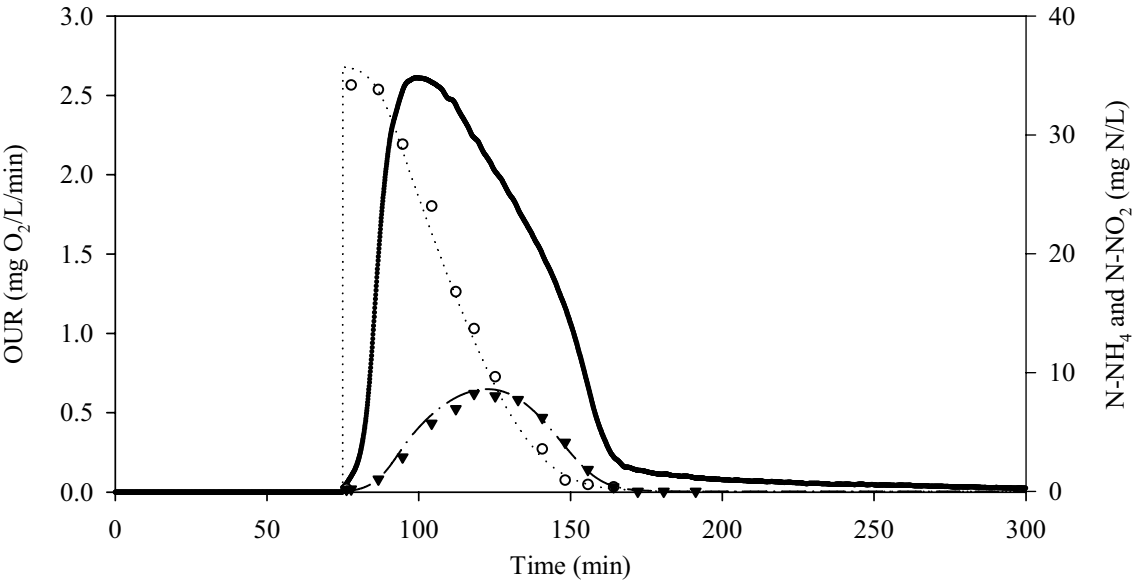

Figure VI.E20. Experimental versus simulated profiles for FIT 5: experimental OUR (solid line), experimental N-NH_4^+ (white circle), simulated N-NH_4^+ (dotted line), experimental N-NO_2^- (black triangle), simulated N-NO_2^- (dash-dotted line).

VI.D.4.2 DISCUSSION ON PARAMETER ESTIMATION RESULTS

This section discusses the parameter estimation values of FIT 5 (see Table VI.E11), which are considered to be the closest to the real ones. The values of the maximum growth rates could not be estimated separately from the active fraction values due to identifiability issues. However, a rough approximation of the maximum growth rate values could be obtained using equation VI.E5 and assuming:

- the ASM2 default value for the lysis fraction of inerts (f_l=0.2)
- b_i =0.14 1/d (Jubany *et al.*,2004).
- The ratio of f_A to f_N to be equal to the ratio between the two yields (Y_A/Y_N) (Gee *et al.*, 1990a). In these experiments, the ratio between yields was 2.62; hence, f_A/f_N=2.62.

The calculated OUR_{END} and VSS were 0.0284 mg O_2/L/min and the VSS were 950 mg VSS/L (1425 mg COD_X/L). The resulting active fractions are: $\mathbf{f_A}$ = 0.185 and $\mathbf{f_N}$ = 0.07. These active fraction values are very similar to the ones obtained in the previous experiments in the LFS respirometer (experiment VI.E1), regarding that the time between experiments was one month. If these were the real values, then σ_A and σ_N would respectively be:

$$\boldsymbol{\sigma_A} = 1.27\ 1/d \text{ and } \#\boldsymbol{\sigma_N} = 1.19\ 1/d$$

The value of σ_N is practically the same as the one previously obtained (1.22 1/d in experiment VI.E1). However, the value of σ_A is around 15% lower. The fact that σ_A was higher than σ_N allowed to distinguish between the two steps of nitrification in the OUR profiles obtained of experiment VI.E1. On the other hand, the values of both σ were too similar in experiment VI.E5 and, hence, the OUR profiles were single steps.

The value of both substrate affinity constants was far too high than the ones obtained in the previous experiments. These parameters are highly correlated with σ and yield as pointed out by many authors (e.g Holmberg, 1982; Baltes *et al.*, 1994; Munack and Posten, 1989; Versyck *et al.*, 1997; Petersen, 2000 or Liu and Zachara, 2001 among many others). Hence, some identifiability problems appeared despite the fact that the yield was previously estimated.

Figure VI.E21 and VI.E22 show the existing correlation between $\sigma_A \cdot f_A$ and $K_{NH,A}$ and $\sigma_N \cdot f_N$ and $K_{NO,}$ respectively. The correlation is much more important in the latter than in the first. The existing correlation was very significant since this graphic was obtained considering the four measurements as measured variable, which was the scenario theoretically with the fewest correlation problems.

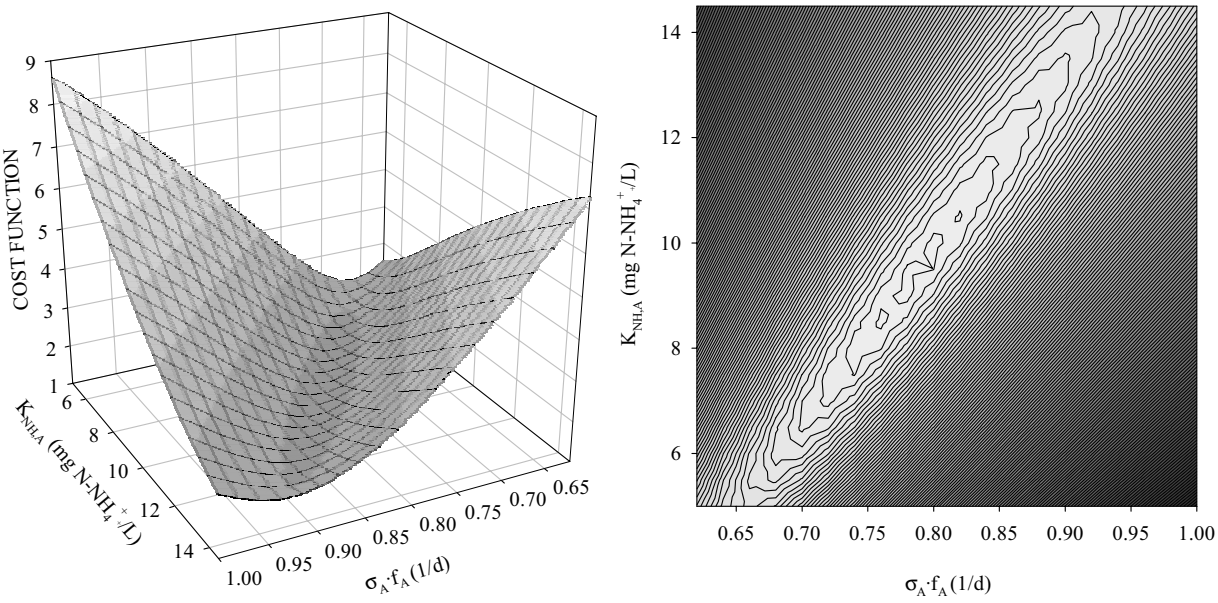

Figure VI.E21 Correlation between $K_{NH,A}$ and $\sigma_{MAXA} \cdot f_A$ for FIT 5

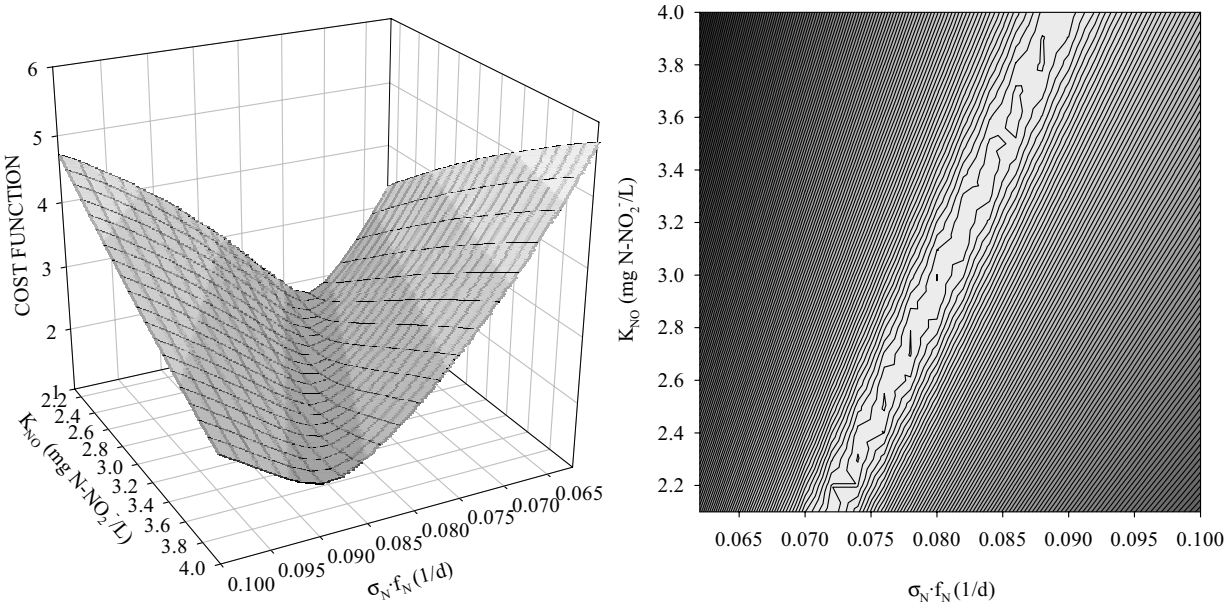

Figure VI.E22 Correlation between K_{NO} and $\sigma_{MAXN} \cdot f_N$ for FIT 5

The fact that the substrate affinity constants (i.e.. $K_{NH,,A}$ and K_{NO}) obtained are so different between experiments VI.E1 and VI.E5 may not only be caused by the identifiability issue but also by the operational conditions. Theoretically, the values of $K_{NH,A}$ and K_{NO} are specific of each population regardless the equipment used (respirometer, fermenter,…). However, as these constants are extremely linked to substrate limitations (and, hence, mass transfer issues), the operational conditions of the system (i.e the stirring efficiency, the aeration,…) may have on influence on this value.

This huge correlation observed between σ_A and K_{NH} and σ_N and $K_{NO,}$ respectively, even in the experiment with all the measurements, indicates that batch experiments are not recommended for estimating the affinity constants. Different experimental desings such as fed-batch systems may improve the parameter identifiability.

VI.E.5 Effect of pH on the nitrification process

VI.E.5.1 EXPERIMENTAL RESULTS

The aim of this section is to examine the pH influence on the nitrification process. For this aim, the value of OUR_{MAX} was measured at different pH set points. Experiment VI.E6 (Table VI.E12) shows different OUR profiles obtained with several ammonia pulses with different pH setpoint values.

Table VI.E12 Experiment VI.E6

EXPERIMENT VI.E6	Effect of pH on the nitrification process
Equipment	BIOSTAT B fermenter (V_0 = 5.5 L)
pH	7.3/7.5/7.8/8/8.2
Temperature	25 ºC
Acid used	HCl = 0.25 M
Base used	NaOH = 0.25 M
Pulses	5 · 200 mg $N\text{-}NH_4$

Figure VI.E23 compares the OUR profiles obtained. At first glance, a variation on the OUR_{MAX} values is observed in the different experiments. In addition there seems to be an optimum pH. Sodium bicarbonate was added before each pulse to avoid TIC limitations.

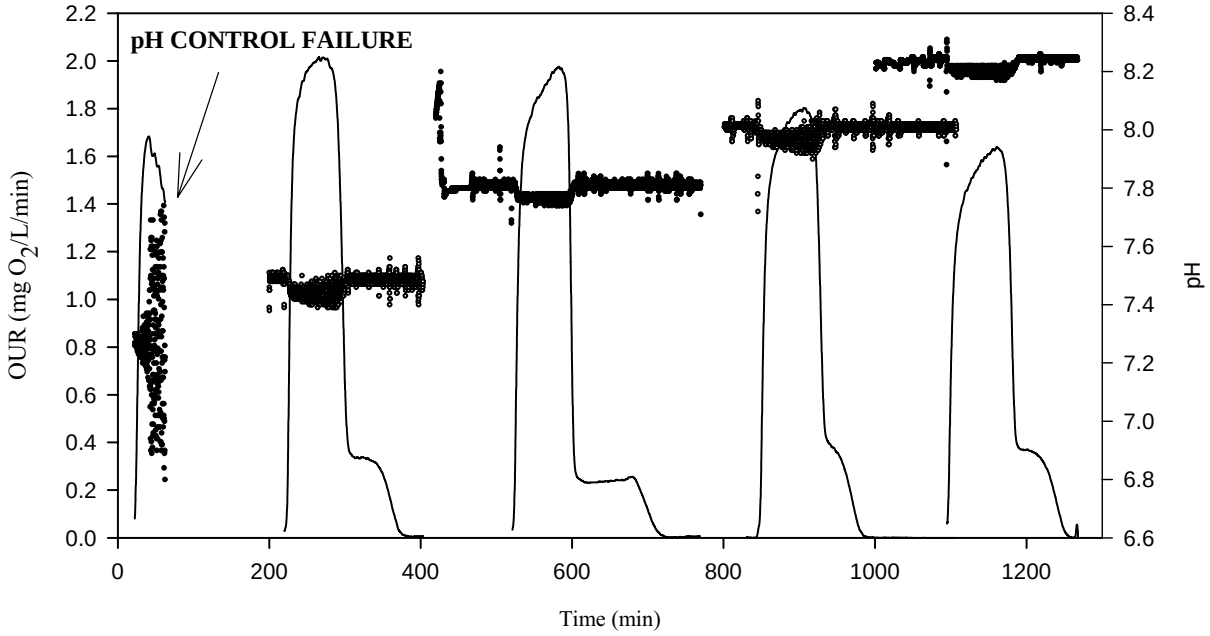

Figure VI.E23 – OUR and pH profiles obtained at different pH setpoint levels.

The biomass used was withdrawn from the same pilot plant (Jubany *et al.*, 2004) with a similar concentration. Hence, for this experiment, studying the dependence of the OUR_{MAX} on pH is analogous to study the dependence of the growth rates on pH because the OUR_{MAX} corresponds to VI.E12 (Table VI.A3):

$$OUR_{MAX} = \left(\frac{3.43}{Y_A} - 1\right)\cdot\sigma_{MAXA}\cdot X\cdot f_A + \left(\frac{1.14}{Y_N} - 1\right)\cdot\sigma_{MAXN}\cdot X\cdot f_N \qquad \text{(VI.E12)}$$

Figure VI.E24 shows the dependence of the OUR_{MAX} on pH for the experiment VI.E6.

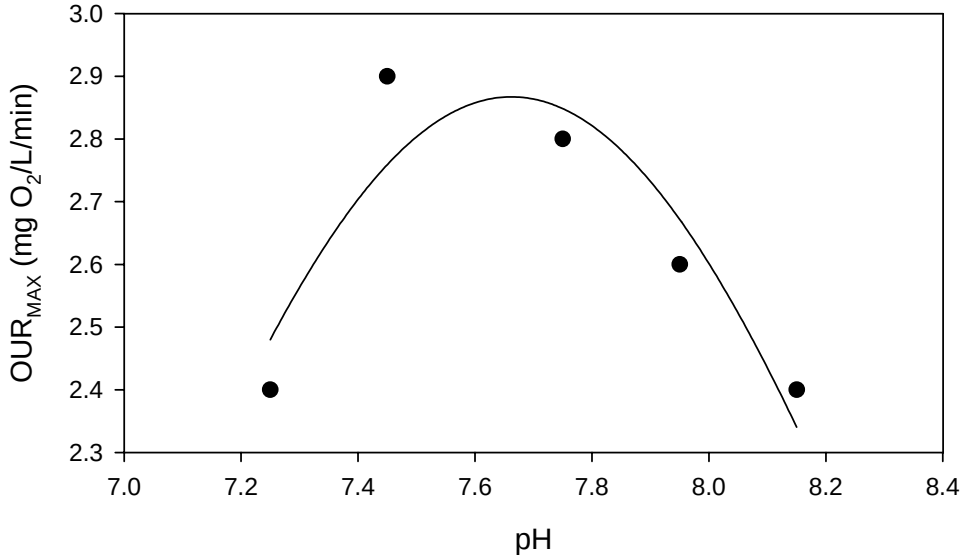

Figure VI.E22 – Dependence of OUR_{MAX} on Ph

In this thesis, a simple Gaussian expression was fitted to the experimental value obtained [eq. VI.E13].

$$OUR_{MAX}(pH) = OUR_{MAX}\cdot e^{-0.5\left(\frac{pH - pH_{OPT}}{\rho}\right)^2} \qquad \text{(VI.E13)}$$

The optimum parameters obtained were:

$$OUR_{MAX} = 2.87 \pm 0.11$$
$$\rho\# = 0.76 \pm 0.13$$
$$pH_{OPT} = 7.63 \pm 0.05$$

VI.E.5.2 COMPARISON WITH OTHER WORKS

Several authors have studied the effect on pH on nitrification in activated sludge systems and reported that the optimum pH for was in the range 7.0-8.0 (Painter and Loveless 1983,; Schlegel and Bowien, 1989; Antoniou *et al.*, 1990, EPA, 1993). Villaverde *et al.* (1996) studied the influence of pH over nitrification in submerged biofilters within a wide range of 5.0-9.0 and found that the highest activity in ammonia oxidisers was at pH 8.2.

Other authors have preferred to work with pure cultures of *Nitrobacter* and *Nitrosomonas* since the activated sludge is variable in time and in place. For example, Alleman (1984) pointed out that for *Nitrosomonas* the optimum range is 7.9 to 8.2 and 7.2 to 7.6 for *Nitrobacter*. Antoniou *et al.* (1990) obtained an equation for pH dependence for *Nitrosomonas* growth. The expression was derived from theoretical arguments based on the activation energy (equation VI.E14). They had three unknown parameters (m,b and c), which were estimated using several experimental data. An optimum pH around 7.8 was determined as a result, which is in agreement with the results obtained in this thesis.

$$\sigma_A 4 b_A | \frac{m}{1 2 \frac{b}{10^{4pH}} 2 \frac{10^{4pH}}{c}} \qquad \text{(VI.E14)}$$

Finally, Grunditz and Dalhammar (2001), studied the effect of both temperature and pH on *Nitrosomonas* and *Nitrobacter* and obtained similar graphs as the one in Figure VI.E22. According to their experimental results, the optimum pH and temperature for *Nitrosomonas* is 35ºC and 8.1 respectively and 38ºC and 7.9 for *Nitrobacter*. As can be observed, the optimum pH values are somehow higher than the ones obtained in this thesis.

CHAPTER VI.E CONCLUSIONS

- Parameter estimation requires the measurement error weighting matrix (Q_K) assessment for the experimental inputs used. This matrix has been calculated for both equipments and the values obtained seem to be underestimated which will result in too low parameter estimation errors. However, the values obtained are in the range of similar works (Petersen, 2000).

- The two-step nitrification model has been successfully calibrated and validated with OUR and HPR experiments. The most important values obtained are σ_A= 1.52 1/d and #σ_N = 1.22 1/d. These values have been calculated with an estimation of the active fraction values using the endogenous OUR value.

- The value of the pK_1 obtained is lower than the default value for pure water (6.36). This is likely due to the huge ionic strength of the medium.

- The influence of the CER measurement was examined. The obtained results showed that minor changes in the pH were much more influent in the CER measurement than the CO_2 consumption linked to the nitrification. Thus, it can be concluded that CER measurement is useless for parameter estimation for a nitrification model.

- Parameter estimation was conducted using different output measurements such as OUR, HPR, ammonium or nitrite. The conclusion was that OUR and HPR contain enough information for a reliable description of the system without neither ammonia nor nitrite measurements, though the profile obtained was a single step.

- A huge correlation was observed between $\sigma_A \cdot f_A$ and K_{NH} and $\sigma_N \cdot f_N$ and $K_{NO,}$ respectively, even in the experiment with all the measurements, indicating that short-term batch experiments are not recommended for estimating Monod parameters.

- Finally, the effect of pH on the nitrification rate was studied by measuring OUR_{MAX} at different pH set points. The results showed that the optimum pH was around 7.6, which is in agreement with the values found in the literature.

CHAPTER VII

ENHANCED BIOLOGICAL PHOSPHORUS REMOVAL

CHAPTER VII.A

Model development for the enhanced biological phosphorus removal process

Part of this chapter has been published as:

Pijuan M., Saunders A.M., Guisasola A., Baeza J.A., Casas C. and Blackall L.L. (2004a) Enhanced biological phosphorus removal in a sequencing batch reactor using propionate as the sole carbon source. Biotechnol. Bioeng. 85, 56-67.

ABSTRACT

This chapter describes the development of a model for the Enhanced Biological Phosphorus Removal (EPBR) process. This model is a modification of the widespread Activated Sludge Model nº2 (ASM2). The modifications introduced are based on other metabolic models for EBPR. The stoichiometry of each process was obtained through elementary mass and reduction balances and the process kinetics proposed are based on Monod kinetics and substrate limitations and/or product inhibition factors. The model was successfully calibrated and validated using acetate and propionate as the sole carbon source. The parameter estimation results, together with the values found in the literature were used to discuss the differences between acetate and propionate as the carbon source for an EBPR system.

VII.A.1 The EBPR process

The EBPR process is based on the enrichment of activated sludge with Polyphosphate Accumulating Organisms (PAO). The detailed metabolic behaviour of these microorganisms is not completely known and there are still different hypotheses pretending to describe the inside of the EBPR process. However, the knowledge of this process is improving faster particularly due to the recent use of new microbial techniques. These techniques can help to identify different populations involved in the process apart from PAO such as Denitrifying Phosphate Accumulating Organisms (DPAO) or glycogen accumulating organisms (GAO).

Under anaerobic conditions, PAO take up organic substrates (preferably volatile fatty acids - VFAs) and store them as poly-hydroxyalkanoates (PHA), while the reducing equivalents are provided by glycolysis of internally stored glycogen (Mino *et al.*, 1987; Arun *et al.*, 1988; Satoh *et al*., 1992; Smolders *et al*., 1994a,b; Pereira *et al.*, 1996). The energy for this process is obtained partly from the glycogen utilisation but mostly from the hydrolysis of the intracellular stored polyphosphate (polyP), resulting in an orthophosphate release into solution. In the subsequent aerobic phase, PAO take up excessive amounts of orthophosphate to recover the intracellular polyP levels by oxidising the stored PHA. Meanwhile they grow and replenish the glycogen pool using PHA as both carbon and energy sources (Arun *et al.*, 1988; Smolders *et al*., 1995). Net phosphorus removal is achieved by wasting sludge after the aerobic period when the biomass contains a high level of polyP.

On the other hand, GAO have the potential to directly compete with PAO for substrate uptake under anaerobic conditions. GAO are capable to obtain the energy required to uptake acetate from the glycolysis (Filipe *et al.*, 2001b). Hence, GAO can be considered detrimental for the EBPR process since these bacteria can store VFA as PHA under anaerobic conditions but without neither phosphorus release nor the subsequent uptake. These bacteria may have been the cause of many detected EBPR failures (Cech and Hartman 1990, 1993). Nowadays, some EBPR works are focused on finding which operational conditions may favour PAO in front of GAO.

VII.A.2 EBPR model development

VII.A.2.1 EBPR MODELLING BACKGROUND

The first modelling attempts in the EBPR field started in the late 1980s. By that time, a controversial point of EBPR was whether the reduction equivalents required for the PHA synthesis were provided by glycogen degradation (i.e. through glycolysis) or by the substrate entering to the TCA cycle.

On the one hand, Comeau *et al. (*1988) and Wentzel *et al.* (1990), proposed the TCA cycle as the most probable reducing power source, whereas Mino *et al.* (1987) supported the glycolysis hypothesis with experimental evidences. Later on, Pereira *et al.* (1996) demonstrated that the reducing power was mainly produced by the intracellular glycogen degradation, although some reducing power was also supplied through acetate oxidation (TCA cycle). Nowadays, the "glycogen hypothesis" seems more widely accepted.

Smolders *et al.* (1994a, 1994b, 1995) proposed the first metabolic model for EBPR. Their model was developed for acetate as the sole carbon source and considered the two different hypotheses for reducing power obtainment. As the metabolic model of Smolders considered only acetate as substrate, PHA fractions different from Poly-η-hydroxybutyrate (PHB) were neglected. Other metabolic models appeared after Smolders' work using acetate as a sole carbon source (e.g. Filipe *et al.*, 2001a, Meijer *et al.*, 2001 or Yagci *et al.*, 2003). Murnleitner *et al.* (1997) from the same research group (Technical University of Delft) extended Smolders' model for the anoxic phosphorus uptake process.

Acetate is usually as chosen as the sole carbon source when modelling EBPR since it is the primary fraction of VFA present in most WWTP. However, the impact of other carbon sources on EBPR is also a focus of interest (Pijuan *et al.*, 2004b). Propionate is a carbon source that requires special attention since it might represent a significant portion of VFA generated through prefermentation. Moreover, it has been shown to be a more favourable substrate for achieving EBPR (Lemos *et al*., 2003). Several authors pointed out that the ratio of acetate to propionate is significant since the type of VFA used by PAOs in EBPR had an effect on their metabolism (e.g. Hood and Randall, 2001 or Chen *et al.*, 2004).

Later on, Oehmen *et al.* (2005) presented the first biochemical model developed with propionate as the sole carbon source. The main difference observed with acetate's model was that propionate was not only stored as PHB, but also as Poly-η-hydroxyvalerate (PHV) and Poly-η-hydroxy-2methylvalerate (PH2MV), two different PHA fractions (Satoh *et al.*, 1992). In fact, and according to stoichiometry of Oehmen's model, only 5 % of the total amount of produced PHA was PHB.

In parallel to these metabolic models, the International Water Association (IWA) developed a different approach to the EBPR modelling by using "grey models" for a macroscopic description of the evolution of the main compounds involved, but without deepening in the metabolic details of these transformations. Examples of these models are ASM2 and ASM2d (Henze *et al.,* 2000) and ASM3-BioP (Koch *et al.*, 2001; Rieger *et al.,* 2001). Baetens deepened in the study of ASM2 models, provided the structural and practical identifiability of them and performed OED for reliable parameter estimation (Baetens, 2000). These models have been proved to be very useful to calibrate pilot-plants or full WWTP as for example in Meijer *et al.* (2001; 2002).

VII.A.2.2 MODEL DESCRIPTION

The model used in this thesis and described below is not a metabolic model. It derived from a modification of the ASM2. ASM2 needed to be modified because it was developed for a macroscopical description of EBPR and, as such, it contained a lot of simplifications. One of the most important simplifications was the omission of glycogen as model compound, partly because its measurement by that time was non-reliable (Aurola *et al.*, 2000). However, glycogen has a very important role, particularly when describing batch experiments and its inclusion has become indispensable in view of process modelling. Hence, glycogen economy was included in the model as in on other models of the literature (Smolders *et al.,* 1994 a,b; Mino *et al.,* 1995; van Veldhuizen *et al*., 1999; Filipe and Daigger 1999; Manga *et al.,* 2001).

ASM2 considers all the different biomass fractions involved in the biological nutrient removal processes. However, only PAO microorganisms were considered in the model development since ordinary heterotrophs and nitrifying bacteria were not favoured due to the operational conditions. Nitrogen was not a state variable because ammonia concentration was high enough to avoid limitations during the experiments. In addition, anoxic processes related to PAO were omitted since nitrates were not detected in the reactor. Hence, the model considered nine reactions involved in PAO mechanisms. Storage polymers (PHA, glycogen and polyP) are treated separately from active biomass to describe reliably the process and, hence, lysis reactions were used to ensure that polymeric storage products decayed together with the biomass.

One of the most important differences among metabolic models and ASM-alike models lays in the energy part. The metabolic models include ATP as a model compound and describe the amount of energy necessary for each process to occur. This energy is mainly provided by PHA oxidation in the aerobic phase. On the other hand, ASM-alike models include some PHA oxidation in each process to avoid ATP as model compound.

In the model developed in this thesis, ATP is not considered as a compound, and each aerobic process includes a certain PHA oxidation. Hence, the stored PHA is used for two purposes (under aerobic conditions):

- part of the internal PHA is oxidised for energy obtainment. This energy is utilised for growth and maintenance purposes, for glycogen restoration and for phosphorus uptake from the medium which was stored as polyP.

- the rest of this PHA was directly used as a carbon source for biomass growth and internal glycogen pools restoration.

1. ACETATE UPTAKE and X_{PHA} STORAGE

This process describes the acetate uptake linked to glycogen degradation, phosphorus release and PHA production which occurs under anaerobic conditions. The metabolic stoichiometry of this process was first deduced by Smolders *et al.* (1994a) for acetate as sole carbon source [eq. VII.A1].

$$CH_2O + \frac{1}{2}CH_{10/6}O_{5/6} + \frac{0.25 + \zeta_1}{\zeta_2}HPO_3 \Downarrow$$
$$1.33CH_{1.5}O_{0.5} + 0.17CO_2 + \frac{0.25 + \zeta_1}{\zeta_2}H_3PO_4 + \left(\frac{5}{12} - \frac{0.25 + \zeta_1}{\zeta_2}\right)H_2O \qquad \text{(VII.A1)}$$

where CH_2O : acetate
HPO_3 : polyphosphate
H_3PO_4 : orthophosphate
ζ_1 : moles ATP required to uptake acetate through the membrane (pH dependent)
ζ_2 : amount of ATP generated from the degradation of polyP
$CH_{1.5}O_{1.5}$: PHB
$CH_{10/6}O_{5/6}$: glycogen

Oehmen *et al.*, (2005) deduced the stoichiometry of the process for propionate as the sole carbon source [eq VII.A2]. Although acetate was mainly stored as PHB, the major fractions of PHA produced with propionate were PHV and PH2MV.

$$CH_2O_{2/3} + \frac{1}{3}CH_{10/6}O_{5/6} + \left(\frac{2}{9} + \zeta_{PAO}\right)HPO_3 \Downarrow$$
$$\frac{1}{18}CH_{1.5}O_{0.5} + \frac{5}{12}CH_{1.6}O_{0.4} + \frac{3}{4}CH_{5/3}O_{1/3} + \frac{1}{9}CO_2 + \left(\frac{2}{9} + \zeta_{PAO}\right)H_3PO_4 + \left(\frac{8}{9} + \zeta_{PAO} + \frac{1}{6}\right)H_2O \qquad \text{(VII.A2)}$$

where $CH_{1.6}O_{0.4}$: PHV
$CH_2O_{2/3}$: propionate
$CH_{5/3}O_{1/3}$: PH2MV
ζ_{PAO}:moles ATP required to uptake acetate through the membrane (pH dependent)

According to the previous stoichiometry, a unique simpler expression was proposed valid for both substrates based on the ASM2 notation (expressed in mass basis) [eq. VII.A3]. All the PHA fractions were gathered in only one compound. The CO_2 stoichiometric coefficient was calculated using mass and degree of reduction balances likewise the other models developed in this thesis (see Chapter V.B or Chapter VI.A) or Heijnen (1999).

$$Y_{VFA}/CH_2O \text{ or } CH_2O_{2/3} + Y_{GLY1}CH_{10/6}O_{5/6} + Y_{PO}HPO_3 \Rightarrow$$
$$CH_{1.5}O_{0.5} + \left(\frac{1}{8}\cdot\frac{Y_{PHA}}{\nu_A} + \frac{Y_{GLY1}}{\nu_G} - \frac{1}{\nu_P}\right)CO_2 + Y_{PO}H_3PO_4 + H_2O \qquad \text{(VII.A3)}$$

where Y_{GLY1} : g COD_{GLY} degraded /g COD_{PHA} produced
Y_{PO} : g P released /g COD_{PHA} produced
Y_{VFA} : g COD_{VFA} taken up /g COD_{PHA} produced
ν_A : degree of reduction of acetate (= 4), (Roels, 1983)
ν_G : degree of reduction of glycogen (= 4)
ν_P : degree of reduction of PHA (if PHA was PHB, ν_P = 4.5)

The kinetics of this process is defined with the next expression [eq. VII.A4], where the substrate uptake rate is limited by a lack of any of three substrates. Filipe *et al.* (2001a) also studied this kinetics and found a dependence on polyP and glycogen content of the biomass cells.

$$r_{VFA\_UPTAKE} = q_{PHA}\cdot\frac{S_{VFA}}{K_S + S_{VFA}}\cdot\frac{X_{PP}/X_{PAO}}{K_{PP} + X_{PP}/X_{PAO}}\cdot\frac{X_{GLY}/X_{PAO}}{K_{GLY} + X_{GLY}/X_{PAO}}\cdot X_{PAO} \qquad \text{(VII.A4)}$$

where K_{GLY} : Affinity constant for the ratio X_{GLY}/X_{PAO} (g COD_{GLY}/ g COD_X)
K_{PP} : Affinity constant for the ratio X_{PP}/X_{PAO} (g P/ g COD_X)
K_S : Substrate affinity constant (mg COD_{VFA}/L)
q_{PHA} : maximum PHA storage rate (1/d)
S_{VFA} : VFA concentration (mg COD_{VFA}/L)
X_{GLY} : Glycogen concentration (mg COD_{GLY}/L)
X_{PAO} : PAO concentration (mg COD_X/L)
X_{PP} : PolyP concentration (mg P/L)

2. <u>AEROBIC polyP STORAGE</u>

This process described the orthophosphate uptake from the medium to be stored as polyphosphate [eq. VII.A5]. This energy required for this process is obtained from PHA oxidation.

$$Y_{PHA}CH_{1.5}O_{0.5} + H_3PO_4 + Y_{PHA}O_2 \Rightarrow HPO_3 + \frac{Y_{PHA}}{8\cdot\nu_p}CO_2 \qquad \text{(VII.A5)}$$

where Y_{PHA}: g COD_{PHA} oxidised/ g P taken up

The kinetics of this process is defined with expression VII.A6, where the process rate is limited by a lack of any of the three substrates and by an excess of polyP in the biomass. Experiments developed showed that the maximum amount of phosphorus in the biomass

observed in bio-P sludge is around 30 % on mass basis (Wentzel *et al.*, 1990). Similarly, ASM2 predicts of value of 0.34 g P/g PAO (Henze *et al.*, 2000).

$$r_{PP\_STORAGE} = q_{PP} \cdot \frac{S_{PO4}}{K_{PS} + S_{PO4}} \cdot \frac{X_{PHA}/X_{PAO}}{K_{PHA\_P} + X_{PHA}/X_{PAO}} \cdot \frac{K_{MAX} - X_{PP}/X_{PAO}}{K_{IPP} + K_{MAX} - X_{PP}/X_{PAO}} \cdot \frac{S_O}{K_O + S_O} X_{PAO} \quad \text{(VII.A6)}$$

where K_{IPP} : Kinetic constant for the X_{PP} storage process (g COD_{PHA}/ g COD_X)
K_{MAX} : Maximum X_{PP}/X_{PAO} ratio (g COD_{PHA}/ g COD_X)
K_O : oxygen affinity constant (mg O_2/L)
K_{PHA_P} : Affinity constant for X_{PHA}/X_{PAO} in X_{PP} storage process (g COD_{PHA}/ g COD_X)
K_{PS} : Orthophosphate affinity constant (mg P/L)
q_{PP} : maximum X_{PP} storage rate (1/d)
S_O : dissolved oxygen concentration (mg O_2/L)
S_{PO4} : Orthophosphate concentration (mg P/L)
X_{PHA} : PHA concentration (mg COD_{PHA}/L)

3. AEROBIC GLYCOGEN STORAGE

This expression was added from scratch to the model since ASM2 did not consider glycogen economy. The stoichiometry of this process for acetate was described by Smolders *et al.*, (1994a) as:

$$\frac{4}{3} CH_{1.5}O_{0.5} + \frac{5}{6} ATP + \frac{5}{6} H_2O \Rightarrow CH_{10/6}O_{5/6} + \frac{1}{3} CO_2 + NADH_2 \quad \text{(VII.A7)}$$

As can be observed, PHB was the carbon source for glycogen production. However, some energy was needed (i.e. ATP). This energy came from the PHB oxidation, which the Smolders *et al.* (1994a) considered as an extra equation. In this thesis, these two equations were gathered in the same expression:

$$CH_{1.5}O_{0.5} + (1 - Y_{GLY3})O_2 \Rightarrow Y_{GLY3} CH_{10/6}O_{5/6} + \frac{1 - Y_{GLY3}}{8\nu_P} CO_2 \quad \text{(VII.A8)}$$

where Y_{GLY3} was the g COD_{GLY} produced for g COD_{PHA} used.

The kinetics of this process is described in equation VII.A9, where the process rate is limited by a lack of any of the two substrates and by an excess of glycogen in the biomass. The kinetics of glycogen storage process consists of typical product saturation kinetics as described in Filipe and Daigger (1999).

$$r_{GLY\_STORAGE} = q_{GLY} \cdot \left(X_{GLY}^{MAX} - X_{GLY}/X_{PAO} \right) \cdot \frac{X_{PHA}/X_{PAO}}{K_{PHA} + X_{PHA}/X_{PAO}} \cdot \frac{S_O}{K_O + S_O} \cdot X_{PAO} \quad \text{(VII.A9)}$$

where q_{GLY} : maximum glycogen storage rate (1/d)
X_{GLY}^{MAX} : maximum X_{GLY}/X_{PAO} ratio (g COD_{GLY}/ g COD_X)

4. PAO GROWTH

The PAO growth process requires PHA as carbon and energy source likewise the glycogen restoration process. According to the model of Smolders *et al.* (1994a,b), the metabolic stoichiometry of this process is [eq. VII.A10]:

$$1.27CH_{1.5}O_{0.5} + 0.2NH_3 + \left(K + \frac{m_{ATP}}{\sigma}\right)ATP + 0.385H_2O + 0.015H_3PO_4 \Rightarrow CH_{2.09}O_{0.54}N_{0.2}P_{0.015} + 0.27CO_2 + 0.615NADH_2 \quad \text{(VII.A10)}$$

where K is the amount of ATP needed for the formation of biomass precursors from acetylCoA and polymerisation of these precursors to 1 C-mol of biomass (K=1.5 mol ATP/C-mol biomass)
m_{ATP} is the specific ATP consumption for maintenance purposes
σ is the growth rate.

As describe above, this process was linked with PHA oxidation through the next equation:

$$\frac{1}{Y_{PAO}}CH_{1.5}O_{0.5} + i_{NB}NH_3 + \left(H_2O + i_{PB}H_3PO_4 \Rightarrow CH_{2.09}O_{0.54}N_{0.2}P_{0.015} + \frac{1}{8}\left(\frac{1}{Y_{PAO}\cdot\nu_P} - 4\right)\frac{1}{\nu_X}\right)CO_2 \quad \text{(VII.A11)}$$

where i_{NB} and i_{PB} were the nitrogen and phosphorus content of the biomass (mass basis) respectively.
Y_{PAO} was the biomass yield in terms of g COD_{PAO} produced per g COD_{PHA} used.
ν_X = degree of reduction of biomass (4.5)

The kinetics of the process was described in equation VII.A12, where the process rate is limited by a lack of any of the three substrates, except for ammonia which was not considered in this model because ammonia concentration was high enough to avoid limitations during the experiments.

$$r_{PAO\_GROWTH} = \sigma_{PAO}\cdot\frac{S_{PO4}}{K_P + S_{PO4}}\cdot\frac{X_{PHA}/X_{PAO}}{K_{PHA} + X_{PHA}/X_{PAO}}\cdot\frac{S_O}{K_O + S_O}\cdot X_{PAO} \quad \text{(VII.A12)}$$

where σ_{PAO} : maximum PAO growth rate (1/d)

5. MAINTENANCE

The maintenance process of the model was used to describe the second P-release observed in all the batch experiments performed with both VFAs when these were completely depleted (see section VII.A.3.2). In fact, this release would take place during all the anaerobic period, but it could only be observed when the substrates were depleted or in the experiments performed without added VFA. When the VFA was still in the medium, this second release was lower than the usual P-release and, then, hidden by this latter. The stoichiometry of the process is the polyP being degraded to orthophosphate and the kinetics is described in expression VII.A13, where the process rate is limited by a lack of polyP. Moreover, a factor was included to prevent this process from occurring under aerobic conditions.

$$r_{MANT} = q_{MANT}\cdot\frac{X_{PP}/X_{PAO}}{K_{PHA} + X_{PP}/X_{PAO}}\cdot\frac{K_O}{K_O + S_O}\cdot X_{PAO} \quad \text{(VII.A13)}$$

where q_{MANT} : maximum maintenance rate (1/d)

6. LYSIS PROCESSES

The lysis processes ensure that the storage compounds decay together with the biomass. The stoichiometry of these processes was obtained from the ASM2 model. The products of the lysis were biodegradable compounds (Table VII.A1). The kinetics of these processes is commonly described with a constant rate multiplying the biomass fraction.

VII.A.2.3 SUMMARY OF THE EBPR MODEL IN MATRIX FORMAT

A description of this model is shown in Figure VII.A1 with a graphical representation, along with the kinetics and stoichiometry (Table VII.A1) and a brief description of the parameters (Table VII.A2).

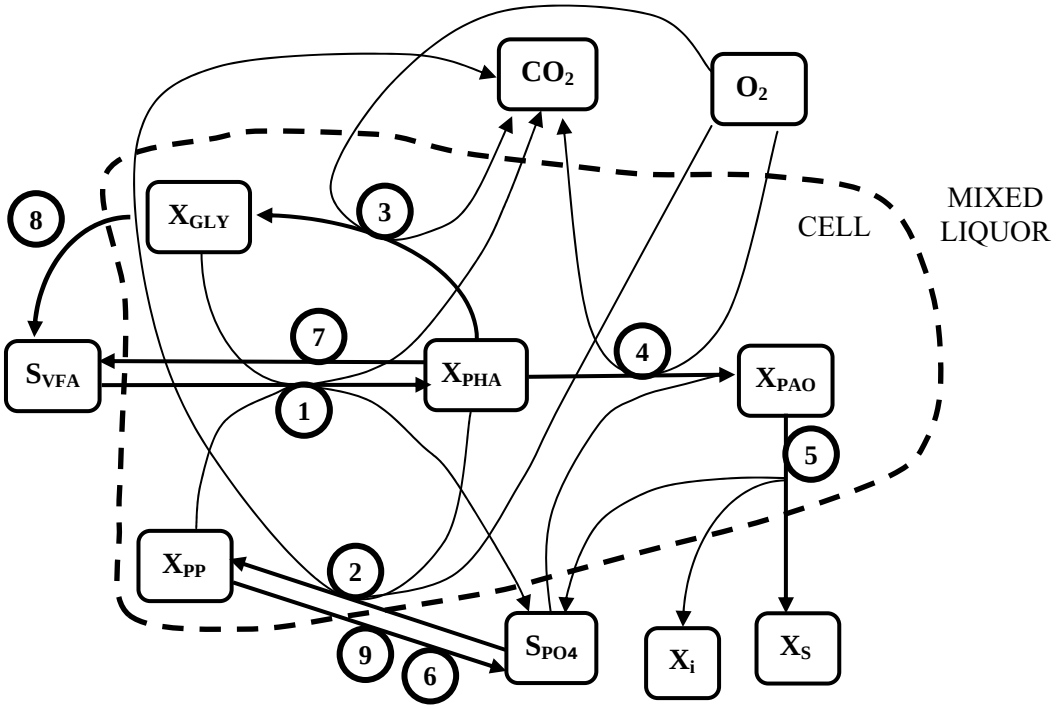

Figure VII.A1 Schematic diagram of the model used in this study (1-PHA storage, 2-Poly-P storage, 3-Glycogen storage, 4-PAO growth, 5- PAO lysis, 6- Poly-P lysis, 7- PHA lysis, 8- Glycogen lysis, 9-Anaerobic poly-P lysis for maintenance).

Table VII.A1 Stoichiometry of the EBPR model

	PROCESS	STOICHIOMETRY								
		S_S	S_{O2}	S_{PO4}	S_{CO2}	X_{PHA}	X_{GLY}	X_{PP}	X_{PAO}	X_I
		mg COD/L		mg P/L	mol/L	mg COD/L	mg COD/L	mg P/L	mg COD/L	mg COD/L
1	X_{PHA} storage	$-Y_{VFA}$		Y_{PO}	$\frac{1}{8}\cdot\left(\frac{Y_{AC1}}{\nu_A} - \frac{Y_{AC1}}{\nu_A} - \frac{1}{\nu_P}\right)$	1	$-Y_{GLY1}$	$-Y_{PO}$		
2	X_{PP} storage		$-Y_{PHA}$	-1	$\frac{Y_{PHA}}{8\nu_P}$	$-Y_{PHA}$		1		
3	X_{GLY} storage		$-(1-Y_{GLY3})$		$\frac{1 - Y_{GLY3}}{8\cdot\nu_P}$	-1	Y_{GLY3}			
4	X_{PAO} growth		$-\left(\frac{1 - Y_{PAO}}{Y_{PAO}}\right)$	$-i_{BPM}$	$\frac{1}{8}\left(\frac{1}{Y_{PAO}\cdot\nu_P} - \frac{1}{\nu_X}\right)$	$\frac{41}{Y_{PAO}}$			1	
5	X_{PAO} lysis			$\hat{I}_{5P}$				-1	$(1-f_{XI})$	f_{XI}
6	X_{PP} lysis			1				-1		
7	X_{PHA} lysis	1				-1				
8	X_{GLY} lysis	1					-1			
	Maintenance			1				-1		

Table VII.A2 Kinetics of the EBPR model

	PROCESS	KINETICS
1	X_{PHA} storage	$r_{VFA\_UPTAKE} = q_{PHA}\cdot\frac{S_{VFA}}{K_S + S_{VFA}}\cdot\frac{X_{PP}/X_{PAO}}{K_{PP} + X_{PP}/X_{PAO}}\cdot\frac{X_{GLY}/X_{PAO}}{K_{GLY} + X_{GLY}/X_{PAO}}\cdot X_{PAO}$
2	X_{PP} storage	$r_{PP\_STORAGE} = q_{PP}\cdot\frac{S_{PO4}}{K_{PS} + S_{PO4}}\cdot\frac{X_{PHA}/X_{PAO}}{K_{PHA\_P} + X_{PHA}/X_{PAO}}\cdot\frac{K_{MAX} - X_{PP}/X_{PAO}}{K_{IPP} + K_{MAX} - X_{PP}/X_{PAO}}\cdot\frac{S_O}{K_O + S_O}X_{PAO}$
3	X_{GLY} storage	$r_{GLY\_STORAGE} = q_{GLY}\cdot\left(X_{GLY}^{MAX} - X_{GLY}/X_{PAO}\right)\cdot\frac{X_{PHA}/X_{PAO}}{K_{PHA} + X_{PHA}/X_{PAO}}\cdot\frac{S_O}{K_O + S_O}\cdot X_{PAO}$
4	X_{PAO} growth	$r_{PAO\_GROWTH} = \sigma_{PAO}\cdot\frac{S_{PO4}}{K_P + S_{PO4}}\cdot\frac{X_{PHA}/X_{PAO}}{K_{PHA} + X_{PHA}/X_{PAO}}\cdot\frac{S_O}{K_O + S_O}\cdot X_{PAO}$
5	X_{PAO} lysis	$b_{PAO}X_{PAO}$
6	X_{PP} lysis	$b_{PP}X_{PP}$
7	X_{PHA} lysis	$b_{PHA}X_{PHA}$
8	X_{GLY} lysis	$b_{GLY}X_{GLY}$
9	Maintenance	$r_{MANT} = q_{MANT}\cdot\frac{X_{PP}/X_{PAO}}{K_{PHA} + X_{PP}/X_{PAO}}\cdot\frac{K_O}{K_O + S_O}\cdot X_{PAO}$

VII.A.3 Model calibration and validation

VII.A.3.1 EXPERIMENTAL SET-UP

Experiments were conducted in a SBR with a working volume of 1.8 litres, inoculated with activated sludge from an EBPR plant (Thornside Sewage Treatment Plant, Queensland, Australia). The experimental work of this chapter was performed in the Advanced Wastewater Management Center of the University of Brisbane. The experimental SBR system used will be named AWMC-SBR from this point on. This SBR was operated in 4 cycles of 6 h per day. Each cycle consisted of 2.5 h anaerobic react, 3 h aerobic react, 30 min settling and, in the last 5 min of settling, extraction of 900 mL supernatant. A volume of 900 mL of synthetic wastewater (Pijuan *et al.*, 2004a) was added during the first 7 min of the subsequent cycle, producing a hydraulic residence time (HRT) of 12 h. The sludge residence time (SRT) was kept at 9 d by periodic sludge wastage during the react phase. Since the pH was not controlled, it increased from 7.2 to 7.6 during the anaerobic react and it increased further to 8.5 during the aerobic react, due to the stripping of CO_2. The SBR operating temperature was 23-24ºC during all stages. To achieve anaerobic conditions, nitrogen gas was bubbled through the liquid and to achieve aerobic conditions, air was bubbled. Further information of the experimental set-up can be found in Pijuan *et al.,* (2004a).

The model was calibrated using acetate and propionate as carbon sources. The majority of studies on EBPR have been carried out using acetate as the sole carbon source or acetate in combination with other substrates. (Satoh *et al.,* 1992; Smolders *et al.,* 1994a,b; Mino *et al.,* 1994; Liu *et al.*, 1997: Bond *et al.,* 1999a ; Hood and Randall, 2001; Levantesi *et al*., 2002; Randall *et al.*, 2003). When acetate is used as the sole carbon source, the PHA produced is mostly PHB, whereas most PHA produced appears as PHV and PH2MV when propionate becomes the predominant carbon source (Satoh *et al.*, 1992; Lemos *et al.,* 1998; Randall and Liu, 2002).

The biomass used in this work was enriched in PAO using propionate as the sole carbon source. After three weeks, the amount of propionate was 140 mg/L at the beginning of the anaerobic phase, and this concentration was maintained until steady state was achieved. The abundance of "*Candidatus* Accumulibacter phosphatis" and "*Candidatus* Competibacter phosphatis" (from now on called *Accumulibacter* and *Competibacter*, respectively) was followed using fluorescence *in situ* hybridization (FISH) probing. After three SRTs (approximately 27 days), the reactor showed substantial P removal and the amount of PAOMIX-binding cells (*Accumulibacter*) rapidly increased from 7% of all bacteria on the 2nd day of operation to 54% of all bacteria on the 17th day of operation. During steady state operation of the SBR, when all cycle study experiments were carried out, 50-55% of all bacteria were *Accumulibacter* and they were presumed to be the dominant PAO. The inoculum for the SBR contained GAOMIX-binding cells (*Competibacter)*, and although their abundance could not be accurately quantified due to such low amounts, they probably comprised 1-2% of all bacteria. On the 17th day of operation, the abundance of *Competibacter* cells had dramatically declined to just a few cells every few fields observed microscopically, which would be substantially less than even 1% of all bacteria. After 6 weeks of operation, *Competibacter* cells were rarely observed in the biomass.

Hence, feeding the system with propionate improved the EBPR start-up in terms of favouring PAO growth against GAO. Hood and Randall (2001) hypothesised that propionate may be relatively easily sequestered and metabolised by PAO, but that it might not be readily utilisable by other microorganisms also requiring VFA in the anaerobic zone. Thomas *et al.* (2002) also provide evidence supporting the GAO competition for acetate and PAO competition for other substrates including propionate.

VII.A.3.2 CYCLE STUDIES WITH PROPIONATE AND ACETATE

After obtaining steady state in the SBR, two sets of cycle study experiments were conducted to assess the behaviour of the EBPR microbial community developed with propionate. The experiments were performed in the same SBR with the same operational conditions and also without pH control. Since cycle studies were generally conducted once per day, at least three 6-h SBR cycles with normal VFA concentration elapsed between each study. The first set of experiments was done with different propionate concentrations at the beginning of the cycle.

After the propionate cycle studies, a second set of cycle studies with acetate was conducted in the reactor. The acetate experiments spanned 5 days, during which the carbon source fed to the SBR was changed from 1.89 mmol propionate/L (196 mg COD/L) to 2.83 mmol acetate/L (187 mg COD/L). During this 5 day period, one cycle per day was used to study different acetate additions. All other SBR cycles were operated with 2.83 mmol acetate/L. The main reason for changing the SBR operating carbon source was to explore the acclimation of the biomass to acetate. After these 5 days, acetate was changed back to propionate in order to return to the original operating conditions of the SBR. In the first SBR cycle with acetate (1.42 mmol C/g VSS), the propionate-enriched biomass was able to use acetate immediately for EBPR. The observed acetate uptake rate did not change remarkably during the 5 days of acetate operation. Hence, it can be deduced that no acclimation period was required.

Figure VII.A2-left depicts the results of the cycle studies performed with different initial concentrations of propionate. During these cycle studies, the anaerobic P-release (mmol P/g VSS) increased with increasing propionate concentration in the feed, but the concomitant aerobic P-uptake for the two higher propionate concentrations employed was not complete. The aerobic P-uptake presented for the normal SBR operating concentration (1.35 mmol propionate/g VSS) was complete after 2 h of aerobiosis.

Figure VII-A2-right depicts the results of the cycle studies performed with different initial concentrations of acetate. During these cycle studies, the anaerobic P-release (mmol P/g VSS) increased with increasing acetate concentration in the feed. The following aerobic P-uptake was complete, with the only exception of the highest acetate concentration. When the SBR operation employed 1.42-1.96 mmol C/g VSS, the aerobic P-uptake was complete after approximately 2 h of aerobiosis.

In addition, ammonia was measured during all the experiments conducted with propionate (Fig. VII.A3-left) and acetate (Fig. VII.A3-right). An increase of ammonia was detected in all the experiments during the anaerobic period likely due to hydrolysis of the organic nitrogen from peptone to ammonia by the microorganisms. The diminution of ammonia in aerobic conditions could not be assigned to nitrification since nitrate was not detected in the reactor. Therefore, the biomass consumed the ammonia for growth, supporting the metabolic models declaring PAO growth under aerobic conditions.

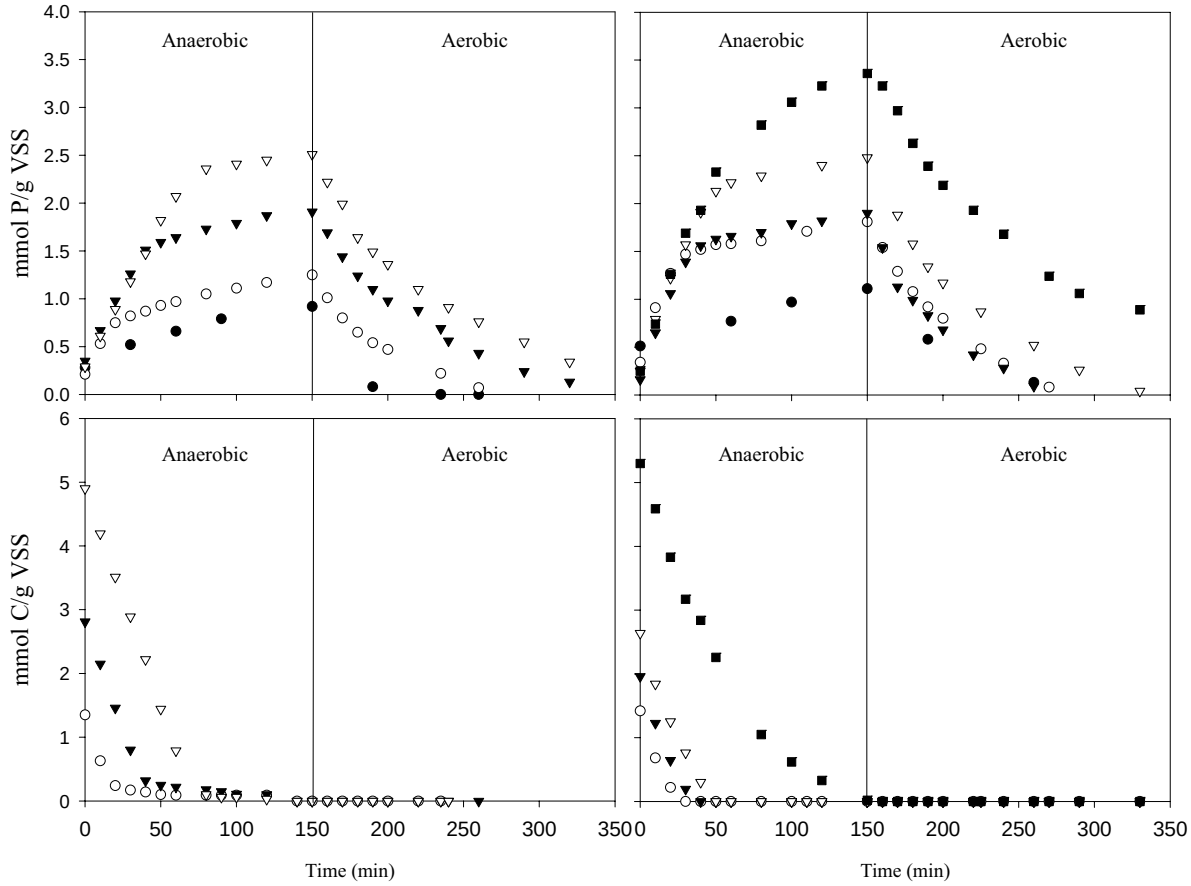

Figure VII.A2. Experimental profiles of the acetate and propionate cycles.
PROPIONATE : Up-left (phosphorus profile), Down-left (propionate profile): ħ 0 mmol C/g VSS, ƺ 1.35 mmol C/g VSS, ƛ 2,81 mmol C/g VSS, ⊆ 4.90 mmol C/g VSS .
ACETATE : Up-right (phosphorus profile), Down-right (acetate profile): ħ 0 mmol C/g VSS, ƺ 1.42 mmol C/g VSS, ƛ 1.96 mmol C/g VSS, ⊆ 2.64 mmol C/g VSS, ƴ 5.30 mmol C/g VSS.

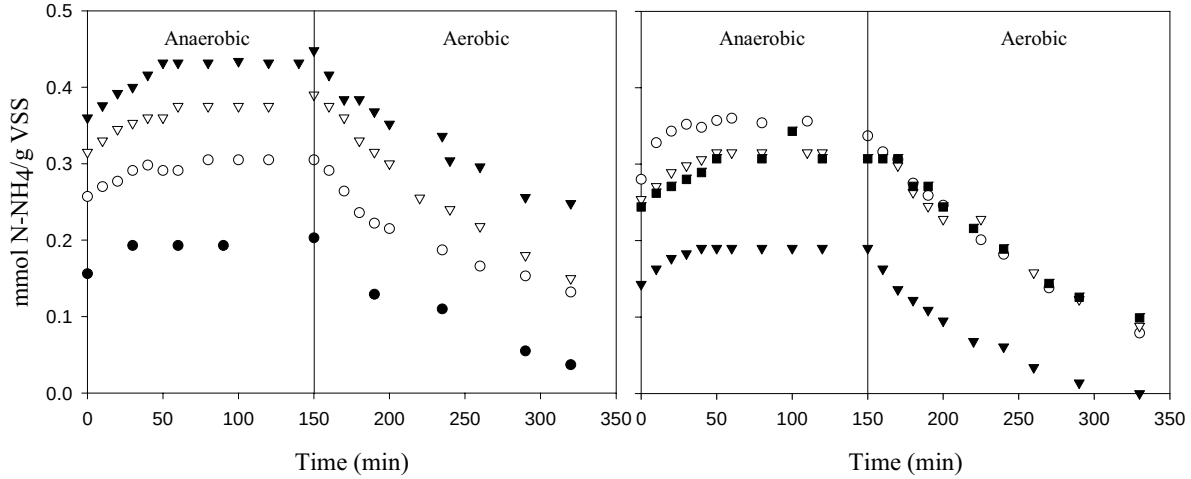

Figure VII.A3. Experimental ammonia profiles of the acetate and propionate cycles.
PROPIONATE - Left ħ 0 mmol C/g VSS, ƺ 1.35 mmol C/g VSS, ƛ 2,81 mmol C/g VSS, ⊆ 4.90 mmol C/g VSS . ACETATE - right ħ 0 mmol C/g VSS, ƺ 1.42 mmol C/g VSS, ƛ 1.96 mmol C/g VSS, ⊆ 2.64 mmol C/g VSS, ƴ 5.30 mmol C/g VSS.

VII.A.3.3 PARAMETER ESTIMATION RESULTS

Experiments VII.A1 and VII.A2 (Tables VII.A1 and VII.A2) were conducted to calibrate the model for each different carbon source. The experimental results together with the model fits are depicted on Figure VII.A4 and VII.A5, respectively. The model was calibrated using propionate, PHA, glycogen and phosphorus as output variables. Not all the model parameters were estimated due to identifiability and some of them were assumed from the literature.

Table VII.A3 Experiment VII.A1

EXPERIMENT VII.A1	Calibration using propionate as the sole carbon source
Equipment	AWMC-SBR
pH	7.2-7.6
Temperature	23-24 ºC
Pulses	4.9 mmol C/ g VSS

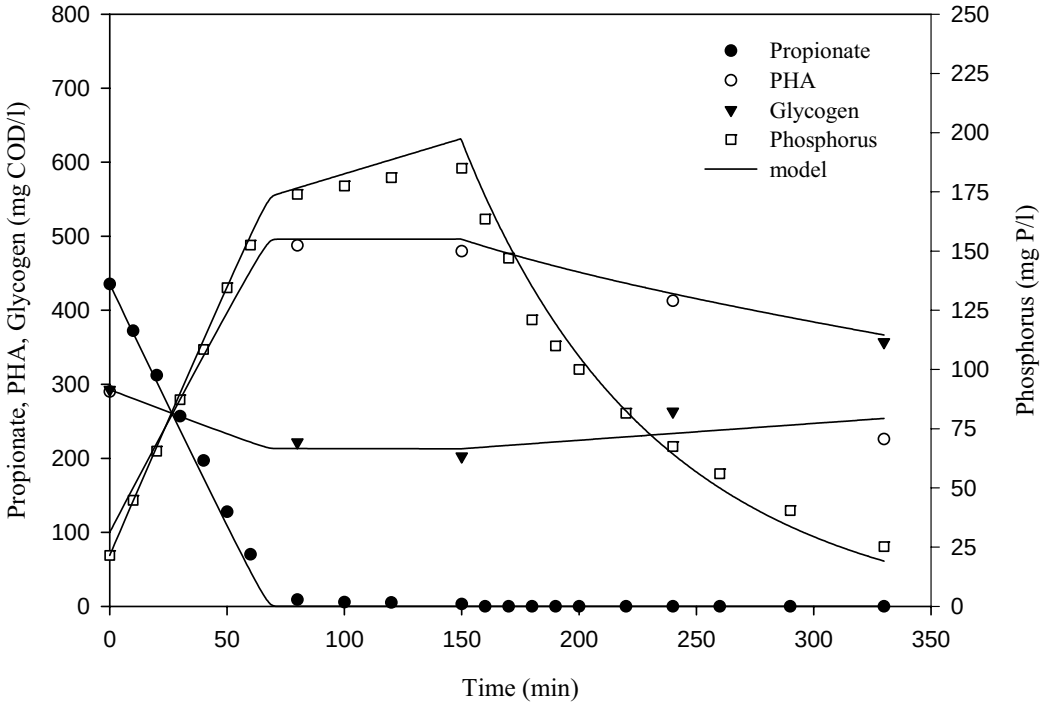

Figure VII.A4 Experimental measures and simulated values for experiment VII.A1 Ž Phosphorus, ƀ VFA, ƍ Glycogen, ƒ PHA, — fitted model

The estimated parameters were: Y_{VFA}, Y_{PO}, q_{PHA}, q_{PP}, K_{PHA_P}, q_{GLY} and $\sigma_{PAO.}$ Similarly to previous models, the active fraction of the PAO in the system could not be estimated with short-term experiments. Hence, its value was lumped in the maximum rate constants estimation. The parameter estimation results for propionate and acetate are shown on Table VII.A5. The parameters in bold are the parameter which were estimated with the experimental results. The parameter estimation values are compared with the values proposed in ASM2, except for the values related to processes including glycogen.

Table VII.A4 Experiment VII.A2

EXPERIMENT VII.A2	Calibration using acetate as the sole carbon source
Equipment	AWMC-SBR
pH	7.2-7.6
Temperature	23-24 ºC
Pulses	1.96 mmol C/ g VSS

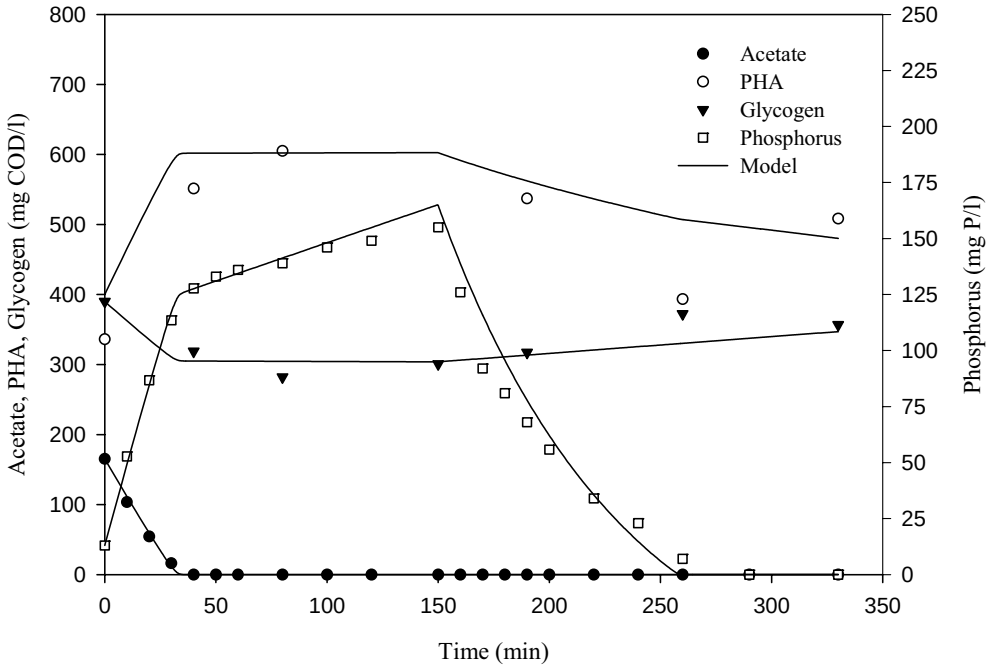

Figure VII.A5 Experimental measures and simulated values for experiment VII.A2. Ž Phosphorus, ƀ VFA, ƍ Glycogen, ƶ PHA, — fitted model

Table VII.A5 Value and description of the parameters of the model and comparison with the ASM2 parameters.

Process	Parameter	ASM2	Propionate	Acetate	Units
1	$\mathbf{Y_{VFA1}}$	1	1.1	0.82	g COD_{VFA}/g COD_{PHA}
1	$\mathbf{Y_{PO}}$	0.4	0.33	0.55	g P/g COD_{PHA}
1	Y_{GLY1}	-	0.2	0.42	g COD_G/g COD_{PHA}
2	Y_{PHA}	0.2	0.2	0.2	g COD_{PHA}/g P
3	Y_{GLY3}	-	1.0 **	1.0 **	g COD_G/g COD_{PHA}
4	i_{BPM}	0.02	0.02	0.02	g P/g COD_X
4	Y_{PAO}	0.625	0.625	0.625	g COD_X/ g COD_{PHA}
5	τ_{5P}	0.01	0.01	0.01	g P/ g COD_X
5	f_{XI}	0.1	0.1	0.1	g COD_I/ g COD_X
1	$\mathbf{q_{PHA}}$	*	5.76	5.76	g COD_{PHA}/ g COD_X/ d
1	K_S	4	4	4	mg COD_{VFA} / L
1,9	K_{PP}	0.0075	0.0075	0.0075	g P/ g COD_X
1	K_{GLY}	-	1e-3 **	1e-3 **	g COD_G /g COD_X
2	$\mathbf{q_{PP}}$	1.5	3.64	4.07	g P/ g COD_X/ d
2	K_{PS}	0.2	0.2	0.2	mg P/L
2	$\mathbf{K_{PHA\_P}}$	*	0.133	0.133	g COD_{PHA}/ g COD_X
2	K_{MAX}	0.255	0.255	0.255	g P/ g COD_X
2	K_{IPP}	0.015	0.015	0.015	g P/ g COD_X
2,3,4,9	K_O	0.20	0.20	0.20	mg OD/L
3	$\mathbf{q_{GLY}}$	-	5.00	5.00	g COD_G/ g COD_X/ d
3	X_{GLYMAX}	-	0.28 ***	0.28 ***	g COD_G/ g COD_X
3,4	K_{PHA}	0.0125	0.0125	0.0125	g COD_{PHA}/ g COD_X
4	$\mathbf{\sigma_{PAO}}$	1.0	0.50	0.50	1/d
4	K_P	0.01	0.01	0.01	mg P/L
5	b_{PAO}	0.2	0.2	0.2	1/d
6	b_{PP}	0.2	0.2	0.2	1/d
7	b_{PHA}	0.2	0.2	0.2	1/d
8	b_{GLY}	0.2	0.2	0.2	1/d
9	q_{MANT}	0.29	0.29	0.29	g P/ g COD_X/ d

* These values of ASM2 parameters are not comparable to the ones obtained in this work, since the kinetics of the process are based on different approaches.
** Manga *et al.* (2001) *** Filipe and Daigger (1999)

Once the model was calibrated, experiments VII.A3 and VII.A4 (Table VII.A6) were conducted to validate the parameter estimation results obtained in the calibration experiments. Figure VII.A6 (A and B) shows one example of this validation for each VFA. The validation experiments showed that this model could give an accurate description of the behaviour of the different compounds involved in the process for each VFA used.

Table VII.A6 Experiment VII.A3 and VII.A4

EXPERIMENT VII.A3, A4	Validation of the parameter estimation results for both the acetate and the propionate
Equipment	AWMC-SBR
pH	7.2-7.6
Temperature	23-24 ºC
Pulses	1.35 mmol C/ g VSS (propionate)
Pulses	1.42 mmol C/ g VSS (acetate)

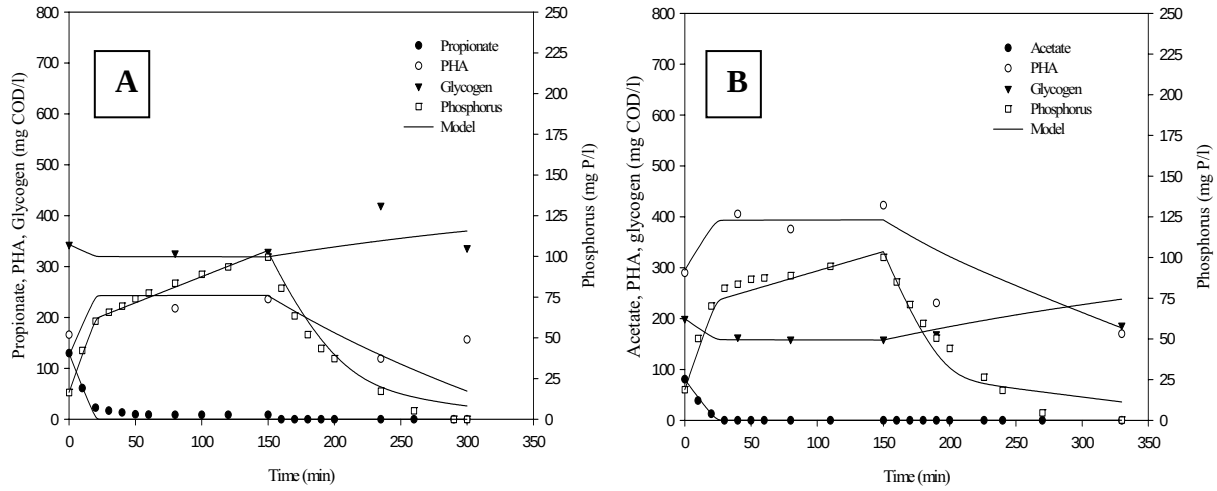

Figure VII.6 Cycle studies used for model validations. **A** - Experimental measures and simulated values for propionate cycle study (1.35 mmol C / g VSS). **B** - Experimental measures and simulated values for acetate cycle study (1.42 mmol C / g VSS). (Ž Phosphorus, ƀ VFA, ξ Glycogen, ε PHA, — model prediction)

VII.A.3.4 DISCUSSION OF THE PARAMETER ESTIMATION VALUES

The parameter estimation results of the experiments performed using the two different VFAs showed some differences between them:

1. PHA storage process

One of the most significant stoichiometric parameters was Y_{VFA}, which described the amount of VFA uptaken per PHA stored. The values obtained were 1.1 g COD_{VFA}/g COD_{PHA} for propionate and 0.82 g COD_{VFA}/g COD_{PHA} for acetate. The Y_{VFA} for acetate was smaller than the one for propionate, which meant that the amount of PHA produced per substrate COD unit was higher for acetate. Table VII.A7 shows that this results agreed with the experimental values presented in the literature as well as with the theoretical results (i.e. deduced from a metabolic model) presented by Smolders *et al.* (1994a) and Oehmen *et al.* (2005). Chen *et al.* (2002) argued that as there was less glycogen consumption when propionate was used, more propionate has to be consumed to produce the same amount of PHA.

As can be observed, the values obtained in this work were somehow higher than the ones proposed in the literature. The most probable reason was that some of the PHA fractions which were important such as PH2MV or even poly-η-hydroxy-2-methylbutyrate

(3H2MB) were not measured in these experiments. Hence, less PHA production and higher yields were calculated. However, it can be argued that probably some of the previous works shown on Table VII.A7 did not measure these compounds. It has to be noted that these works used biomass enriched with acetate as the sole carbon source and PHB production was more favoured than in the case of this thesis where biomass was enriched with propionate and switched to acetate only for a week. In any case, the experimental results obtained in this thesis coincided showed that the Y_{VFA} value for propionate is 33 % higher than the one for acetate. This ratio is very similar to the one obtained using the theoretical ratios of Smolders *et al.* (1994a) and Oehmen *et al.* (2005).

Table VII.A7 Comparison of the substrate uptake yields with biographical values

Reference	Substrate	mol C_{VFA}/ mol C_{PHA}	g COD_{VFA}/ g COD_{PHA}
BIOCHEMICAL MODELS			
Smolders *et al.* (1995)	Acetate	0.75	0.67
Wentzel *et al.* (1991)	Acetate	0.75	0.67
Mino *et al.* (1987)	Acetate	0.75	0.67
Oehmen *et al.* (2005)	Propionate	0.81	0.88
EXPERIMENTAL RESULTS			
Satoh *et al.* (1992)	Acetate	0.77	0.68
Satoh *et al.* (1992)	Propionate	0.83	0.87
Liu *et al.* (1997)	Acetate	0.77-0.85	0.68-0.75
Bond *et al.* (1999a)	Acetate	0.73	0.65
Filipe *et al.* (2001b)	Acetate	0.77	0.68
Manga et al. (2001)	Acetate	-	0.75
Randall *et al.* (2003)	99 % Ac 1% Prop.	0.69	
Randall *et al.* (2003)	38 % Ac 62 % Prop.	0.97	
Yagci *et al.* (2003)	Acetate	0.59	0.53
This thesis: Y_{VFA}	Acetate	-	0.82
This thesis: Y_{VFA}	Propionate	-	1.1

Table VII.8 shows the mean rates of phosphorus release, substrate and phosphorus uptake, and the ratios calculated in experiments VII.A1 and VII.A2. As can be observed, acetate uptake was more rapid than propionate uptake in terms of mmol VFA uptaken/g VSS min. However, these molecules have different number of carbon moles and when converted to mmol C uptaken/g VSS min, the VFA uptake rate was very similar for propionate and acetate. Hence, the maximum rate of substrate uptake in both cases is very similar if the number of carbons of each specie is considered.

Table VII.A8 shows the mean rates of phosphorus release, substrate and phosphorus uptake, and the ratios calculated in experiments VII.A1 and VII.A2.

Parameters average	Propionate experiments	Acetate experiments
Phosphorus release rate * (mmol P/g VSS min)	0.0274 ∂ 0.0016	0.0427 ∂ 0.0026
VFA uptake rate (mmol C/g VSS min)	0.0622 ∂ 0.0065	0.0604 ∂ 0.0015
VFA uptake rate (mmol VFA/g VSS min)	0.0198 ∂ 0.0011	0.0288 ∂ 0.0015
P release/VFA uptake (mmol P/mmol VFA)	1.33 ∂ 0.18	1.40 ∂ 0.11
P release/ C uptake* (mmol P/mmol C)	0.46 ∂ 0.03	0.72 ∂ 0.04
Phosphorus uptake rate ** (mmol P/g VSS min)	0.0120 ∂ 0.0001	0.0154 ∂ 0.0016

* Values calculated when there was substrate in the mixed liquor.
** Values calculated without using the cycle study without substrate.

The phosphate released per PHA stored (Y_{PO}) also differed when propionate or acetate were used as sole carbon sources (0.33 g P/g COD_{PHA} with propionate and 0.50 g P/g COD_{PHA} with acetate). These values indicated that more phosphate is released to produce the same amount of PHA with acetate (in mass basis). The results of this study contrasted with some of those reported in the literature (Hood and Randall, 2001) where the experiments performed with propionate showed a higher P-release than with acetate. In any case, Table VII.A9 compares these values with the values presented in the literature. As can be observed, the biochemical models also predict a higher P release in the case of acetate. In addition, the values of Y_{PO} found in this work are again somehow higher than the ones found in the literature. Again, a possible underestimation of the PHA produced as abovementioned may be the reason.

Table VII.A9 Comparison of the phosphorus release values with biographical values

Reference	Substrate	mol P/ mol C_{PHA}	g P/ g COD_{PHA}
BIOCHEMICAL MODELS			
Smolders et al. (1995)	Acetate	0.37	0.32
Wentzel *et al.* (1991)	Acetate	0.33	0.28
Mino *et al.* (1987)	Acetate	0.5	0.43
Oehmen et al. (2005)	Propionate	0.34	0.29
EXPERIMENTAL RESULTS			
Satoh et al. (1992)	Acetate	0.33	0.28
Satoh et al. (1992)	Propionate	0.27	0.23
Filipe et al. (2001b)	Acetate	0.44	0.38
Bond et al. (1999a)	Acetate	0.34	0.29
Liu et al. (1997)	Acetate	0.47-0.49	0.4-0.421
Randall et al. (2003)	99 % Ac 1% Prop.	0.29	
Randall et al. (2003)	38 % Ac 62 % Prop.	0.33	
Yagci *et al.* (2003)	Acetatte	0.46	0.39
ASM2	Any		0.4
This thesis: Y_{PO}	Acetate	-	0.5
This thesis: Y_{PO}	Propionate	-	0.33

On the other hand, the P-release per VFA taken up (in molar basis) for propionate (1.33) was very similar to the results obtained in the case of acetate (1.40) as shown in Table VII.A8. The highest P-release detected with acetate (in terms of C-mmol) agreed with Liu *et al.* (2002). This observation could indicate that the same amount of ATP was required to convert propionate to propionyl-CoA (3 carbons) as was required to convert acetate to acetyl-CoA (2 carbons). Hence, more energy could be required per C-mol to convert acetate to acetyl-CoA than to convert propionate to propionyl-CoA. This difference in energy requirement could also be related to the fact that each substrate produces different fractions of PHB, PHV or PH2MV in the PHA. Another hypothesis would be that acetate transfer from the exterior is more energy-expensive than propionate. However, such detailed metabolic explanations are beyond the scope of this thesis.

The results obtained for glycogen degraded per PHA stored (Y_{GLY1}) were also quite different when propionate or acetate was used. A value of 0.20 g COD_{GLY}/g COD_{PHA} was obtained for propionate, while 0.42 was obtained for acetate. These values indicated that less amount of reducing power is required to store propionate than acetate, which is in agreement with the values obtained comparing the metabolic models of Smolders *et al.*, (1994a) and Oehmen *et al.*, (2005). Hood and Randall (2001) summarised the $NADH_2$ production of probable pathways for PHA biosynthesis and they found that less reducing power is required to store propionate, which is in agreement with the results of this work. There was a greater need for reducing equivalents to convert acetate to PHB than to convert propionate to PHV and/or PH2MV, which are respectively PAOs normal PHA storage compounds. Table VII.A10 compares these values when some experimental and theoretical values of the literature and again the value obtained for acetate seems a bit higher probably for a PHA production underestimation.

Table VII.A10 Comparison of the glycogen degradation values with biographical values

Reference	Substrate	mol C_{GLY}/ mol C_{PHA}	g COD_{GLY}/ g COD_{VFA}
BIOCHEMICAL MODELS			
Smolders *et al.* (1995)	Acetate	0.375	0.33
Wentzel *et al.* (1991)	Acetate	0.375	0.33
Mino *et al.* (1987)	Acetate	0.375	0.33
Oehmen *et al.* (2005)	Propionate	0.26	0.23
EXPERIMENTAL RESULTS			
Satoh *et al.* (1992)	Acetate	0.46	0.41
Satoh *et al.* (1992)	Propionate	0.31	0.28
Filipe *et al.* (2001b)	Acetate	0.38	0.34
Bond *et al.* (1999a)	Acetate	0.49	0.43
Manga *et al.* (2001)	-		0.25
Liu *et al.* (1997)	Acetate	0.33	0.29
Randall *et al.* (2003)	99 % Ac 1% Prop.	0.15	
Randall *et al.* (2003)	38 % Ac 62 % Prop.	0.02	
Yagci *et al.*, (2003)	Acetate	0.375	0.33
This thesis: Y_{GLY1}	Acetate	-	0.42
This thesis: Y_{GLY1}	Propionate	-	0.2

2. Second P-release

During the anaerobic period, phosphorus was released at two different rates with both VFA. The first rate took place when the VFA was present in the mixed liquor. The second P-release, slower than the first one, was detected after the VFA depletion. The second P-release rates seemed to be independent of the initial VFA concentration according to the experimental results (Table VII.A11). Similar second P-release rates were obtained with different initial concentrations of VFA including that measured with no added VFA. These rates were about one order of magnitude lower than P-release rates when VFA was still present. Moreover, both cycle studies performed without VFA addition demonstrated P-release could occur without any VFA consumption (Fig. VII.A2).

Table VII.A11 Second P-release rates

	VFA concentrations during cycle studies (mmol C/g VSS)				
ACETATE	0	1.42	1.96	2.64	5.30
Second release rate (mmol P/g VSS min)	0.0040	0.0029	0.0033	0.0040	**
PROPIONATE	0	1.35	2.81	4.90	
Second release rate (mmol P/g VSS min)	0.0046	0.0035	0.0035	0.0021	

** not observed experimentally

The observed second P-release could be explained with the hypothesis that PAO used their intracellular polyP to generate energy for maintenance purposes. An alternative hypothesis could be that the microorganisms were using substrates other than propionate such as peptone or yeast extract for their P-release. The SBR medium contained peptone at levels slightly higher than those typically used by other researchers (Bond *et al.* 1999a; Smolders *et al.* 1994a; Zeng *et al.* 2003).

Barnard (1984) first described this second P-release in the anaerobic zone after VFA removal. Smolders *et al.* (1995) introduced a maintenance parameter in their anaerobic metabolic model of 0.0013 mmol P/g VSS min, which was almost three times lower than that obtained in this thesis, either with propionate or acetate. However, no further comment is made about this fact in their work and, moreover, it is mostly absent in other EBPR literature. In this thesis, the secondary P-release measured could not be neglected since it was equivalent to 18% of the total amount of P-released under anaerobic conditions.

The kinetic parameter linked to this second P-release in the model was the maintenance rate constant (q_{MANT}) which was the same for both VFA (0.29 gP/g COD_X/d), since the type of VFA seemed not to affect this release. This finding could support for the hypothesis that PAO were using peptone in the medium for P-release, since this component was common to both experiments.

3. Aerobic values

The only kinetic parameter different for both VFA in the aerobic phase was the Poly-P storage rate constant (q_{PP}). The value obtained for acetate (4.07 g P / g COD_X /d) was higher than the one obtained for propionate (3.64 g P / g COD_X /d). As suggested Randall and Liu (2002), this P-uptake can be influenced by the PHA composition at the beginning of the aerobic phase. The hypothesis that higher PHB percentages imply higher P-uptake agrees with the experimental results of this work.

Chapter VII.A - Conclusions

- An EBPR model, developed as a modification of ASM2 and including glycogen economy, described successfully anaerobic-aerobic batch tests with acetate and propionate as the sole carbon source.

- When propionate and acetate were used as carbon sources for EBPR, PAOs demonstrated similar anaerobic VFA-uptake rates (mmol C/g VSS min), The major differences observed between both carbon sources are that the amount of PHA produced per substrate COD unit was higher for acetate, more phosphate is released to produce the same amount of PHA with acetate (in mass basis), the P-release per VFA taken up (in molar basis) for propionate (1.33) was very similar to the results obtained in the case of acetate (1.40) and that less amount of reducing power is required to store propionate than acetate

- A remarkable second P-release possibly linked to PAO maintenance or to use of peptone as a carbon source is reported. It was only detectable after the VFA substrate was exhausted but it probably occurred throughout the anaerobic period.

- A maintenance reaction is added in order to explain the second P-release detected in the experiments.

- When fitted to experimental data, the model presented in this study gives a good prediction of the behaviour of the EBPR systems for either propionate or acetate and the parameter estimation values obtained are in agreement with the results in the literature.

CHAPTER VII.B

Improving an EBPR system start-up using OUR and HPR: a simulation study

Part of this chapter has been published as:

Improving the start-up of an EBPR system using OUR to control the aerobic phase length: a simulation study (2005). A. Guisasola, M. Pijuan, J.A. Baeza, J. Carrera, J. Lafuente. Proceedings of 2nd IWA Conference on Instrumentation, Control and Automation for Water and Wastewater Treatment and Transport System. Pusan.South Korea, 2005.

ABSTRACT

This chapter is a simulation study to test possible new control strategies to improve an Enhanced Biological Phosphorus Removal (EBPR) system start-up in a Sequencing Batch Reactor (SBR). This study is conducted using the EBPR model presented in Chapter VII.A. The conceptual basis of this improvement is that both the anaerobic and aerobic phases could be shortened without any negative effect on the process of enriching the biomass with Polyphosphate Accumulating Organisms (PAO). Both the anaerobic and the aerobic phases can be reduced according to the Volatile Fatty Acids (VFA) and orthophosphate profiles, respectively. These improvements, though verified by simulation to be successful, require good on-line VFA and orthophosphate sensors. To avoid this technical limitation, a link between these compounds and more habitual measurements such as H^+ Production Rate (HPR) and Oxygen Uptake Rate (OUR) is proposed in this chapter. This link allows the development of an efficient and practical control strategy which is also verified by simulation.

VII.B.1 Conceptual basis of the improvement

VII.B.1.1 PROBLEM STATEMENT

EBPR is based on the enrichment of activated sludge with PAO, which are scarce in a conventional non-EBPR WWTPs, the most frequent plants nowadays. An EBPR start-up commonly consists of inoculating a pilot plant with biomass withdrawn from a conventional WWTP and subjecting it under classical anaerobic/ aerobic conditions. Then, after certain period of time (i.e. some SRTs) the population (enriched in PAO) becomes able to remove biologically phosphorus in a successful way. Hence, the start-up of EBPR systems from conventional WWTP sludge becomes slow and complex because of the low PAO fraction at the *inoculum* sludge and may last from one to three months. Hence, scientists should put some effort in finding new start-up strategies to reduce its length by favouring PAO growth.

The aim of this chapter is to reduce the start-up length of EBPR systems by improving its efficiency. As it is a simulation study, a conventional EBPR system in a SBR was modelled. Then, the start-up of this system was simulated using different control strategies that shortened the cycle to the strictly necessary length. Both the anaerobic and the aerobic phases could be reduced according to the VFA and orthophosphate profiles by omitting periods where PAO were not favoured. The objective function to evaluate the possible start-up improvement was the PAO fraction in the biomass after 30 days of start-up.

Experiment VII.B1 (Table VII.B1) consists of a typical EBPR anaerobic-aerobic cycle with two hours of anaerobic phase and three hours of aerobic phase. It was conducted to illustrate the conceptual basis of the control strategies proposed in this chapter. Figure VII.B1 shows the experimental profiles obtained.

Table VII.B1 Experiment VII.B1

EXPERIMENT VII.B1	EBPR cycle experiment
Equipment	EBPR-SBR (10 L)
pH	7.0
Temperature	25 ºC
Acid used	HCl = 1 M
Pulses	260 mg COD_{VFA}/L (acetate)

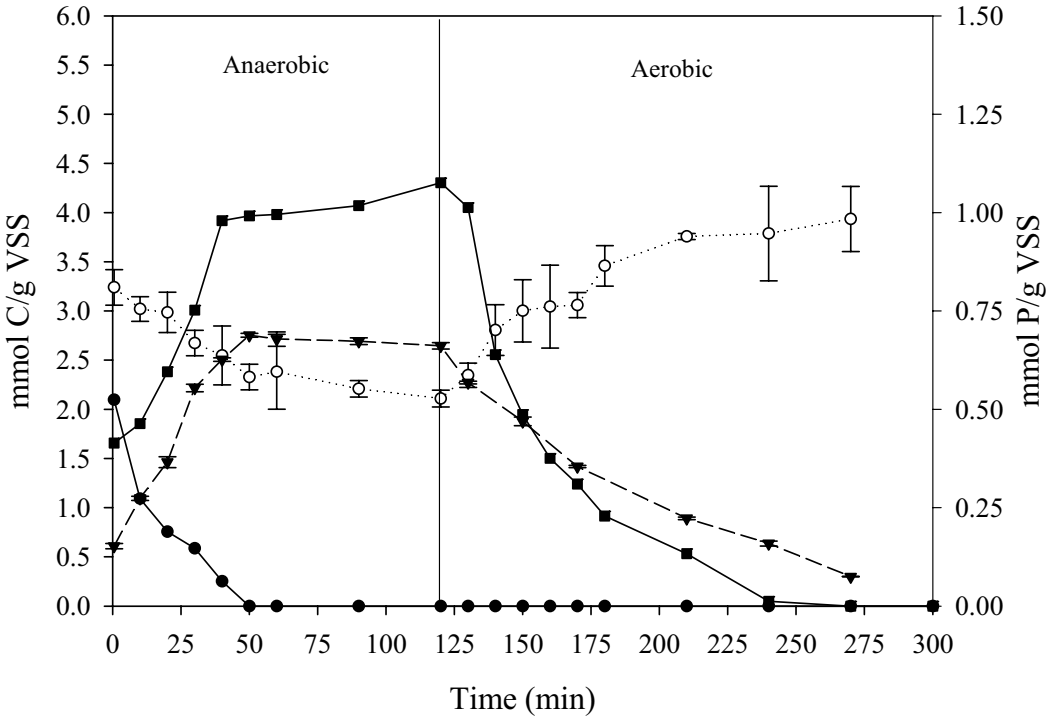

Figure VII.B1 Experimental profiles of the different compounds during experiment VII.B1 (♦) VFA -acetate, (▽) phosphorus, (■) glycogen, (○) PHB.

Under anaerobic conditions, PAO take up VFA and store them as PHA, while the degradation of intracellular glycogen provides reducing equivalents (Mino *et al.* 1987, Smolders *et al*., 1995). The energy for this process is obtained partly from the glycogen degradation but mostly from the hydrolysis of the intracellular stored polyP, resulting in an orthophosphate release into solution. In the subsequent aerobic phase, PAO take up excessive amounts of orthophosphate to recover the intracellular polyP levels by oxidising the stored PHA. Meanwhile they grow and replenish the glycogen pools using PHA as both carbon and energy sources (Smolders *et al*., 1995). Net phosphorus removal is achieved by wasting sludge after the aerobic period when the biomass contains high levels of polyp.

VII.B.1.2 ANAEROBIC AND AEROBIC PHASE LENGTH REDUCTION

Figure VII.B1 shows that once the VFA (acetate in this example) was depleted from the medium (~50 min.), the rest of compounds only suffered small variations. Under anaerobic conditions (i.e. without an electron acceptor available), the stored products could not be used for growth purposes. Hence, the period from the VFA depletion to the end of the anaerobic phase could be considered useless. In the example shown on Figure VII.B1, the period without VFA lasted approximately 70 minutes, which indicated that in this example more than a half of the anaerobic period could be deleted (Figure VII.B2)

In some of the existing EBPR systems, the aerobic phase is longer than the time required by PAO to uptake orthophosphate from the medium. Figure VII.B1 shows that the last half an hour of the aerobic phase (from minute 270 to 300) could be deleted. From the depletion of orthophosphate until the end of the aerobic phase, PAO are not favoured in front of other organisms present in the biomass, such as ordinary heterotrophic organisms (OHO) and/or glycogen accumulating organisms (GAO). Hence, the rest of aerobic phase could be not necessary (it could even be detrimental) for PAO growth (Brdjanovic *et al.* 1998).

A control strategy proposed to improve an EBPR start-up consisted of controlling the length of the aerobic phase by avoiding periods with no orthophosphate in the medium (Figure VII.B2). Dassanayake and Irvine (2001) pointed out this strategy could be beneficial for enriching the sludge with PAO and designed a system with shorter aerobic phase.

Figure VII.B2 shows the time reduction available in experiment VII.B1 (filled area). If the previous control strategies were applied, the anaerobic and aerobic phases would have been 130 minutes shorter and the total cycle length would be reduced in almost 36 %.

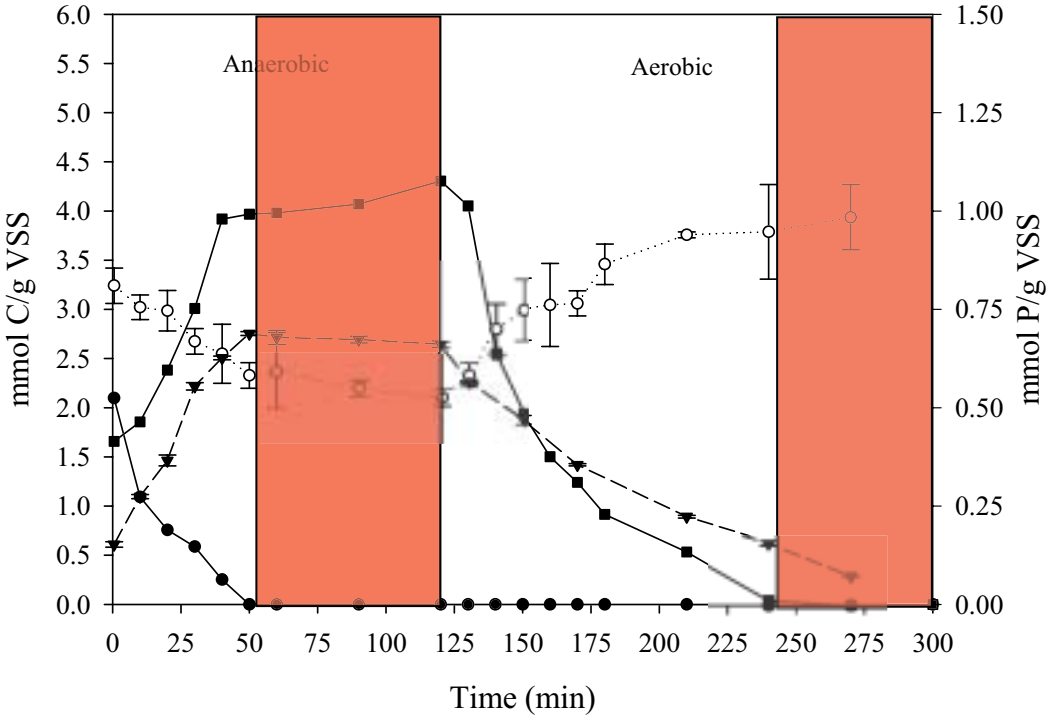

Figure VII.B2. Time reduction available in experiment VII.B1 (filled area) (b) VFA -acetate, (y) phosphorus, (z) glycogen, (Σ) PHB.

VII.B.2 Description of the start-up simulations

VII.B.2.1 SBR MODEL DEVELOPMENT

Thirty days of SBR start-up were simulated using a model which included all the SBR phases. The model had a hydraulic part characteristic of SBR and a biological part which described the occurring processes. The biological model was a modification of the Activated Sludge Model 2d (ASM2d) (Henze *et al.* 2000) including glycogen economy (see Chapter VII.A). The model for the whole SBR cycle simulation could be divided in five sequential phases: feed, anaerobic, aerobic, settling and extraction. Biological reactions were only considered in the anaerobic and in the aerobic phases.

Feed phase: This phase was simulated as an instantaneous process using mass balances. The influent flow was 5 litre and contained COD (as acetate) and P and enough essential micronutrients for microbial growth so that no limitations occurred in the reactor. The total volume of the reactor is 10 L.

Anaerobic phase: This phase was characterised by a constant length of two hours and an oxygen setpoint of zero mg O_2/L. The length of this phase could be constant (2 hours) or variable depending whether there was control or not.

Aerobic phase: The oxygen set point value in this phase was set to 8 mg O_2/L to avoid any oxygen limitation. The length of this phase could be constant (3 hours) or variable depending whether there was control or not.

Settling and *extraction phases:* These two phases lasted one hour in total and were considered together and non-reactive for model simplification. The concentrations of the state variables at the end of the cycle were calculated with mass balances according to the waste and the total volume extracted (5 L).

The model used for the description of the biological processes was an extension of the model described in chapter VII.A. The extension consists of including the processes that may acquire importance in long-term experiments (i.e. lysis, hydrolysis and fermentation processes). The Ordinary Heterotrophic Organisms (OHO) population was included in the biological model, since the competition between OHO and PAO had a strong influence on PAO dynamic behaviour. Moreover, if an EBPR system was inoculated with WWTP biomass, the ratio of PAO to OHO in biomass will be very low, and the OHO behaviour would be significant, particularly in the first days of operation. The nitrifying population was not considered in these simulations since the influent of EBPR pilot plants generally contains ATU, which is a nitrification inhibitor (Pijuan *et al.*, 2004a).

The model stoichiometry and kinetics are shown on Table VII.B2 and VII.B3. The default parameters of ASM2d were used except for the parameters related with glycogen which were taken from the experiments performed in chapter VII.A.

Table VII.B2 Model stoichiometry and kinetics*

	Process	Stoichiometry										Kinetics
		S_A	S_F	S_{PO4}	S_O	X_{PHA}	X_{GLY}	X_{PAO}	X_H	X_S	X_I	X_{PP}	
1	Aerobic hydrolysis		$(1-f_{SI})$	τ_{1P}						-1			$k_H \cdot (X_S/X_H)/(K_X+X_S/X_H) \cdot M_O \cdot X_H$
2	Anaerobic hydrolysis		$(1-f_{SI})$	τ_{2P}						-1			$k_H \cdot \xi_{FE} \cdot (X_S/X_H)/(K_X+X_S/X_H) \cdot K_O/(K_O+S_O) \cdot X_H$
3	X_{PHA} storage	$-Y_{AC3}$		Y_{PO}		1	Y_{GLY3}					$-Y_{PO}$	$q_{PHA} \cdot M_A \cdot (X_{PP}/X_{PAO})/(K_{PP}+X_{PP}/X_{PAO}) \cdot (X_{GLY}/X_{PAO})/(K_{GLY}+X_{GLY}/X_{PAO}) \cdot X_{PAO}$
4	X_{PP} storage			-1	$-Y_{PHA}$	$-Y_{PHA}$						1	$q_{PP} \cdot (X_{PHA}/X_{PAO})/(K_{PHA}+X_{PP}/X_{PAO}) \cdot$ Ą Ą $\cdot (K_{MAX}-X_{PP}/X_{PAO})/(K_{IPP}+K_{MAX}X_{PP}/X_{PAO}) \cdot M_O \cdot M_P \cdot X_{PAO}$
5	X_{GLY} storage				$-(1-Y_{GLY5})$	-1	Y_{GLY5}						$q_{GLY} \cdot (X_{GLYMAX}-X_{GLY}/X_{PAO}) \cdot (X_{PHA}/X_{PAO})/(K_{PHA}+X_{PHA}/X_{PAO}) \cdot M_O \cdot X_{PAO}$
6	X_{PAO} growth			$-i_{BPM}$	$1-1/Y_{PAO}$	$-1/Y_{PAO}$		1					$\sigma_{PAO} \cdot M_P \cdot (X_{PHA}/X_{PAO})/(K_{PHA}+X_{PHA}/X_{PAO}) \cdot M_O \cdot X_{PAO}$
7	X_{PAO} lysis			τ_{7P}				-1		$(1-f_{XI})$	f_{XI}		$b_{PAO} \cdot X_{PAO}$
8	X_{PP} lysis			1								-1	$b_{PP} \cdot X_{PP}$
9	X_{PHA} lysis	1				-1							$b_{PHA} \cdot X_{PHA}$
10	X_{GLY} lysis		1				-1						$b_{GLY} \cdot X_{GLY}$
11	X_H growth on S_A	$-1/Y_H$			$1-1/Y_H$				1				$\sigma_H \cdot M_O \cdot M_A \cdot M_P \cdot S_A/(S_F+S_A) \cdot X_H$
12	X_H growth on S_F		$-1/Y_H$		$1-1/Y_H$				1				$\sigma_H \cdot M_O \cdot M_F \cdot M_P \; S_F/(S_F+S_A) \cdot X_H$
13	X_H lysis								-1	$(1-f_{XI})$	f_{XI}		$b_H \cdot X_H$
14	Fermentation	1	-1										$q_{FE} \cdot K_O/(K_O+S_O) \cdot S_F/(K_F+S_F) \cdot X_H$

* M_I stands for the Monod limitation kinetics: $M_I = S_I / (K_I + S_I)$

Table VII.B3 Model parameters

Parameter	Description	Value	Parameter	Description	Value	Parameter	Description	Value
k_H (1/d)	Hydrolysis maximum rate	3	K_P (mg P/L)	S_P semisaturation (growths)	0.01	Y_{GLY3}	X_{GLY} degraded/ X_{PHA} stored	0.42
K_X (g X_S/gX_H)	Hydrolysis semisaturation	0.1	b_{PP} (1/d)	X_{PP} lysis constant	0.1	K_{MAX} (gX_{PP}/gX_{PAO})	Maximum X_{PP}/X_{PAO} ratio	0.34
f_{XI}	Lysis Inert fraction	0.1	b_{GLY} (1/d)	X_{GLY} lysis constant	0.1	K_{IPP} (g X_{PP}/gX_{PAO})	X_{PP} storage inhibition	0.02
q_{PHA} (g X_{PHA}/g X_{PAO}/d)	X_{PHA} maximum storage rate	5.76	τ_{7PO}	Biomass P release in lysis	0.01	q_{GLY} (1/d)	X_{GLY} production rate	22
K_{PP} (gX_{PP}/gX_{PAO})	X_{PP} semisaturation	0.01	Y_H	X_H growth yield	0.7	Y_{GLY5}	X_{GLY} produced / X_{PHA} degraded	1
Y_{PO} (g P/gCOD)	S_P release / S_A uptake	0.55	i_{BPM} (gP/gX)	P content biomass	0.02	Y_{PAO}	X_{PAO} growth yield	0.625
K_{GLY}	X_{GLY} semisaturation	0.001	K_F (mg COD/L)	S_F semistaturation	4	b_{PAO} (1/d)	X_{PAO} lysis constant	0.1
q_{PP} (gX_{PP}/gX_{PAO}/d)	X_{PP} maximum storage rate	4.07	ξ_{FE}	Anaerobic Reduction factor	0.4	b_{PHA} (1/d)	X_{PHA} lysis constant	0.1
K_{PS} (mg P/L)	S_P semisaturat. X_{PP} storage	0.02	τ_{1PO}, τ_{2PO}	Hydrolysis P release	0	b_H (1/d)	X_H lysis constant	0.1
K_{PHA} (mg COD/L)	X_{PHA} semisaturation	0.07	Y_{PHA} (g COD/gP)	X_{PHA} degraded /S_P accumulated	0.2	f_{SI}	Hydrolysis S_I production	0
X_{GLYMAX}	Maximum X_{GLY}/X_{PAO} ratio	0.28	Y_{AC3}	S_A uptaken / X_{PHA} stored	0.82	σ_H (1/d)	X_H maximum growth rate	6
σ_{PAO} (1/d)	X_{PAO} maximum growth rate	1	K_S (mg COD/L)	S_A semisaturation	4	q_{FE} (g S_F/g X_H/d)	Fermentation maximum rate	3

VII.B.2.2 BASIC START-UP SIMULATION

The initial values of each simulation are shown on Table VII.B4. All the simulations were run for thirty days. Table VII.B5 shows the amount of P and COD in the feed, which was designed so that it increased proportionally to the PAO fraction in the biomass. Moreover, this feed pattern was chosen so that PAO were favoured against other species (i.e. all the COD and the P should have been taken up in the anaerobic phase and aerobic phase respectively). An optimum feed pattern could be found for each one of the control strategies. However, the scope of this study was not feed pattern optimisation but comparing different start-up strategies with the same feed pattern.

A waste of 0.25 L at the end of the aerobic phase was also included from the tenth cycle on to describe more reliably a real start-up sequence. Hence, for a 10 L reactor the SRT of the system is 10 days.

Table VII.B4 Initial values for start-up simulations

Parameter	Initial value	Parameter	Initial value
X_{PAO} (mg PAO/L)	200	X_{GLY} (mg COD/L)	30
X_H (mg COD/L)	1600	X_S (mg COD/L)	0
X_{PHA} (mg COD/L)	10	X_{PP} (mg P/L)	20
X_I (mg COD/L)	0		

Table VII.B5 Feed pattern.

Cycles	1-10	10-20	20-30	30-50	50-75	75-100	100-125	125-150	150-175
mg P/L Feed	6	10	14	18	22	26	30	34	40
mg COD/L Feed	50	100	200	250	350	400	450	500	550

As each cycle lasted 6 hours, 120 cycles could be placed in the thirty days of start-up. The profiles of the main compounds along this simulation without any control strategy implemented are depicted in Figure VII.B3.

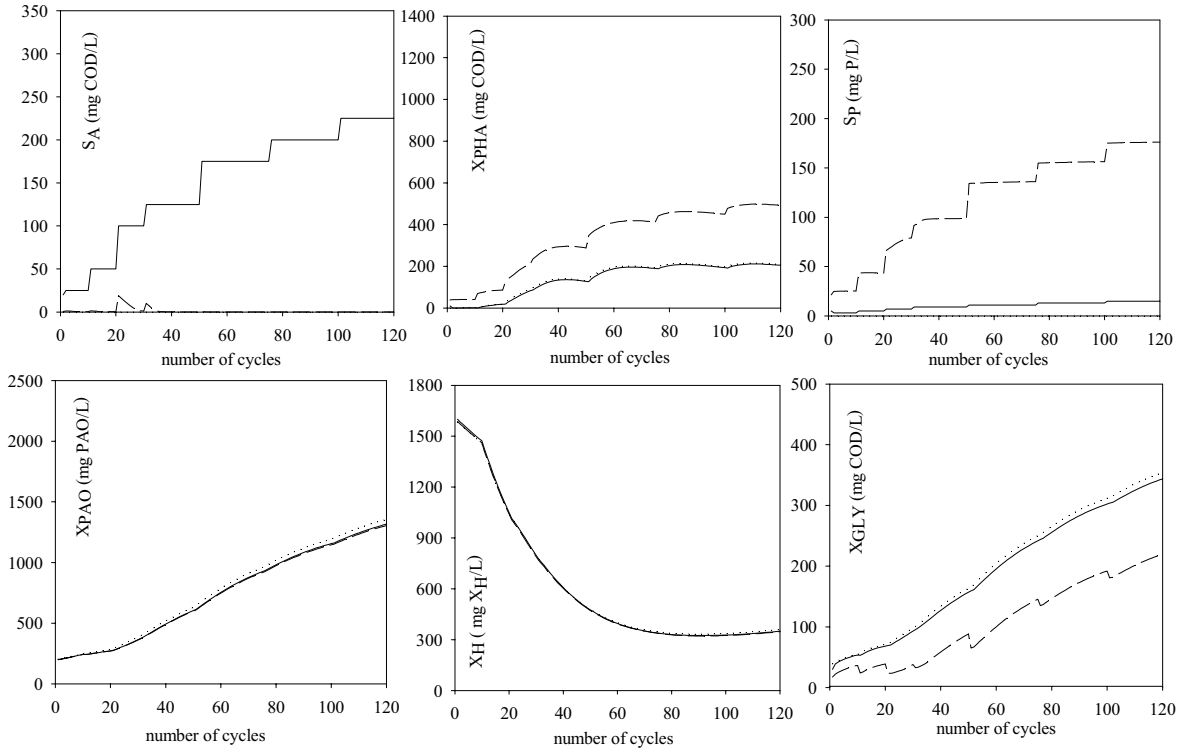

Figure VII.B3 Start-up period without any phase length control (6-hour cycle). Anaerobic phase initial (solid), aerobic phase initial (dashed) and aerobic phase end (dash-dotted).

As can be observed, both VFA and orthophosphate in the influent increased along the experiment following the feed pattern of Table VII.B5. There was some VFA left at the end of the anaerobic phase in the cycles where the amount of acetate in the feed was increased. On the contrary, phosphorus was taken up in the aerobic phase in all cycles. This indicated the amount of P in the feed could have been increased although the absolute value in the last cycles was already very high.

The OHO population decreased along the start-up period because they could only grow on COD under aerobic conditions and the only COD present in the aerobic phase was due to the hydrolysis and fermentation processes, which was a very low COD value. However, according to the simulations, this population did not disappear from the system completely, but a small fraction was always present in the system. This fact was quite significant, since it showed that a certain fraction of OHO should be always considered in the bio-P sludge On the contrary, PAO rose considerably, because under aerobic conditions they could grow on the previously stored X_{PHA}. Hence, it was proven that the start-up without any control strategy fixed aerobic phase length could be successful.

In the last section of this chapter (VII.B.6), several parameters such as the ratio PAO to OHO or the amount of PAO after the start-up are examined in order to evaluate the improvements of each of the control strategies

VII.B.3 Anaerobic phase control length

VII.B.3.1 *VFA-CONTROL* STRATEGY

The *VFA-control* strategy consisted of stopping the anaerobic phase and starting the 3 hour aerobic phase when the concentration of VFA became lower than 1 mg COD/L. This control strategy avoided unnecessary periods without VFA and without neither storage nor growth. This strategy allowed the completion of the 120 cycles in only 635 hours. That meant 85 hours less than the simulations without control. Hence, 12 % of the start-up length was ineffective for PAO enrichment and as such it could be omitted. Hence, during the 30 days of start-up simulation a total of 133 cycles could be completed.

Figure VII.B4 displays the values of the main components of the simulation obtained during these 133 cycles. The EBPR system start-up became more efficient since more cycles could be performed with the *VFA-control* strategy (in the same period of time) than in the start-up without any control.

The length of the anaerobic phase in the normal SBR operation (without anaerobic control) was 120 min. Figure VII.B5 shows the relation between the length of anaerobic phase and the amount of acetate in the feed. As can be observed, few cycles require the maximum length to uptake all the VFA of the feed. As discussed, another analysis of this simulation is that the feed pattern could be optimised so that the amount of VFA at the inlet was just depleted before the anaerobic phase finished.

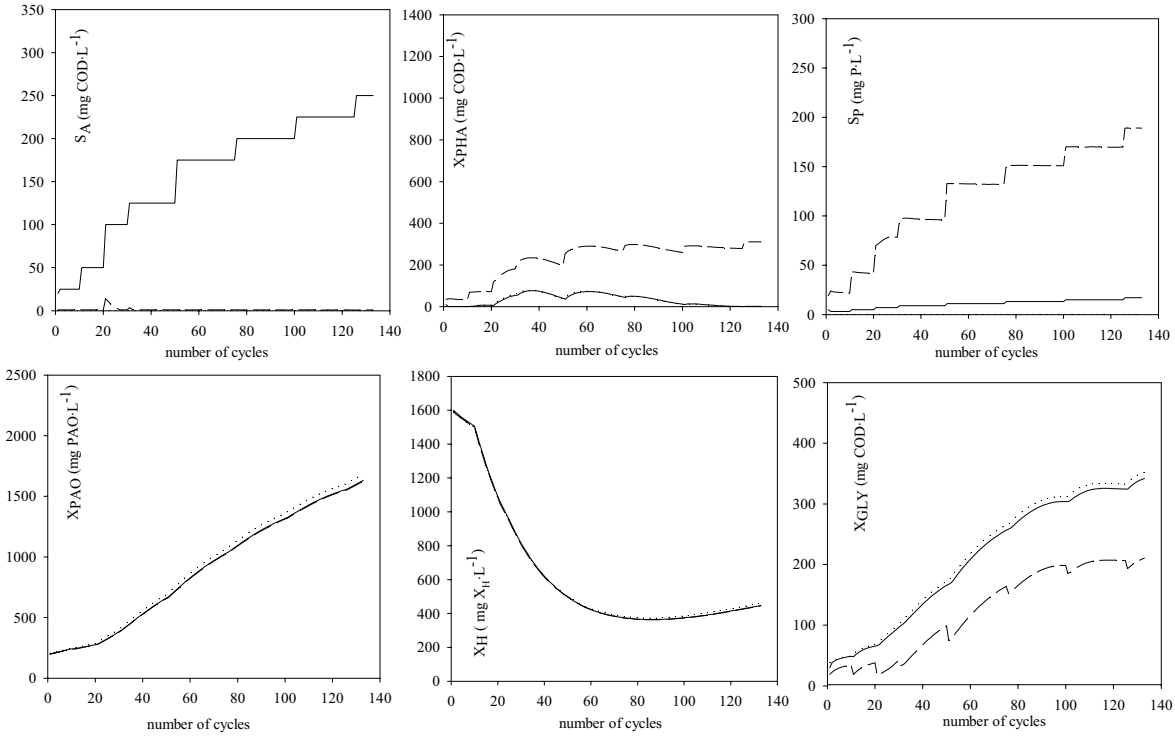

Figure VII.B4 Start-up period with *VFA-control* strategy. Anaerobic phase initial (solid), aerobic phase initial (dashed) and aerobic phase end (dash-dotted).

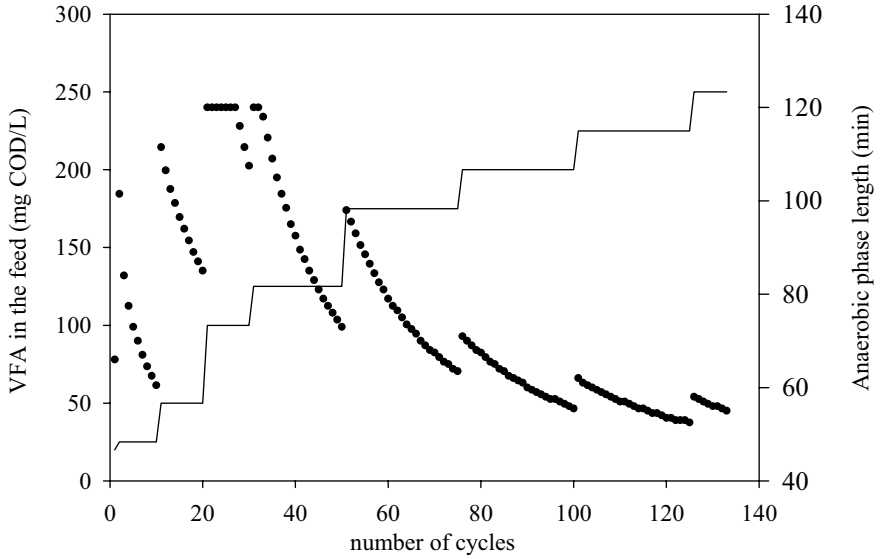

Figure VII.B5 Anaerobic phase length (dotted) and amount of VFA in the feed (solid) versus the number cycles.

This *VFA-control* strategy has one technical limitation. The success of this control strategy (in view of implementation to real systems) is strongly dependent on the quantity and quality of the measured data. However, the truth is that the on-line measurement of VFA, i.e. COD measurement, cannot be considered optimum (i.e. low data frequency, high confidence intervals and long time delays). Hence, this strategy could not be used in a real scenario. An online measurement that predicted the VFA depletion would be a great advance for control purposes since the control strategies proposed could be easily developed. An alternative measurement, suitable for control purposes such as pH (or HPR) should be linked to the VFA uptake process. This study links the depletion of VFA with a conventional online measurement such as pH.

VII.B.3.2 LINKING HPR TO VFA DEPLETION

The link between anaerobic VFA uptake (and P release) with pH is described in many EBPR studies, particularly studying the influence of pH on the P/C ratio (Smolders *et al.*, 1994a; Fleit, 1995; Carlsson *et al.*, 1996; Liu *et al.*, 1996) and to study the competition between PAO and GAO (Jeon *et al.*, 2001 or Schuler and Jenkins, 2002). Bond *et al.* (1999b) went one step beyond and affirmed that anaerobic P release was caused by intracellular alkalinisation, and not because typical EBPR carbon compounds transformations. According to their work, these events (i.e. VFA uptake, PHA production and glycolysis) result in a cell alkalinisation which is balanced with internal polyP degradation to maintain the pH. Anyway, the pH changes because of the all the anaerobic processes involved in VFA uptake and, hence, HPR (i.e. acid/base dosage to maintain pH) could be used as a measured variable. Finally, Serralta *et al.* (2004) proposed an extension of the ASM2d model including a chemical model to predict the pH evolution in EBPR systems. This model was based on the chemical equilibriums of all the ionic species present in the system. They affirmed that EBPR process was very sensitive to pH changes. Actually, they observed a decrease in the polyP storage rate as phosphorus was taken up and included a inhibition factor due to pH to describe this process. However, this factor is not necessary if the PHB limitation on polyP storage rate is considered.

The processes which have a major influence on the pH under anaerobic conditions are:

1. VFA uptake: The pKa of the VFA (acetic and propionic acids) is lower than 5 (see Table VII.B6). Hence, the VFA is mostly in ionised form at pHs close to neutrality. The molecule of VFA is supposed to be transported through the membrane in the non-ionised form. Hence, a mole of proton is required to transport a mole of VFA molecule through the membrane to maintain internal electroneutrality. Hence, the VFA uptake process results in a pH increase and acid dosage is required to balance this effect. This deduction is analogous to the one used when examining the substrate uptake monitoring with titrimetry (see chapter V.B).

2. Carbonic acid-carbonate equilibrium: the system was bubbled with nitrogen and CO_2 was stripped. As described in previous chapters, the CO_2 stripping process results in a pH increase and acid dosage is required to balance this effect.

3. Phosphoric acid-phosphate equilibrium: H_3PO_4 is released to the medium because of VFA uptake. Table VII.B6 shows the pKas of the different phosphoric acid species. As can be deduced, approximately half of the total phosphorus content is in $H_2PO_4^-$ form and the rest is on HPO_4^{2-} form in the equilibrium when pH is around 7.2. Hence when H_3PO_4 is released, it is transformed to $H_2PO_4^-$ and HPO_4^{2-} resulting in proton release to the media. Qualitatively, a value between 1.5 and 2 moles of H^+ should be released to the media per mol of P released at pH 7.5. Hence, the P release process results in a pH decrease and base dosage is required to balance this effect.

Table VII.B6 pKas for phosphoric, acetic and propionic acids (Burriel *et al.*, 1989)

Acid - base	pKa
H_3PO_4 – $H_2PO_4^-$	2.2
$H_2PO_4^-$ - HPO_4^{2-}	7.2
HPO_4^{2-} - PO^{3-}	12.3
CH_3COOH – $CH3COO^-$	4.8
CH_3CH_2COOH - $CH_3CH_2COO^-$	4.9

Each of the three processes has a different effect on pH. Experiment VII.B2 (Table VII.B7) was conducted to assess the experimental link between the VFA presence and HPR in the anaerobic phase.

Table VII.B7 Experiment VII.B2

EXPERIMENT VII.B2	Relation between VFA uptake and HPR
Equipment	LFS respirometer (V_0 = 1 L)
pH	7.5
Temperature	25 ºC
Acid used	HCl = 0.5 M
Base used	NaOH = 0.2 M
Pulses	150 mg HPr /L (t = 40 min)

Biomass was withdrawn from the end of the aerobic phase of an EBPR-SBR (see chapter III.1.3) system. This system was operating on steady state conditions and the biomass used had a high PAO fraction. The biomass was introduced in the LFS respirometer (see chapter III.1.1) and was bubbled with nitrogen gas to obtain anaerobic conditions. Then, a pulse of propionic acid was added and HPR, propionic acid and phosphorus were measured.

Figure VII.B6 depicts the experimental profiles obtained. Once a pulse of VFA was added, the HPR became positive and base dosage was required to maintain the pH at the setpoint value. This indicated that the influence of the phosphoric acid-phosphate equilibrium on pH was higher than the other proton consuming processes (i.e. CO_2 stripping and VFA uptake). This fact is supported by the important P release measure together with propionic acid consumption (P/C = 0.46 mol P/ mol C_{PROP}).

Moreover, the base dosage is clearly linked with the VFA uptake (and P release), and once this process stops (i.e. propionic is depleted) the HPR returns again to negative values because of CO_2 stripping. As the VFA uptake process produces CO_2 (see EBPR stoichiometry – Table VII.A1), the HPR after the VFA pulse is higher (in absolute terms, i.e. is more negative) than the HPR before the pulse because of the higher CO_2 stripping.

As a conclusion of this experiment, HPR is a valuable tool for detecting the depletion point of the VFA in the anaerobic system and a control strategy using HPR as measured variable to shorten the anaerobic phase can be proposed (section VII.B.3).

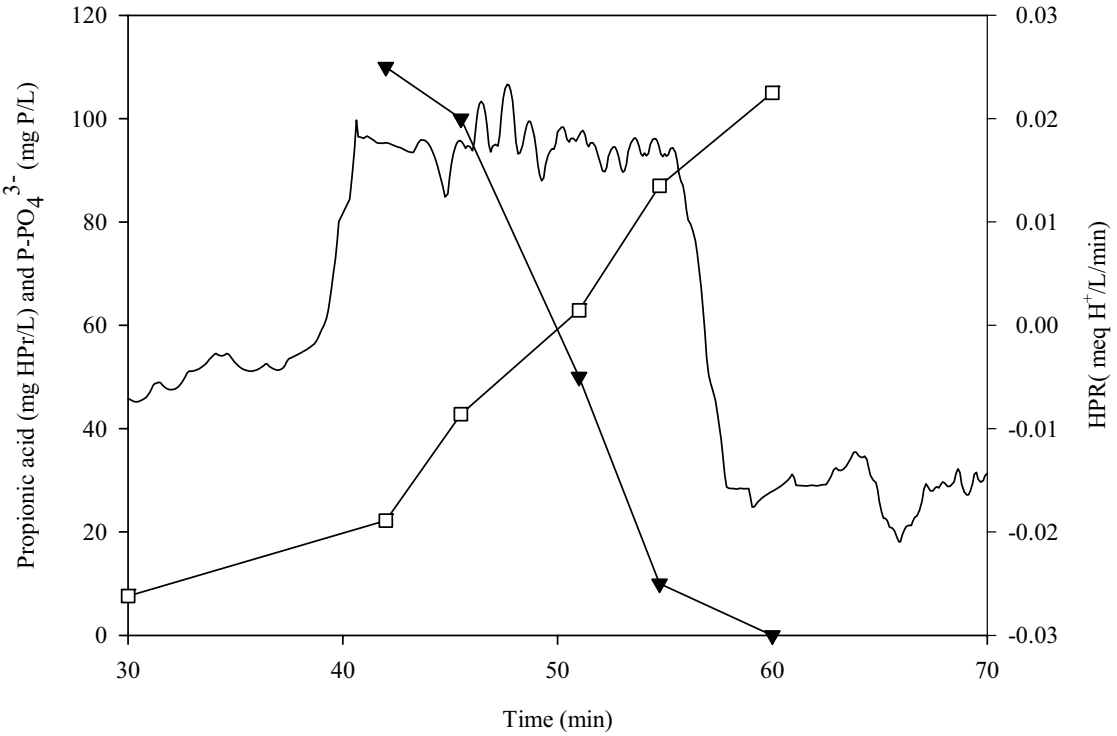

Figure VII.B6 Experimental HPR, propionic acid and phosphorus profiles for experiment VII.B2: VFA (ζ),phosphorus (Ž), HPR (solid line).

Hence, HPR could be used for detecting VFA depletion. This strategy has not been simulated because the introduction of HPR in the model implies increasing the complexity with many different processes such as aeration, CO_2 stripping and the carbonic and phosphoric acid equilibrium. However, this model extension is a future perspective of our research group but further experimental data and more focusing is required. In any case, it can be considered that a control strategy with HPR as the measured variable would result in the same number of cycles and the same start-up improvement with as the *VFA-control* strategy.

VII.B.4 Aerobic phase control length

VII.B.4.1 *P-CONTROL* STRATEGY

The *P-control* strategy was based on controlling the aerobic phase length using orthophosphate as the measured variable. Hence, it consisted of stopping the aerobic phase and starting the settling/extraction phases when the concentration of orthophosphate became lower than 0.1 mg P/L. This control strategy avoided unnecessary PHA oxidation in absence of P and allowed to complete 120 cycles in only 513 hours due to the reductions in the aerobic phase length. That meant 207 hours less than the simulations without control. Hence, 29 % of the start-up time was ineffective for PAO growth and as such it could be omitted. Figure VII.B7 displays the values obtained during 170 cycles. These were the number of cycles that could be placed in thirty days of simulation with the P-control strategy. Hence, the EBPR system start-up became more efficient since more cycles could be performed with this strategy (during the same period) than with fixed aerobic length.

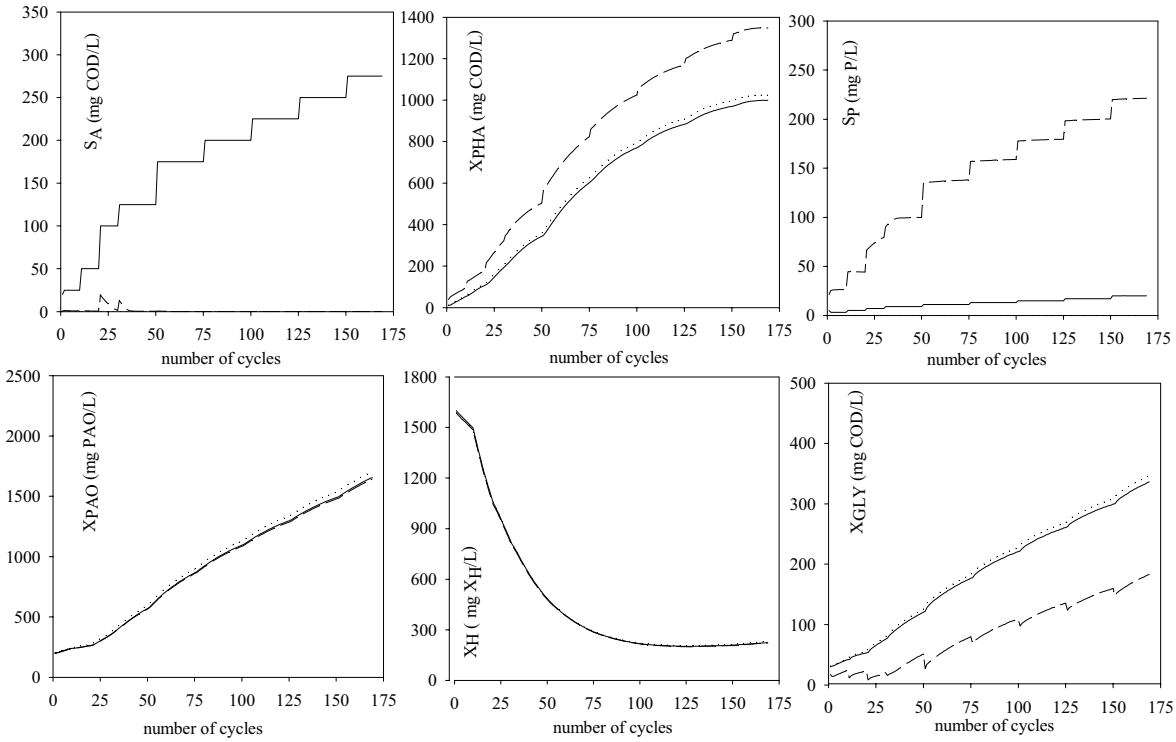

Figure VII.B7 Start-up period with *P-control* (variable aerobic phase length). Anaerobic phase initial (solid), aerobic phase initial (dashed) and aerobic phase end (dash-dotted).

The main difference between this strategy and the simulation without control (Figure VII.B4) was in the X_{PHA} trend. The simulations without control had lower and more fluctuating X_{PHA} levels. The internal polymer was continuously oxidised for maintenance purposes during the aerobic phase. As this phase was reduced, less X_{PHA} was oxidised. The increase in the PHA levels was a positive secondary effect of the P-control strategy because the amount of PHA present at the end of the anaerobic phase governed the extent of P uptake in the subsequent aerobic period. The *P-control* strategy improved the start-up of an EBPR system to a great extend, since the ratio of X_{PAO}/X_H was increased more than 90% and the final amount of X_{PAO} was increased almost 30%.

However, likewise the *VFA-control* strategy, the *P-control* strategy required an accurate on-line sensor for its implementation. Again, the measurement of orthophosphate does not seem the optimum for a control loop. Hence, an alternative was proposed which linked an easily measurable variable as dissolved oxygen (i.e. OUR) to the orthophosphate presence.

VII.B.4.2 LINKING OUR TO ORTHOPHOSPHATE DEPLETION

Linking the aerobic phase length to orthophosphate presence was tested to be successful but difficult and expensive to implement in real EBPR systems since it required an on-line orthophosphate measurement. However, as shown on experiment VII.B3, OUR could also be linked to the orthophosphate concentration. Hence, the control on the aerobic phase length could be developed using OUR as the measured variable, which is more suitable for control purposes. This experiment (Table VII.B4) was conducted to assess the relation of the orthophosphate with OUR in the aerobic phase.

Table VII.B8 Experiment VII.B3

EXPERIMENT VII.B3	Relation between phosphorus uptake and OUR
Equipment	LFS respirometer (V_0 = 1 L)
pH	7.5
Temperature	25 ºC
Acid used	HCl = 0.25 M
Pulses	none

The biomass was withdrawn from the EBPR-SBR pilot plant before the anaerobic phase was finished and it was introduced in the LFS respirometer (chapter III.1.1) under anaerobic conditions (i.e. nitrogen bubbling). Then, the gas inlet was switched to conventional air and the aerobic phase started. The airflow was introduced through an airflow meter for a reliable OUR calculation. Once orthophosphate was totally depleted and the S_O value reached a constant value (S_{OE}) typical of endogenous conditions, the k_La_{O2} of the system was calculated through stopping the aeration and subsequently turning it on as described in chapter III.1.1 (Bandyopadhyay *et al.*, 1976).

Figure VII.B8 shows the experimental OUR and orthophosphate profiles and demonstrates that both components could be linked. A decrease and a slope change on the OUR is observed together with the orthophosphates depletion (around min 110). This slope change is also predicted by the model as shown above. The process of polyP storage requires some energy which is provided by the oxidation of the internal PHA. When the polyP storage process stops, the OUR value sharply decreases.

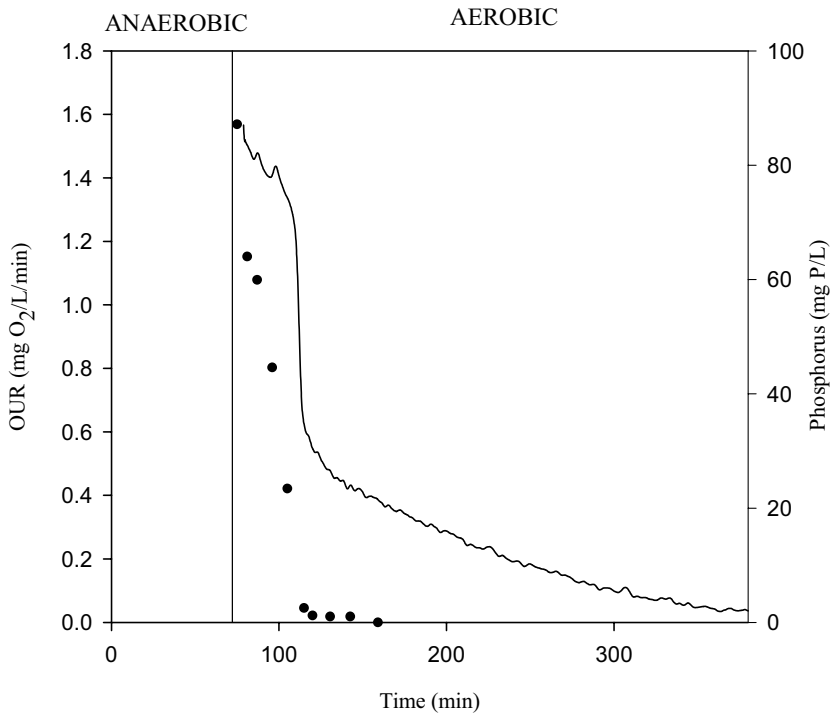

Figure VII.B8 OUR (solid line) and orthophosphate (dotted) profiles of experiment VII.B3

Linking OUR measurement and EBPR process is not very common in the literature since the characteristic phase of EBPR is anaerobic. In this phase, OUR is zero. Under aerobic conditions, PAO use the previously stored PHA to restore its internal glycogen pools, to uptake orthophosphate from the medium and store it as polyP, to grow and, finally, it is oxidised for maintenance purposes. Figure VII.B9 depicts a simulation of the VFA, P and OUR in a conventional EBPR cycle with fixed aerobic phase.

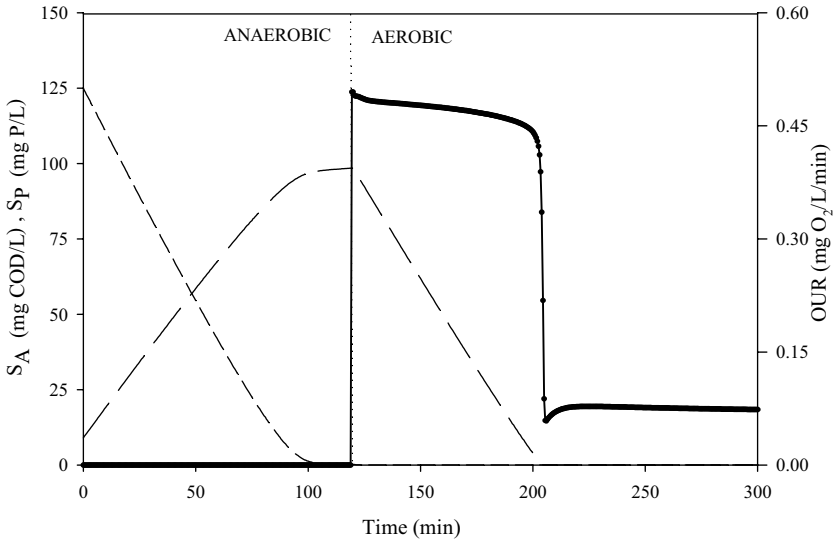

Figure VII.B9 Profiles of the main compounds in a conventional EBPR cycle with fixed aerobic phase. OUR (solid), S_P (dashed) and S_{VFA} (dotted)

As can be observed, the OUR reaches a high value at the start of the aerobic phase and drops off once the orthophosphate is totally depleted. The model stoichiometry (Table VII.B2) shows the oxygen consumption linked to the polyP storage process. PAO growth decreases sharply while orthophosphate is depleted (~200 min).

Hence, the time period between the depletion and the aerobic phase end becomes a waste of time and energy according to the aim of enriching the SBR population with PAO. The last 100 minutes could have been removed without any negative effect.

VII.B.4.3 *OUR-CONTROL* STRATEGY

OUR is a suitable output variable for modelling purposes because it is relatively easy to measure while it provides a lot of information. Although it has not been commonly used in the literature when dealing with EBPR process, experiment VII.B2 showed that there existed a clear link between EBPR and OUR. This link is deeply studied and detailed in the chapter VII.C.

Due to the close link between OUR and orthophosphate concentration, a possible strategy could be to stop the aerobic phase and start the settling/extraction phases when OUR became lower than a certain value. OUR did not decrease to zero after P depletion, but remained in a low constant value because of lysis and hydrolysis processes (Figure VII.B9). The set-point value chosen to test this *OUR-control* strategy was 0.1 mg O_2/L/min. The experimental profiles after thirty days of simulation are shown on Figure VII.B10. The *OUR-control* strategy improved the start-up without control, since 153 cycles could be placed in the period of simulation (thirty days). However, the improvement is lower than the one observed with the *P-control* strategy. As an example, the increase of the ratio X_{PAO}/X_H with the OUR control strategy was only 47 % when compared to the 90 % obtained using the *P-control* strategy.

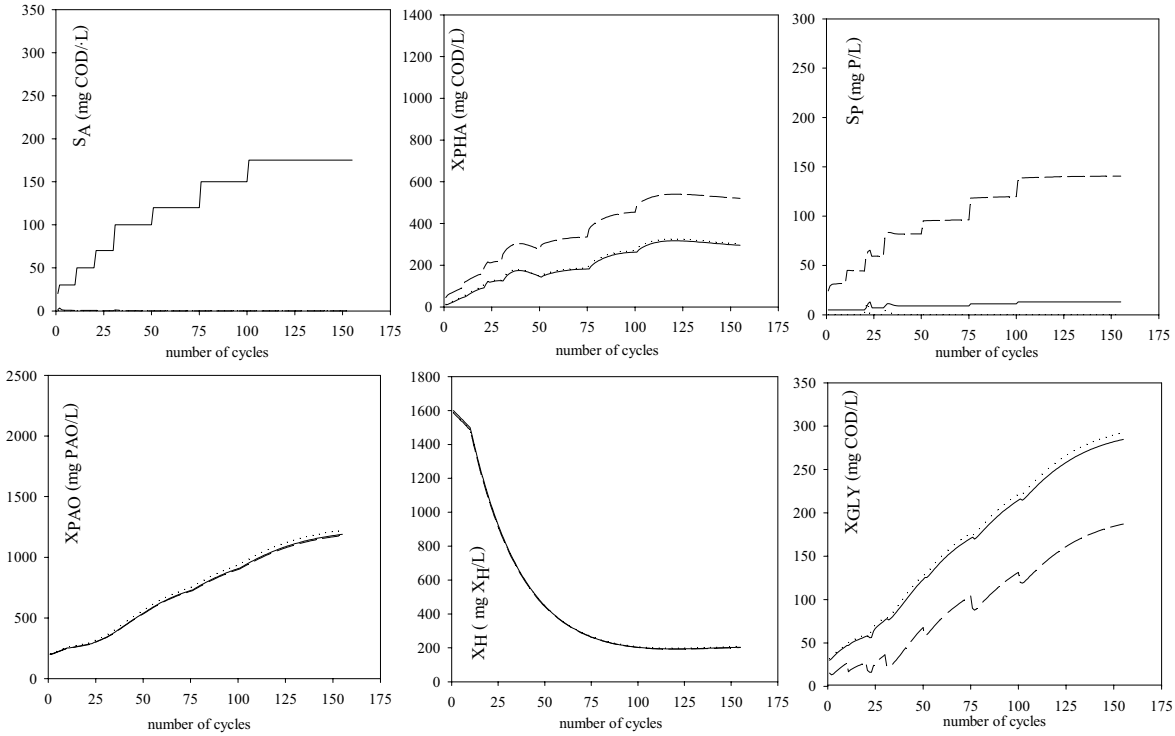

Figure VII.B10 Start-up period with *OUR-control* (variable aerobic phase length). Anaerobic phase initial (solid), aerobic phase initial (dashed) and aerobic phase end (dash-dotted).

VII.B.4.3 *dOUR-CONTROL* STRATEGY

The *dOUR-control* strategy was planned to obtain a more efficient strategy using OUR as the measured variable and to improve the results of the *OUR-control* strategy. Hence, a new approach using the OUR first derivative (dOUR) was planned. Figure VII.B11 shows a simulation of the OUR, dOUR and orthophosphate profiles obtained in the aerobic phase of a conventional EBPR cycle.

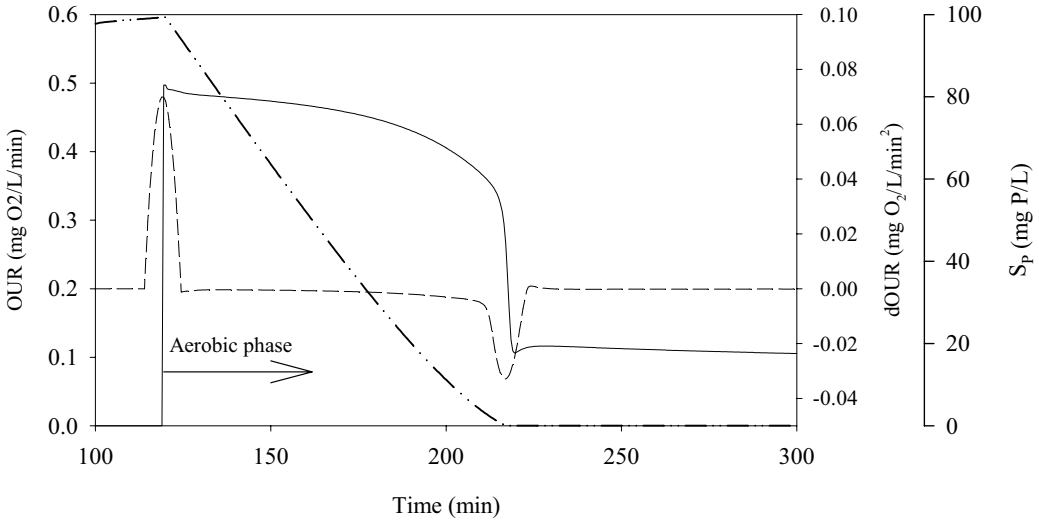

Figure VII.B11 Simulation of orthophosphate, OUR and dOUR profiles in an aerobic phase. OUR (solid), dOUR (dashed), S_P (dash-dotted).

A minimum could be observed in the OUR profile when P was depleted. The OUR was always decreasing along the aerobic phase until this minimum was attained. Hence, if the dOUR was calculated, the depletion point could be estimated because the dOUR at this point should move from a negative to a positive value. This hypothesis was the basis of the *dOUR-control* strategy: stop the aerobic phase and start the settling/extraction phases when the first derivative of the OUR became positive. The experimental results of this simulation are practically the same as the *P-control* strategy (Figure VII.B7). It has to be noted that this minimum may not always be experimentally observed (as in Figure VII.B8) and this control strategy could not be always applicable.

This strategy was shown to be a very successful since 169 cycles could be placed in thirty days of simulation (only one cycle less than the *P-control* strategy). The reason for this "lost" cycle was that OUR values after and before a certain instant of time were needed for a proper estimation of the OUR first derivative in this instant of time. This implied a certain time delay in assessing the minimum of the OUR profile, and consequently, in stopping the aerobic phase. Lower frequency in OUR calculation would imply higher time delays and this last strategy would become less efficient. In this work, an OUR estimation frequency of 10 seconds is used and, then, the delay becomes irrelevant since the start-up process is highly improved using an easy measurable output variable such as OUR.

VII.B.5 Anaerobic and aerobic phase control length

Finally, a last simulation was performed reducing both the anaerobic and the aerobic phases. The strategies used were *VFA-* and *P-control* strategies together. Coupling both strategies together implied that 120 cycles could be placed in 440 hours and then a reduction of 280 hours was accomplished. Hence, almost 40% of the start-up time could have been reduced with any detrimental effect on the EBPR system.This was a significant

improvement since, 219 cycles could be completed in the first 30 days of start-up. Moreover, this improvement was accomplished using control strategies with two conventional measurements such as DO and pH. These measurements are online, generally available and essential for the monitoring of any biological system.

Figure VII.B12 shows the experimental results obtained. Table VII.B9 compares the final results obtained with all the strategies proposed in this chapter. In addition, Figure VII.B13 compares the length of the anaerobic and the aerobic phases with the amount of COD in the feed as acetate. This figure shows that the aerobic phase was always longer than required (it never reached values of 180 min). On the other hand, the anaerobic phase reduction was efficient, particularly from the fortieth cycle on since the length of this phase was close to 60 min.

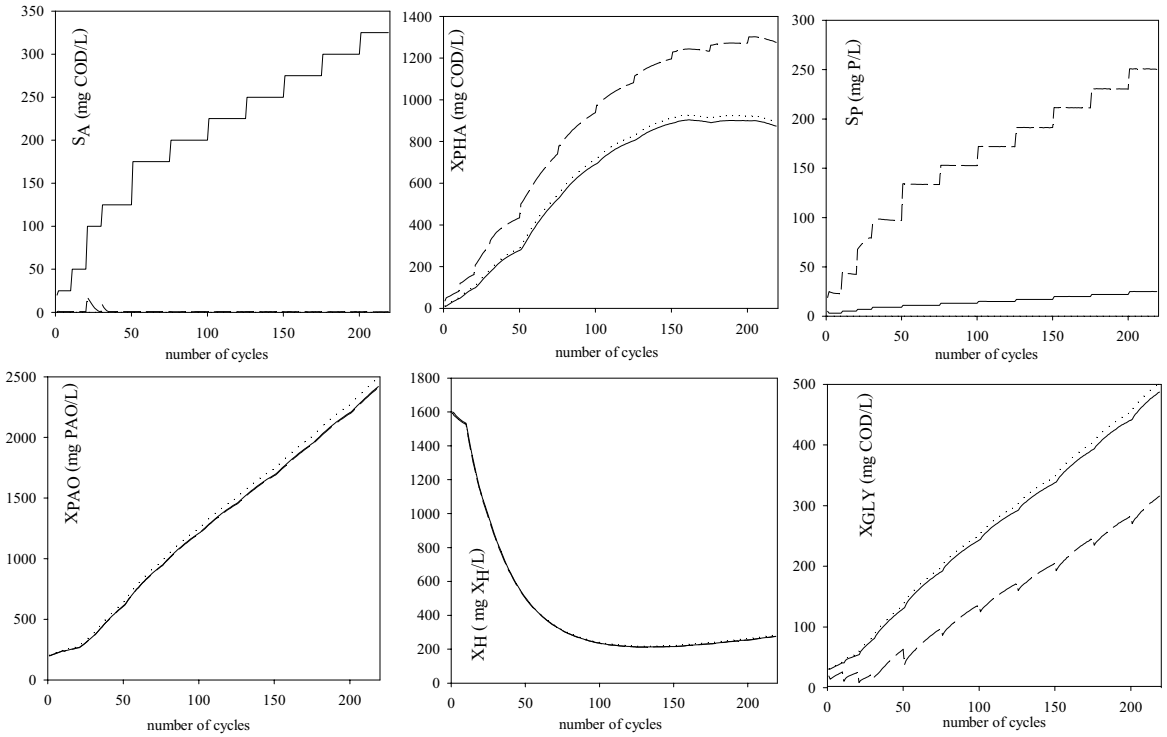

Figure VII.B12 Start-up period with *VFA-P-control* (variable aerobic phase length). Anaerobic phase initial (solid), aerobic phase initial (dashed) and aerobic phase end (dash-dotted).

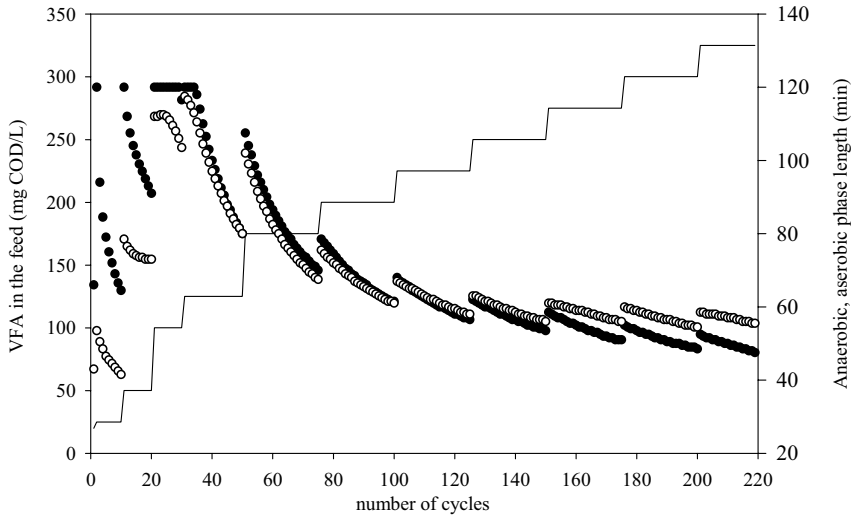

Figure VII.B13 Anaerobic phase length (black dots), aerobic phase length (white dots) and amount of VFA in the feed (solid) versus the number cycles.

VII.B.6 Summary of the control strategies

Table VII.B9 summarises the final steady-state values obtained with all the control strategies used in this chapter.

Table VII.B9 Values of the state variables after thirty days of simulation (SA, SO and EO stand for Start Anaerobic, Start Aerobic and End Aerobic, respectively)

	NO CONTROL			**VFA-CONTROL**			**P CONTROL**		
Cycles placed	120 cycles			133 cycles			170 cycles		
Compound	SA	SO	EO	SA	SO	EO	SA	SO	EO
S_A (mg COD/L)	225	0	0	250	1	0	275	0	0
X_{PHA} (mg COD/L)	205	492	209	1	310	1	998	1349	1024
X_{PAO} (mg COD/L)	1316	1305	1356	1631	1625	1683	1664	1650	1714
S_P (mg COD/L)	15	176	0	17	189	0	20	221	0
X_{PP} (mg COD/L)	274	111	282	477	305	493	515	312	531
X_S (mg COD/L)	6	11	6	8	11	8	13	18	14
X_H (mg COD/L)	349	347	360	447	446	462	225	223	231
X_{GLY} (mg COD/L)	344	220	354	342	211	352	338	185	347
S_{CO2} (mg COD/L)	71	141	142	75	149	150	88	175	176
X_I (mg COD/L)	111	112	114	109	110	113	80	81	82
S_F (mg COD/L)	1	1	2	0	0	0	0	1	1
X_{PAO}/X_H	3.8	3.8	3.8	3.6	3.6	3.6	7.4	7.4	7.4

	OUR CONTROL			**dOUR CONTROL**			**VFA-P-CONTROL**		
Cycles placed	153 cycles			169 cycles			219 cycles		
Compound	SA	SO	EO	SA	SO	EO	SA	SO	EO
S_A (mg COD/L)	275	0	0	275	0	0	325	1	0
X_{PHA} (mg COD/L)	546	897	562	990	1340	1015	871	1273	890
X_{PAO} (mg COD/L)	1597	1583	1647	1658	1645	1708	2429	2422	2502
S_P (mg COD/L)	20	219	0	20	221	0	25	250	0
X_{PP} (mg COD/L)	404	203	418	512	309	528	786	560	809
X_S (mg COD/L)	9	15	9	13	18	13	16	20	17
X_H (mg COD/L)	284	282	293	224	222	231	277	276	285
X_{GLY} (mg COD/L)	387	235	399	338	185	348	489	318	504
S_{CO2} (mg COD/L)	87	172	174	88	175	176	99	196	198
X_I (mg COD/L)	97	99	100	80	81	82	67	68	69
S_F (mg COD/L)	1	1	3	0	1	1	0	1	1
X_{PAO}/X_H	5.6	5.6	5.6	7.4	7.4	7.4	8.8	8.8	8.8

Several interesting conclusions can be obtained observing the Table above. The highest amount of PAO and the ratio X_{PAO}/X_H was obtained with the last strategy (reducing both phases). This new control strategy resulted in an increase of 85 % on the amount of PAO of with respect to the conventional EBPR system without control. Moreover, the ratio of X_{PAO}/X_H was increased around 131 % which are exceptional results. This strategy is planned to be experimentally tested in further works of the Environmental Engineering Group of UAB.

As can be observed, the number of cycles placed in the *VFA-control* strategy (i.e. 133) was lower than number of cycles placed in the *P-control* strategy (i.e. 170). However, the amount of X_{PAO} in both systems at the steady state was very similar. The reason is that the premise that "when orthophosphate was depleted from the reactor, PAO growth did not occur" was never accomplished since some orthophosphate was always present in the reactor due to the polyP lysis process. This small P-release enabled some PAO growth. This hypothesis is supported by the X_{PHA} trend. In the *VFA-contro*l strategy the

PHA values at the end of the aerobic phase are close to zero since all the PHA has been used for growth (among other purposes).

As can be observed in Figure VII.B13, the aerobic phase was usually reduced around 100 min using the aerobic shortening control strategies and the amount of PAO growth in this period might become noticeable.

Chapter VII.B Conclusions

- The simulations performed in this work reveal that it is feasible to improve the start-up of an EBPR system in a SBR by reducing the length of both the anaerobic phase and the aerobic phase so that they coincide with the depletion of VFA and orthophosphate, respectively.

- According to the results of the simulations, if the anaerobic phase is reduced linked to VFA presence, 12 % of the start-up length was ineffective for PAO enrichment and as such it could be omitted. Hence, during the 30 days of start-up simulation a total of 133 cycles could be completed. On the other hand, if the aerobic phase was reduced linked to orthophosphate presence, 120 cycles would be completed in only 513 hours due to the reductions in the aerobic phase length. That meant 207 hours less than the simulations without control. Hence, 29 % of the start-up time was ineffective for PAO growth and as such it could be omitted

- The main improvements observed with the simulations are the increase of the start-up efficiency in terms of PHA internal levels, PAO presence in the final sludge, the achievement of higher orthophosphate removal capacity and higher PAO to OHO ratio.

- If an on-line VFA measurement is not available, the HPR can be used as an indicator of VFA depletion and, hence, as a measured variable for controlling the anaerobic phase length. According to the results of the simulations, 12 % of the start-up length was ineffective for PAO enrichment and as such it could be omitted.

- If an on-line orthophosphate measurement is not available, the OUR can be used as an indicator of its presence. Both the absolute OUR value and the OUR first derivative can be used as a measured value in the control strategy.

- The on-line OUR first derivative calculation allows a satisfactory estimation of the S_P depletion point. This was simulated in a control strategy to reduce the aerobic phase length with almost the same results as the ones obtained using orthophosphate as measured variable

- As a conclusion, the best control strategy obtained is a control strategy including both the *P-control* and the *VFA-control* strategy. 120 EBPR cycles could be placed in 440 hours and then a reduction of 280 hours was accomplished. Hence, almost 40% could be considered useless. This was a significant improvement since, 219 cycles could be completed in the first 30 days of start-up.

CHAPTER VII.C

Aerobic phosphorus release linked to acetate uptake in bio-p sludge: process modelling using oxygen uptake rate

Part of this chapter has been published as:

Guisasola A., Pijuan M., Baeza J.A., Carrera J., Casas C., Lafuente J. (2004). Aerobic phosphorus release linked to acetate uptake in bio-P sludge: process modelling using oxygen uptake rate. Biotechnol. Bioeng. 85, 722-733.

ABSTRACT

The main processes involved in the Enhanced Biological Phosphorus Removal (EBPR) process under anaerobic and subsequently aerobic conditions are fully described in the literature as shown in Chapter VII.A. However, the mechanisms of Polyphosphate Accumulating Organisms (PAO) are not fully established yet under conditions that differ from the classical anaerobic / aerobic conditions. This chapter compares the behaviour of PAO when they take up Volatile Fatty Acids (VFA) under aerobic conditions with the classical anaerobic VFA uptake behaviour. In addition, Oxygen Uptake Rate (OUR) was measured in the set of experiments under aerobic conditions to improve the characterisation of the process. Two different hypotheses for describing the experimental measurements were proposed and modelled. Both hypotheses consider that PAO, under aerobic conditions, take up acetate coupled to PHB storage, glycogen degradation and phosphorus release as in anaerobic conditions. One hypothesis (PAO-hypothesis) considered that PAO were able to store acetate as PHB linked to oxygen consumption and the other (OHO-hypothesis) considered that this storage was due to ordinary heterotrophic organisms (OHO). Both hypotheses were evaluated by simulation extending the model presented in Chapter VII.A to take into account the process involved in the OHO mechanisms.

VII.C.1 Significance of this topic

As described and modelled in Chapter VII.A, EBPR is based on the physical separation between the electron donor (COD) and the final electron acceptor (oxygen or nitrate). One step beyond in PAO knowledge is the analysis of the effect of the simultaneous presence of both the electron donor and the final electron acceptor. Some research can be found in the literature about the effects of the coexistence of COD as electron donor and nitrate as electron acceptor (as for example in Kuba *et al.*, 1996; Pereira *et al.*, 1996 or Filipe and Daigger, 1999). These works are mainly focused in studying the importance of the Denitrifying Polyphosphate Accumulating Organisms (DPAO) in the bio-P sludge.

On the other hand, the coexistence of oxygen and VFA with bio-P sludge is a less studied scenario although P-release under strictly aerobic conditions linked to external substrate uptake can be found in the literature (Henze *et al.*, 2000; Ahn *et al.*, 2002; Serafim *et al.*, 2004; Pijuan *et al.*, 2005). This P release is obviously related to PAO, which are also capable to take up organic substrates under aerobic conditions. However, it is not clear whether, under aerobic conditions, PAO store VFA using oxygen as electron acceptor or linked to glycogen degradation and P-release, as under anaerobic conditions. The analysis of PAO activity under strictly aerobic conditions will contribute to a deeper knowledge of these organisms.

Moreover, this chapter demonstrates that PAO consume a significant amount of oxygen when they take up VFA under aerobic conditions. Hence, the knowledge and quantification of this consumption will provide a better understanding of the respirometric batch profiles obtained with pulses of readily biodegradable substrates to a biomass coming from a WWTP with EBPR.

VII.C.2 Experimental design

VII.C.2.1 EXPERIMENTAL EQUIPMENTS

Two different sets of experiments were conducted. On the one hand, experiments conducted under classical anaerobic/aerobic conditions in the EBPR-SBR equipment (see Chapter III.1.3 for a description of this equipment). On the other hand, batch experiments under aerobic conditions were conducted in a separate SBR identical to the ones of the EBPR-SBR equipment.

Two batch tests were performed under anaerobic/aerobic conditions (AnOx experiments). These experiments were conducted after 150 days of normal SBR operation, when the reactor was working under steady state conditions. Acetate was used as the sole carbon source with an initial concentration of 500 and 250 mg COD_{VFA}/L and the same cycle configuration as the normal operation.

The reactor used for the aerobic batch experiments was inoculated with biomass withdrawn from the EBPR-SBR at the end of the aerobic phase, and left only with aeration during 12 hours to ensure the absence of any external organic substrate. Afterwards, and once the DO level reached a constant value, a pulse of feed was added. This pulse included substrate (COD) and the corresponding amount of P, ammonium and micronutrients as in the normal EBPR operation. Two different tests were performed with initial concentrations in the SBR of 300 and 250 mg COD_{VFA}/L as acetate. The biomass concentration during these experiments was around 2200 mg VSS/L, with a VSS/TSS ratio of 0.80. The pH was controlled during all the experiments at 7.0 ± 0.1 with 1M HCl and the DO was higher than 2 mg/L throughout the experiments.

VII.C.2.2 OUR MEASUREMENT

The OUR profile was obtained by measuring the DO profile in the liquid phase of the reactor, which was working on static conditions (there were neither inputs nor outputs). In addition, it was continuously aerated with a steady flow so that it was operated as a LFS respirometer. Hence, the OUR can be obtained from a simplification of the DO balance in the liquid phase (equation VII.C1):

$$OUR_{EX}(t) = k_L a_{O2} \cdot (S_{OE} - S_O(t)) - \frac{dS_O}{dt} \qquad \text{(VII.C1)}$$

where S_{OE} is the constant equilibrium value of DO reached when the biomass is aerated under endogenous conditions (see Chapter III.1.1 for a detailed description of the respirometer operation). The k_La_{O2} of the reactor was calculated following the procedure originally described by Bandyopadhyay *et al.* (1967) (i.e. a least square optimisation process on the reaeration profile obtained with the action of turning the aeration off and subsequently turning it on).

VII.C.2.3 PARAMETER ESTIMATION

The criterion for selecting the identifiable parameters was based on the Fisher information matrix (FIM) as in many other studies (e.g. Weijers and Vanrolleghem, 1997 or Dochain and Vanrolleghem, 2001 among many others). This method is described in detail in Chapter IV. The least squares parameter estimation method implemented in the MATLAB® function *"fminsearch"* was used. Hence, the weighed sum J (equation VII.C2) of squared errors between model outputs $y(k,\chi)$ and the measured outputs $y_M(k)$, with Q_K as weighting matrix, was minimised:

$$J = \sum_{k=1}^{N} (y(k,\chi) - y_M(k))^T Q_K (y(k,\chi) - y_M(k)) \qquad \text{(VII.C2)}$$

where N is the number of measurements.

Each one of the output signals can be linearised in the neighbourhood of the optimal vector of parameters χ_O as can be seen in equation VII.C3.

$$y(t,\chi_O + \delta\chi) = y(t,\chi_O) + \left(\frac{\delta y(t,\chi_O)}{\delta \chi^T}\right)_{\chi_O} \cdot \delta\chi = y(t,\chi_O) + Y_\chi^T(t)\,\delta\chi \qquad \text{(VII.C3)}$$

where $Y_\chi(t)$ is the so called output sensitivity function. The information related to the dependencies among parameters is also summarised in the FIM (Mehra, 1974). If Q_K is the covariance matrix of the measurement noise, the FIM is defined as equation VII.C4.

$$FIM \mid \sum_{k \mid 1}^{N} Y_\chi^T(k) Q_K^{41} Y_\chi(k) \qquad \text{(VII.C4)}$$

Then, the FIM matrix summarises the quantity and quality of information obtained in each experiment because it gathers the output sensitivity functions and the measurement accuracy. In addition, assuming white measurement noise and no model mismatch, the inverse of the FIM provides the lower bound of the parameter estimation error covariance matrix, which can be used for assessing the estimation uncertainty of χ_O (equation VII.C5).

$$COV(\chi_O) \varnothing FIM^{41} \qquad \text{(VII.C5)}$$

VII.C.3 AnOx experiments modelling

VII.C.3.1. EXPERIMENTAL RESULTS

Experiment VII.C1 (Table VII.C1) was conducted to obtain information about the steady-state operation of the EBPR-SBR.

Table VII.C1 Experiment VII.C1

EXPERIMENT VII.C1	Calibration and validation of AnOx model
Equipment	EBPR-SBR
pH	7.0
Temperature	25 ºC
Acid used	HCl = 1 M
Pulses	500 mg COD_{VFA}/L (calibration)
	250 mg COD_{VFA}/L (validation)

The model used to describe these experiments was developed as a modification of the ASM2 (Henze *et al.*, 2000). The main modification introduced consisted in the inclusion of glycogen economy, as many other models found in the literature (Smolders *et al.*, 1994a,b; Mino *et al.*, 1995; Filipe and Daigger, 1999; Van Veldhuizen *et al.*, 1999; Manga *et al.*, 2001; Hao *et al.*; 2001). The complete development of this model is detailed in Chapter VII.A and the stoichiometry and kinetics are depicted in Tables VII.A1 and VII.A2.

The estimated parameters were q_{PHA}, Y_{AC1}, Y_{GLY1}, Y_{PO}, q_{PP}, σ_{PAO}, q_{GLY} and $X_{GLYMAX,}$ which were practically identifiable with the measured outputs (acetate, PHB, glycogen and phosphate). The fact of having four different measurements facilitated a lot the identifiability of these parameters. The covariance matrix of the measurement noise (Q_K) was required for FIM calculation (equation VII.C4). This matrix was calculated with the measurement errors of the experimental data. Glycogen and PHB measurements were done by triplicate and the covariance error was estimated as the standard deviation. For acetate and phosphorus measurements, the covariance error was estimated as 5% of the measurement. The rank of the FIM gave an indication of the theoretical parameter identifiability since this matrix represented an approximation of the Hessian matrix of the cost function (J). In this study, FIM was found to be non-singular so the model could be considered locally identifiable (Weijers *et al.*, 1996) and, hence, these eight parameters were practically identifiable with the experimental data of this work. Then, the inverse of FIM was calculated to achieve the estimation uncertainty of the parameters according to the procedure described in Dochain and Vanrolleghem (2001).

Figures VII.C1 and VII.C2 show the experimental results of acetate, phosphate, PHB and glycogen obtained for the calibration and validation experiments, which showed the typical EBPR trend. PHA are polymers of different hydroxyalkanoic acids, but when acetate is used as the only carbon source, PHA appears mainly as PHB (Satoh *et al.*, 1992). For simplification, in this chapter PHA was considered as PHB. As can be seen in both figures, the model describes reasonably well the experimental profiles obtained.

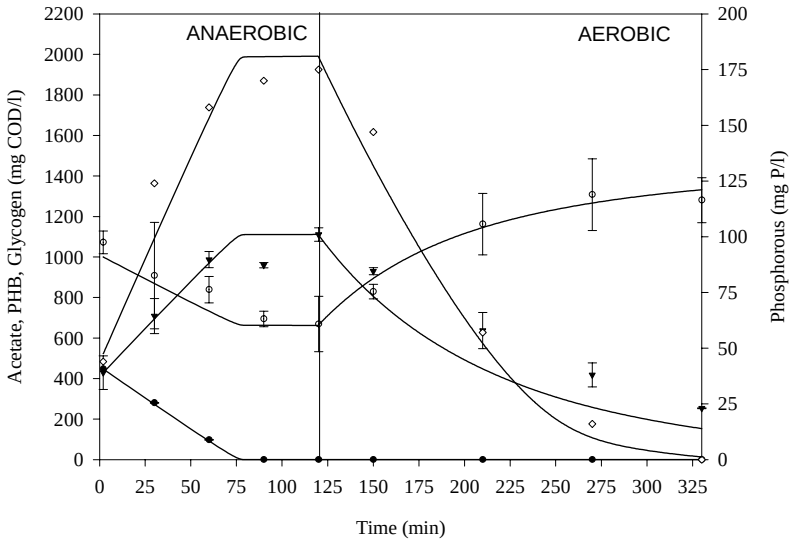

Figure VII.C1 Experimental measurements and simulated values for calibration cycle study with an initial concentration of acetate of 500 mg COD_{VFA}/L
(¸-Acetate, Ã-Phosphorus, ¡-Glycogen, q-PHB, ∝∝ model)

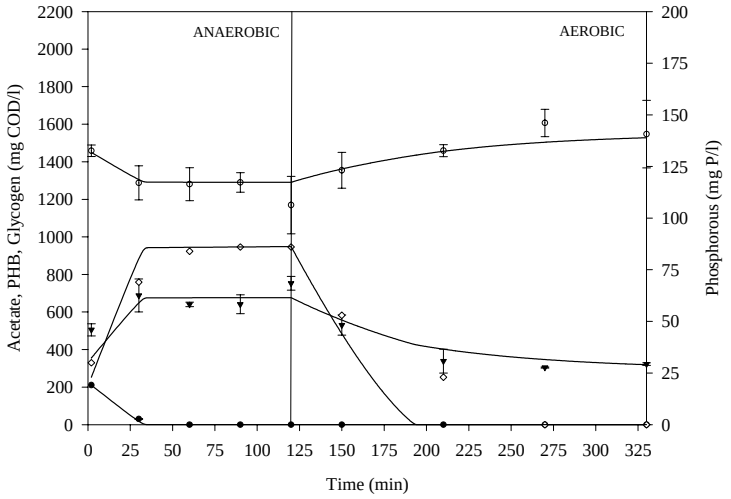

Figure VII.C2 Experimental measurements and simulated values for validation cycle study with an initial concentration of acetate of 250 mg CODVFA/L.
(¸-Acetate, Ã-Phosphorus, ¡-Glycogen, q-PHB, ∝∝ model)

VII.C.3.2 PARAMETER ESTIMATION RESULTS

The parameters which were not estimated were either assumed from ASM2 (Henze *et al.*, 2000), or from Manga *et al.* (2001) (indicated with *). The values obtained for the yields in the anaerobic phase could indicate that a fraction of GAO were present in the EBPR-SBR. Table VII.C2 compares the values for Y_{PO} and Y_{GLY} with the values obtained in the experiments of chapter VII.A and the values of the metabolic model of Smolders *et al.* (1994). As can be observed both yield values indicate the presence of GAO since more glycogen is degraded and less P is released per gram of PHA produced.

Table VII.C2 Comparison of Y_{PO} and Y_{GLY} with literature values

	Experiment VII.C1	Experiments VII.A2	Smolders *et al.* (1994)
Y_{PO} (gP/gCOD$_{PHA}$)	0.195	0.5	0.32
Y_{GLY} (gCOD$_{GLY}$/gCOD$_{PHA}$)	0.54	0.42	0.33

Actually, it is shown to be quite difficult to avoid the presence of GAO in a typical bio-P sludge coming from a standard AnOx process, particularly when acetate is used as a sole carbon source (Pijuan *et al.*, 2004a). A lot of research about GAO and PAO competition is being conducted, as for example in Liu *et al.* (1996), Filipe *et al.* (2001a,b), Manga *et al.* (2001) or Zeng *et al.* (2003). However, distinguishing between the two populations was beyond the scope of this study. This chapter aimed at analysing the behaviour of a bio-P sludge (which may contain GAOs) when organic carbon source and oxygen were present simultaneously. Moreover, further work on this topic with a bio-P sludge population without GAO showed the same behaviour (Pijuan *et al.*, 2005a,b),.

The parameter estimation results obtained for the experiments VII.C1 and VII.C2 are presented in Table VII.C3.

Table VII.C3 Value and description of the parameters of the AnOx model (COD_X = biomass COD, COD_{VFA} = external substrate (acetate) COD, COD_{PHA} = PHA COD, COD_G = Glycogen COD, COD_I = Inert COD).

Parameter	Description	Value	Units
Y_{AC1}	Ac consumed per PHA stored	0.663 ∂ 0.016	g COD_{VFA} / g COD_{PHA}
Y_{PO}	P released per PHA stored	0.195 ∂ 0.007	g P / g COD_{PHA}
Y_{GLY1}	Glycogen degraded per PHA stored	0.54 ∂ 0.05	g COD_G / g COD_{PHA}
Y_{PHA}	PHA degraded per poly-P stored	0.20	g COD_{PHA} / g P
$^{(*)}Y_{GLY3}$	Glycogen stored per PHA converted	1	g COD_G / g COD_{PHA}
Y_{PAO}	PAO Yield biomass/PHA	0.3	g COD_X / g COD_{PHA}
q_{PHA}	PHA storage rate constant (PAO)	8.0 ∂ 0.3	g COD_{PHA} / g COD_X /d
q_{PP}	Poly-P storage rate constant	1.350 ∂ 0.001	g P / g COD_X/ d
q_{GLY}	Glycogen storage rate constant	22 ∂ 9	g COD_G / g COD_X / d
σ_{PAO}	Maximum PAO growth rate	0.463∂ 0.021	1/d
b_{PAO}	PAO lysis rate constant	0.2	1/d
b_{PP}	Poly-P lysis rate constant	0.2	1/d
b_{PHA}	PHA lysis rate constant	0.2	1/d
b_{GLY}	Glycogen lysis rate constant	0.2	1/d
K_O	Saturation coefficient for DO	0.20	mg DO/L
K_S	Saturation coefficient for acetate	4	Mg COD_S /L
K_{PP}	Saturation coefficient for poly-P	0.01	g P/g PAO
$^{(*)}K_{GLY}$	Saturation coefficient for glycogen	0.001	Mg COD_G /L
$^{(*)}K_{PHA-P}$	Saturation coefficient for PHA in polyP storage	0.07	g COD_{PHA}/g COD_X
K_{PS}	Saturation coefficient for P in polyP storage	0.2	mg P/L
K_{MAX}	Maximum ratio of X_{PP}/X_{PAO}	0.34	g P/g PAO
K_{IPP}	Inhibition coefficient for X_{PP} storage	0.02	g P/g PAO
X_{GLYMAX}	Maximum ratio of X_{GLY}/X_{PAO}	0.71 ∂ 0.06	g COD_G /g COD_X
K_{PHA-G}	Saturation coefficient for PHA	0.01	g PHA/g^{-1} PAO
K_P	Saturation coefficient for P in PAO storage	0.01	mg P/L^{-1}
i_{BPM}	P content of biomass	0.02	g P/g COD_X
τ_{5P}	P released in PAO lysis	0.01	g P/g COD_X
f_{XI}	X_I produced in PAO lysis	0	g COD_I/g COD_X

The parameters which were not estimated were taken from ASM2, except for three parameters (*) from Manga et al. (2001)

The CO_2 production under anaerobic conditions due to the PHB storage process predicted in this work (0.16 C-mol / C-mol) agreed with the ratio obtained in these other studies such as Smolders *et al.* (1994a) or Zeng *et al.* (2003). Besides, some rates were higher than those found in the literature, as q_{PHA} (Henze *et al.*, 2000) and q_{GLY} (Manga *et al.*, 2001). The reason could be that the system of this study was more dynamic in the COD variations compared to the cited systems of the literature. Hence, SBR would probably be more effective in the selection for biomass that take up and store substrate very fast (Dircks *et al.*, 2001).

The confidence intervals of the obtained parameters were low, with the exception of the glycogen storage rate constant (q_{GLY}). The reason was that the experimental glycogen measures showed an important measurement error (high standard deviation).

VII.C.4 Modelling aerobic experiments

VII.C.4.1 EXPERIMENTAL RESULTS

Experiments VII.C2 (Table VII.C4) were conducted to assess the behaviour of bio-P sludge under strictly aerobic conditions. This biomass was withdrawn from the reactor where the AnOx set of experiments was previously performed.

Table VII.C4 Experiment VII.C2

EXPERIMENT VII.C2	Aerobic calibration experiment
Equipment	Aerobic-SBR
pH	7.0
Temperature	25 ºC
Acid used	HCl = 1 M
Pulses	300 mg COD_{VFA}/L (calibration)

Figure VII.C3 shows the experimental profiles obtained in experiment VII.C2. Two different phases could be distinguished, despite the aeration conditions were not changed along the experiment. The first phase coincided with the presence of acetate, which was stored as PHB. In this phase, P was released and glycogen was degraded. Afterwards, in the second phase, PHB was consumed and biomass grew on the accumulated polymer. In these phase P was uptaken and glycogen was produced.

These two phases of accumulation and subsequent growth are known in the literature as feast / famine phases when referring to heterotrophic consumption of an external substrate (e.g. Majone *et al.*, 1999; Dircks *et al.*, 2001). In this work, these phases were also analogous to the anaerobic / aerobic phases of the EBPR process according to the trends of acetate, phosphate, PHB and glycogen.

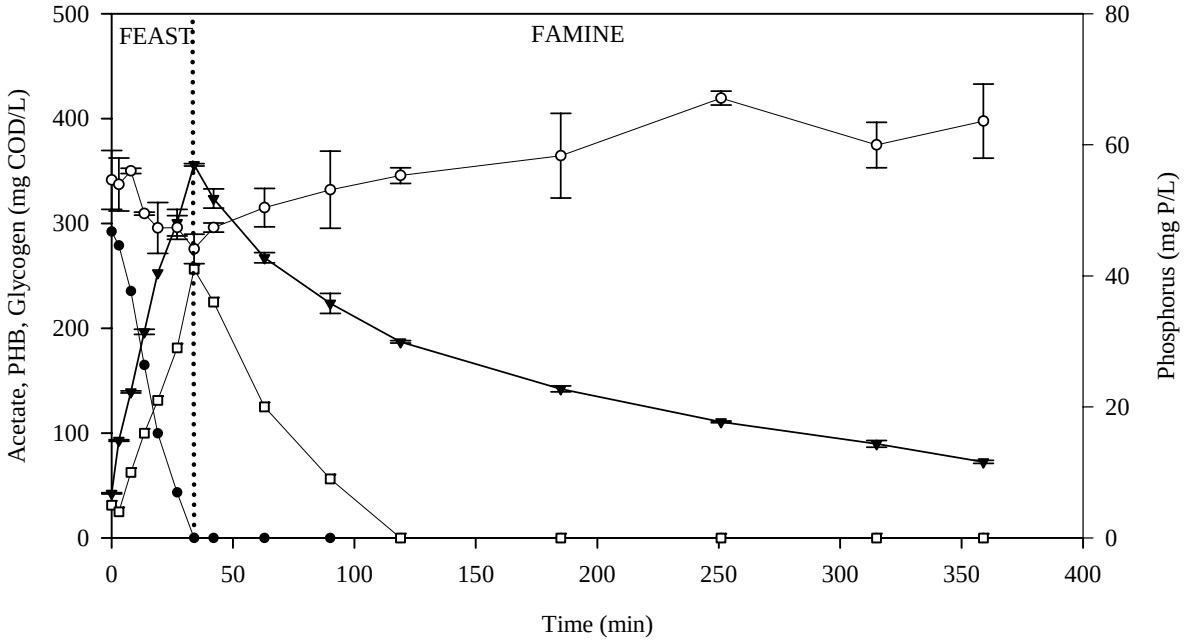

Figure VII.C3 Measured profiles of experiment VII.C2.
¸-Acetate, Ã-Phosphorus, ¡-Glycogen, q-PHB

Accordingly, while acetate was consumed in the feast phase, PHB was stored. In this storage process, glycogen degradation and phosphate release were experimentally observed. These events are uniquely characteristic of PAO behaviour, and they are carried out in order to obtain the necessary reducing power and energy to store PHB. Hence, these experimental results were very interesting since PAO seem to behave the same way than under anaerobic conditions despite the oxygen presence.

In addition, OUR was measured (Figure VII.C4) in order to obtain supplementary information about the process. The OUR value obtained was considerably high during acetate consumption (from 0 to 35 min). When acetate was depleted, the OUR value decreased, but some oxygen consumption was observed until minute 370. The high OUR in the feast phase could be assigned to acetate storage as PHB. Hence, it can be concluded that the acetate uptake is linked to oxygen consumption despite PAO are used to taking up acetate under anaerobic conditions.

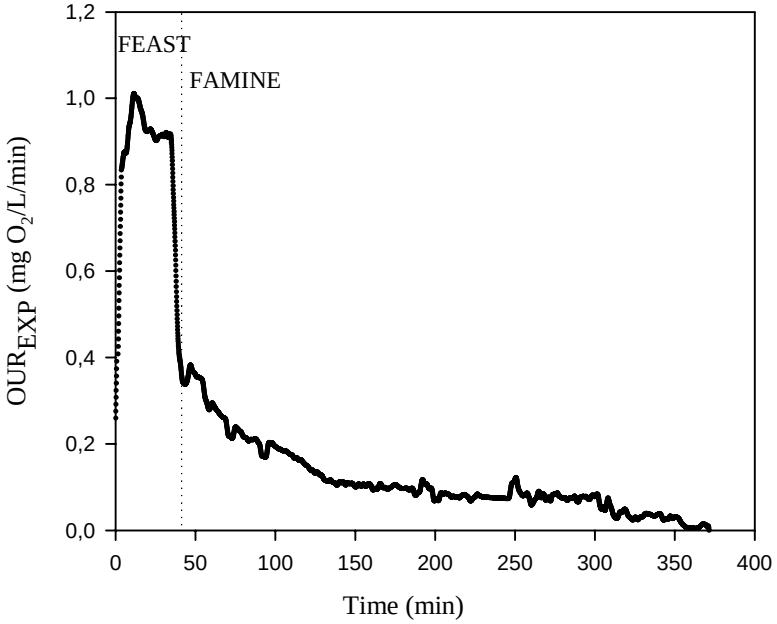

Figure VII.C4 OUR profile for experiment VII.C2

In the famine phase, once the acetate was exhausted, the profiles obtained coincided with the typical EBPR behaviour under aerobic conditions: PHB was degraded (allegedly for PAO growth and to restore the glycogen internal pool), glycogen was accumulated and orthophosphate was taken up.

VII.C.4.2 MODELLING WITH THE CONVENTIONAL AnOx MODEL

At this point, the AnOx model previously described was simulated with the initial conditions of the relevant compounds of the aerobic experiment (Figure VII.C5 solid line) and compared with the experimental data. The kinetic and stoichiometric parameters of the PAO processes were not modified with respect to the parameters estimated in experiment VII.C1, except for the X_{GLYMAX} parameter of the glycogen storage process. This parameter was changed from 0.71 to 0.40 g COD_{GLY}/g COD_X because the initial glycogen levels were very different between both sets of experiments.

Moreover, the kinetics of the three typical EBPR aerobic processes (i.e. poly-P storage, glycogen storage and PAO growth) were slightly modified. As these processes are supposed to occur under aerobic conditions, a new term was required in order to prevent these processes from occurring simultaneously with PHB storage when acetate was present. This term was a switch on acetate: $K_{AC}/(S_{AC}+K_{AC})$, with K_{AC} estimated as 10 mg COD_{VFA}/L.

In the AnOx model (i.e. conventional EBPR operation), these processes cannot occur simultaneously because they include an inhibition term on oxygen. Hence, in the AnOx model the oxygen concentration was the switch between the two phases, whereas under strictly aerobic conditions the depletion of acetate was the switching factor.

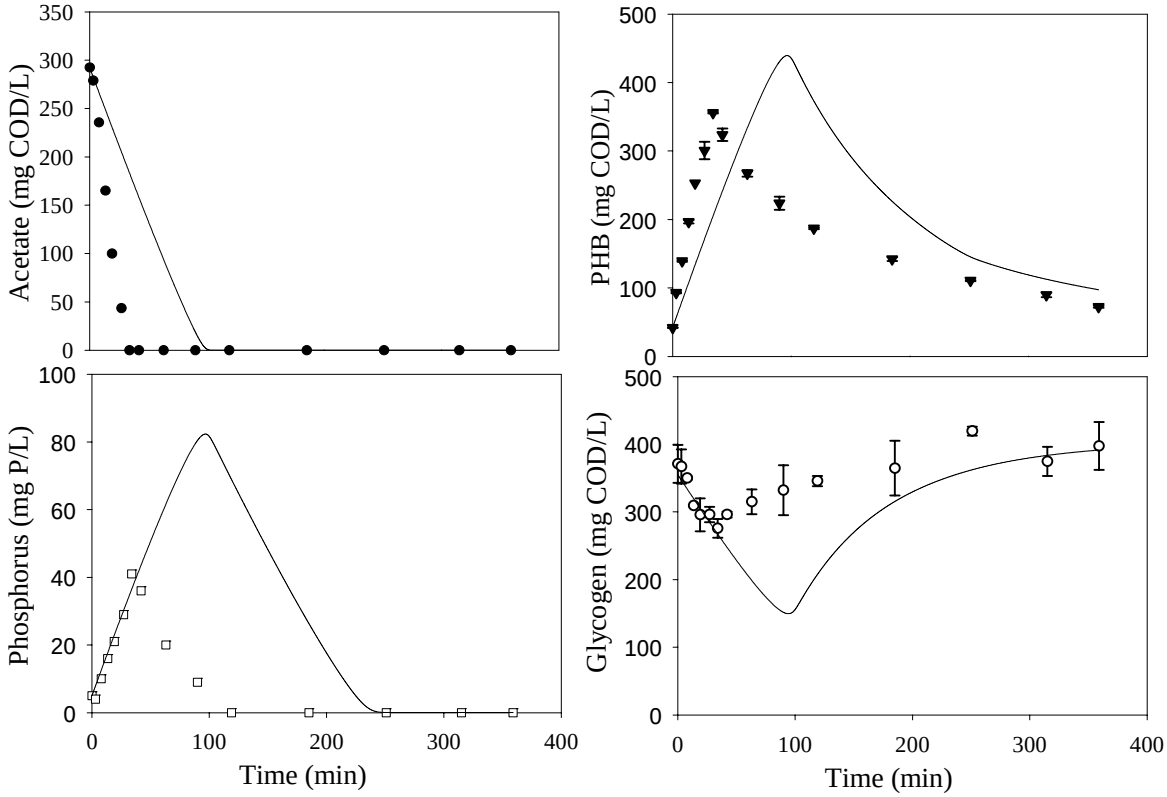

Figure VII.C5 Experimental measurements of experiment VII.C2 (¸ -Acetate, Ã-Phosphorus, ¡ -Glycogen, q -PHB). Simulated values with the AnOx model (∝ ∝).

As can be observed, P-release and glycogen degradation in the feast phase were well predicted by the AnOx model. These profiles were characteristic of PAO behaviour. However, the model prediction did not agree with the evolution of these compounds along the famine phase, because the point where the acetate was totally consumed (end of the feast phase) was not well predicted. Moreover, the AnOx model underestimated the rates of acetate consumption and PHB storage, as observed Kuba *et al.* (1996) in their experiments with nitrate as final electron acceptor. This fact indicated that existed an additional consumption of acetate for PHB storage, with neither P-release nor glycogen degradation. Kuba *et al.* (1996) also observed that part of acetate was oxidised through the tricarboxylic acid cycle (TCA), to obtain energy and reduction equivalents for PHB storage, when nitrate was present. In addition, the high OUR observed in the feast phase (Figure VII.C4) could not be predicted with the model of Chapter VII.A and probably the consumption of this "excess" of acetate for PHB storage was linked to oxygen consumption.

At this point, two different hypotheses were proposed. Both hypotheses considered that PAO, under aerobic conditions, uptake acetate coupled to PHB storage, glycogen degradation and phosphorus release as under anaerobic conditions. Moreover, the first hypothesis (PAO-hypothesis) considered that PAO were able to store additional acetate as PHB linked to oxygen consumption. The second one (OHO-hypothesis) considered that a different biomass fraction, OHO, was the only responsible for this additional consumption of acetate. Both hypotheses were evaluated by simulation, extending the AnOx model with additional equations, and using the parameters of Table VII.C3 without modifications.

VII.C.4.3 PAO HYPOTHESIS

The PAO-hypothesis implies that PAO can oxidise part of the acetate using oxygen as electron acceptor in order to obtain energy to store PHB. Then, PAO should take advantage of the much more efficient aerobic metabolism. In addition, P-release was observed under aerobic conditions, which meant that PAO also used the classical polyP hydrolysis mechanism for energy supply. This hypothesis was considered and modelled by extending the AnOx model with process 9a (Table VII.C5), so that PAO can store aerobically as PHB as described in the ASM3 model (Henze *et al.*, 2000).

A factor was added to this PHB storage process in order to describe the time delay in reaching the maximum OUR value experimentally observed after adding acetate. This phenomenon, known as "start-up", is probably caused by many factors such as mixing, substrate diffusion or metabolic pathways activation (Vanrolleghem *et al.*, 2004), and can be mathematically described by a first order delay (Guisasola *et al.*, 2003; Vanrolleghem *et al.*, 2004). The model was simulated maintaining the previous parameter values for the processes 1-8. For the process 9a, the value for the yield Y_{STO} was assumed to be the same of ASM3 (Henze *et al.*, 2000), and the storage rate constant (k_{STO}) was modified in order to fit the experimental profiles for acetate. Figure VII.C6 shows the experimental results versus the modelling profiles. As can be observed, the feast phase was well described using this new process but, in the famine phase, PHB degradation was underestimated.

Table VII.C5 Stoichiometry and kinetics of the PAO-hypothesis model (9a).

PROCESS		STOICHIOMETRY				KINETICS
		S_S	S_{O2}	S_{CO2}	$X_{PHA,HET}$	
9a	Aerobic X_{PHA} storage by X_{PAO}	$\frac{41}{Y_{STO}}$	$\frac{4(1\ 4\ Y_{STO})}{Y_{STO}}$	$\frac{1}{8\hat{A}_{STO}}\cdot(\frac{\hat{A}_{STO}}{Y_{STO}\cdot\hat{A}_S}-1)$	1	$k_{STO}\cdot M_{AC}\cdot M_O X_{PAO}\cdot(1-e^{-t/\vartheta})$

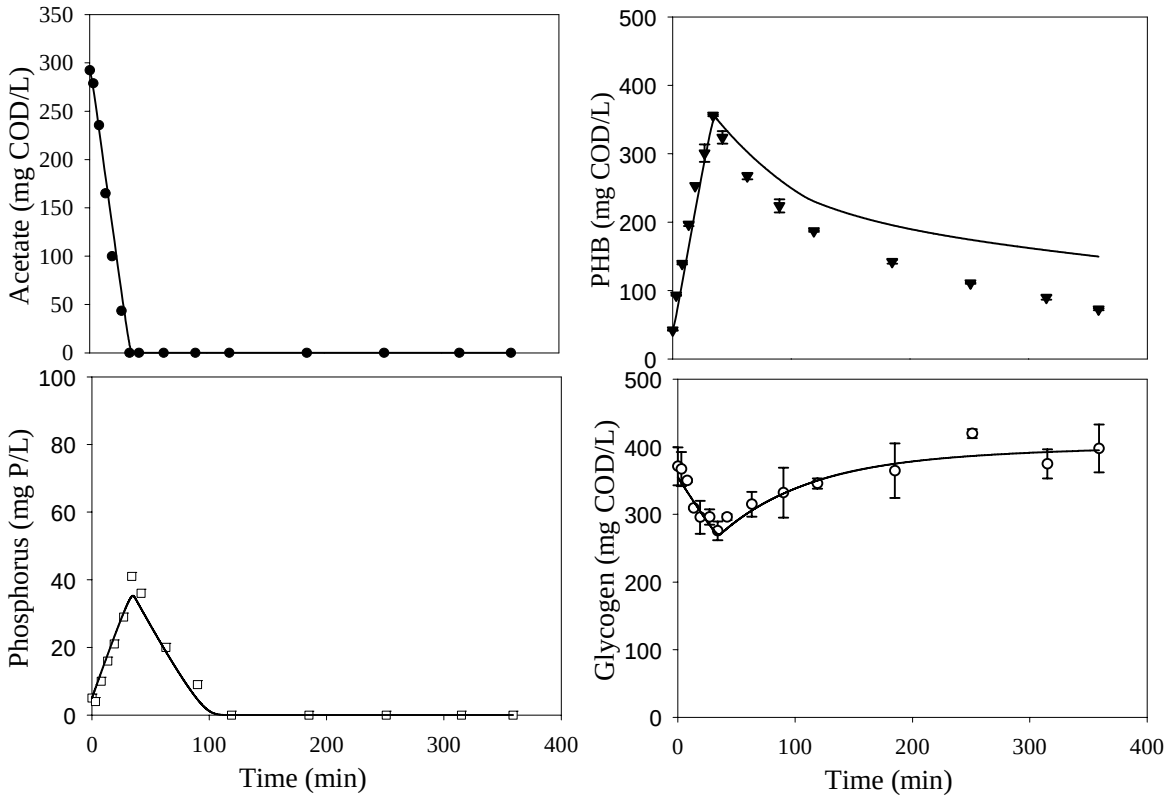

Figure VII.C6 Experimental measurements of experiment VII.C2 (¸-Acetate, Ã-Phosphorus, ¡-Glycogen, q-PHB). Simulated values with the PAO hypothesis model (∝ ∝).

VII.C.4.4 OHO HYPOTHESIS

The model presented in Chapter VII.A was extended with two new processes (9b and 10 of Table VII.C6) to simulated the OHO-hypothesis. These processes were adapted from the ASM3 model. Two different contributions of PHB were considered: PHB from PAO and PHB from OHO. The sum of both contributions should be equal to the PHB measured.

Table VII.C6 Stoichiometry and kinetics of the OHO-hypothesis model (9b and 10).

	PROCESS	STOICHIOMETRY					KINETICS
		S_S	S_{O2}	S_{CO2}	$X_{PHA,HET}$	X_H	
9b	Aerobic X_{PHA} storage by X_H	$\frac{41}{Y_{STO}}$	$\frac{4(1\ 4\ Y_{STO})}{Y_{STO}}$	$\frac{1}{8\hat{A}_{STO}}\cdot(\frac{\hat{A}_{STO}}{Y_{STO}\cdot\hat{A}_S} - 1)$	1		$k_{STO}\cdot M_{AC}\cdot M_O X_H\cdot(1 - e^{-t/\vartheta})$
10	X_H growth		$\frac{4(1\ 4\ Y_H)}{Y_H}$	$\frac{1}{8\hat{A}_X}\cdot(\frac{\hat{A}_X}{Y_H\cdot\hat{A}_{STO}} - 1)$	$\frac{41}{Y_H}$	1	$\sigma_H\cdot M_O\cdot\frac{X_{PHA}/X_H}{K_{STO}\ 2\ X_{PHA}/X_H} X_H$

The model was fitted maintaining the previous values for the parameters of the 8 first processes. In the processes 9b and 10, the value for the yield Y_{STO} was assumed to be the same of ASM3. The practical identifiability of the five parameters optimised (k_{STO}, μ_H, Y_H, Ű, and $K_{S,HET}$) with the 5 outputs measured (acetate, PHB, glycogen, phosphate and OUR) was checked with the FIM procedure as in the AnOx model. Likewise, the confidence interval of the parameters was also estimated.

The parameters used in these processes are presented in Table VII.C7. The confidence intervals for the estimated parameters were much lower than the previous case. The reason was the extra amount of information provided by the OUR measurement (measuring interval: 5 seconds). Moreover, the number of parameters in this case was only 5 compared to the 8 of the previous case. The obtained k_{STO} (8.9 $gCOD_{PHA}/gCOD_X/d$) was higher than default value of ASM3 (i.e. 5 $gCOD_{PHA}/gCOD_X/d$). The reason could be the same as previously discussed for q_{PHA} and q_{GLY}. In addition, the obtained Y_H (0.7 $gCOD_X/gCOD_{PHA}$) was higher than the default ASM3 value (i.e. 0.63). The variability of this parameter is already discussed in Chapters V.C and V.B.

Table VII.C7 - Value and description of the parameters (COD_X = biomass COD, COD_{VFA} = external substrate (acetate) COD, COD_{PHA} = PHA COD, COD_G = Glycogen COD)

Paramteter	Description	Value	Units	From
Y_{STO}	PHA produced per acetate uptaken	0.85	$gCOD_{PHA}/gCOD_{VFA}$	Henze *et al*. (2000)
Y_H	Heterotrophic growth yield	0.70 ± 0.06	g COD_X/g COD_{PHA}	This study
k_{STO}	Storage rate constant	8.93 ± 0.04	g COD_{PHA}/g COD_X/d	This study
σ_H	Heterotrophic growth rate	2.88 ± 0.03	1/d	This study
K_{STO}	Storage process constant	1	g COD_{PHA}/g COD_X	Henze *et al*. (2000)
K_{S_HET}	Heterotrophic sat. coeff. for Acetate	10.00 ± 0.06	mg COD_{VFA}/L	This study
ϑ#	Time constant	3.0 ± 0.1	min	This study

Figure VII.C7 shows that the model from the OHO-hypothesis described accurately the evolution of all the components in both feast and famine phases.

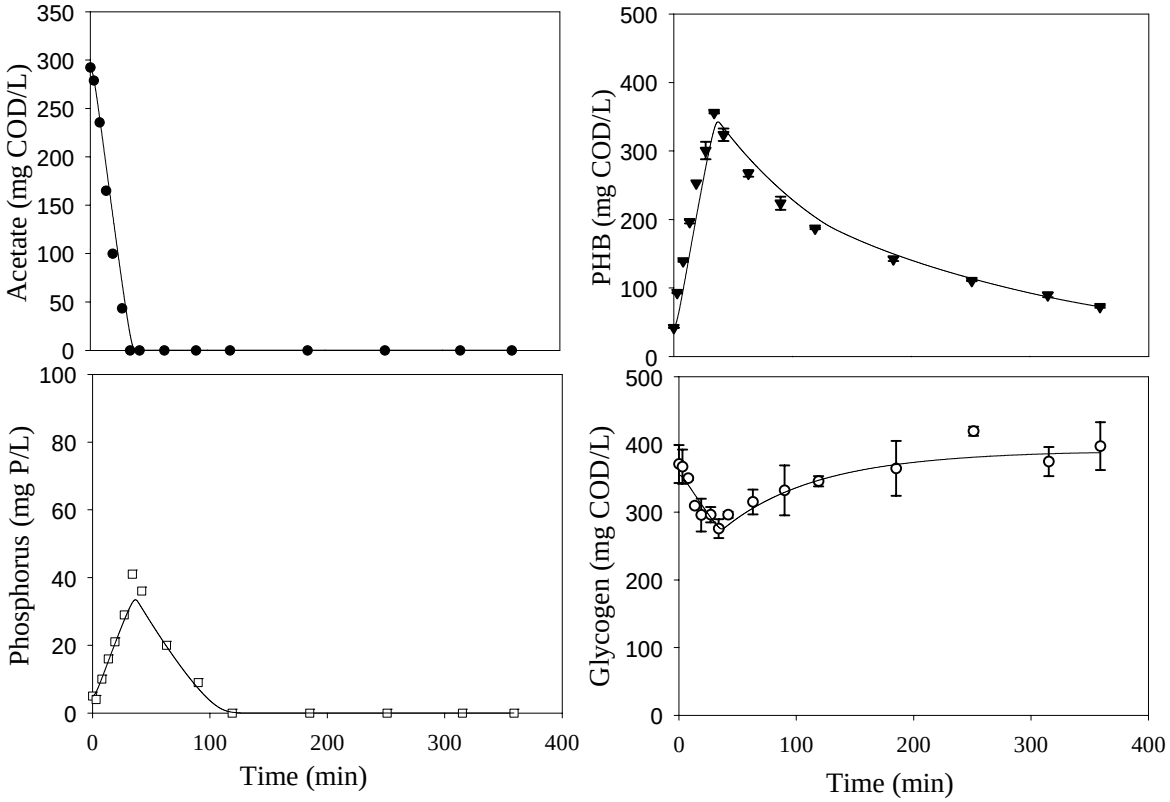

Figure VII.C7. Experimental measurements of experiment VII.C2 (¸ -Acetate, Ã-Phosphorus, ¡ -Glycogen, q -PHB). Simulated values with the OHO-hypothesis model (∝ ∝).

Figure VII.C8 shows the predicted OUR profiles with both the PAO- and OHO-hypothesis. As can be observed, the latter made a better prediction of the OUR profile (dashed-dotted line) than the PAO-hypothesis (dashed line) during both phases.

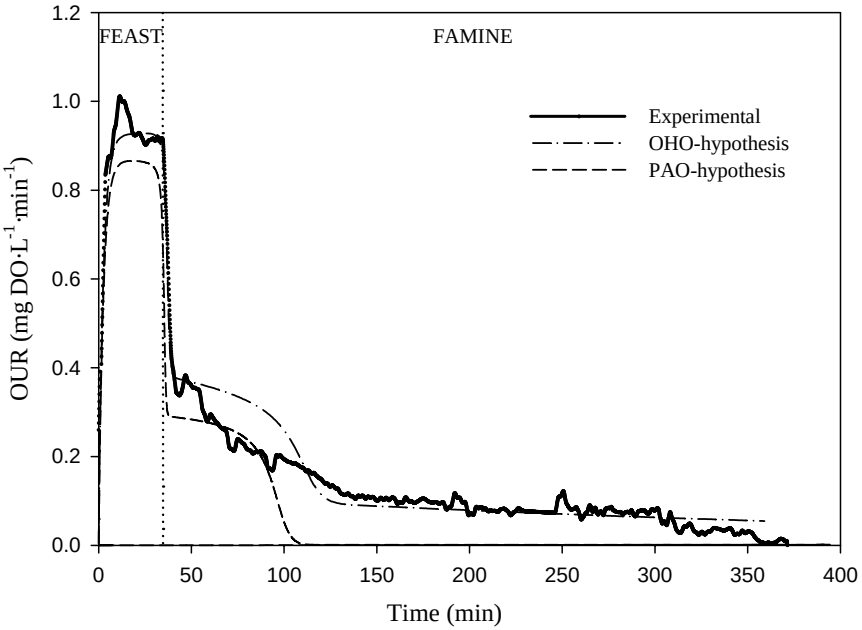

Figure VII.C8 Experimental and simulated OUR profiles of experiment VII.C2. Experimental OUR (solid), OHO-hypothesis (dash-dotted) and PAO-hypothesis (dashed)

Experiment VII.C3 (Table VII.C8) was conducted to validate the results of experiment VII.C2.

Table VII.C8 Experiment VII.C3

EXPERIMENT VII.C3	Aerobic validation experiment
Equipment	Aerobic-SBR
Ph	7.0
Temperature	25 ºC
Acid used	HCl = 1 M
Pulses	250 mg COD_{VFA}/L (validation)

In addition, it was tested whether the calibrated model for each hypothesis was able to describe the new experimental data. The experimental results shown in Figure VII.C9, confirm that, under aerobic conditions, P-release occurred simultaneously to acetate uptake, glycogen degradation and PHB storage. This figure also shows the predicted profiles for both hypotheses.

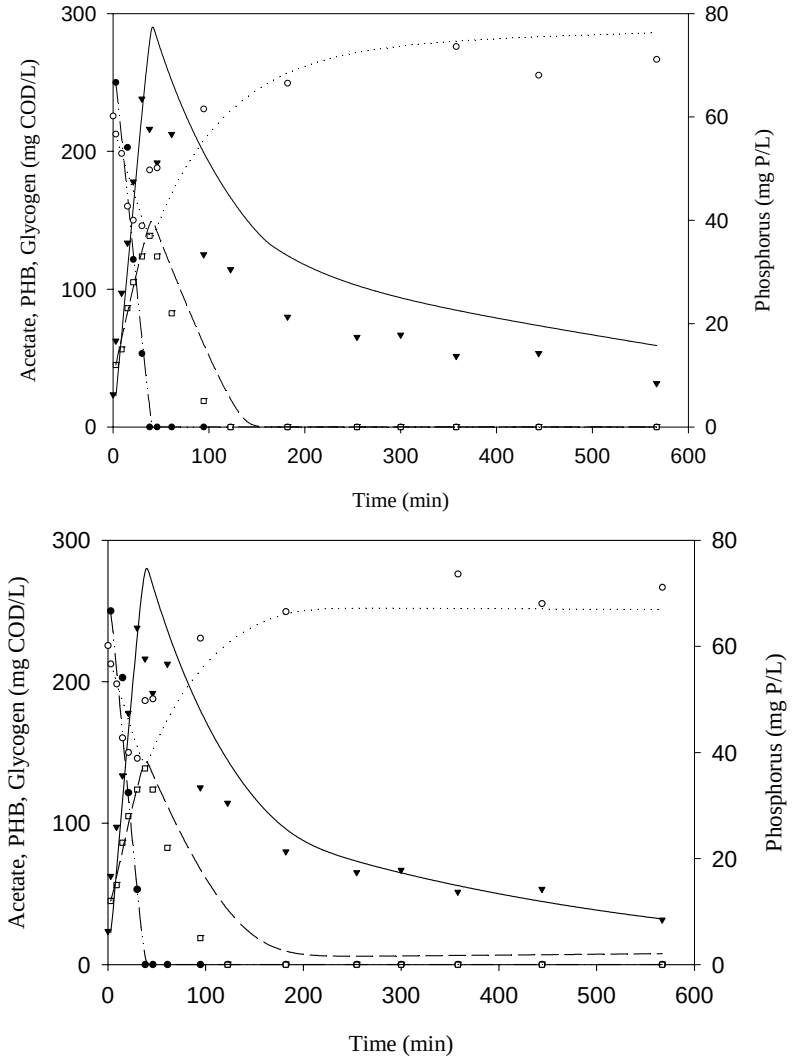

Figure VII.C9 Experimental measurements of different compounds experiment VII.C3. PAO hypothesis (UP) and OHO hypothesis (DOWN)
¸-Acetate, Ã-Phosphorus, ¡-Glycogen, q-PHB, -·-· Acetate model, -- Phosphorus model, ··· Glycogen model, ∝ PHB model.

The PAO-hypothesis model described adequately the feast phase, although the PHB degradation and the poly-P storage in the famine phase were underestimated. The observed behaviour for PHB was quite similar to the observed in the calibration experiment of this hypothesis (Figure VII.C3).

However, the poly-P storage process was better described in the calibration experiment. The OHO-hypothesis model also described adequately the feast phase and underestimated the poly-P storage in the famine phase. However, the OHO-hypothesis provided a better description of the PHB degradation in the famine phase.

VII.C.5 Discussion of the results

A conventional bio-P sludge obtained from a SBR operated with normal EBPR conditions (anaerobic/aerobic cycles) was used to test its behaviour under aerobic conditions. The results obtained showed that this bio-P sludge stored acetate as PHB, linked to glycogen degradation and P-release under aerobic conditions. These results could not be reliably described using a modified ASM2 model, calibrated with the same bio-P sludge in anaerobic/aerobic conditions since it underestimated the acetate uptake and the PHB storage in the feast phase (Figure VII.C5). Moreover, it did not describe the high experimental OUR observed during the feast phase (Figure VII.C8).

Two hypotheses were proposed to describe the experimental measures. Both hypotheses considered that PAO, under aerobic conditions, uptake acetate coupled to PHB storage, glycogen degradation and phosphorus release as in anaerobic conditions. However, the additional consumption of acetate was attributed to different biomass fractions depending on the hypothesis.

Both hypotheses were evaluated by simulation, extending the AnOx model with additional equations. The OHO-hypothesis described the experimental profiles more accurately than the PAO-hypothesis (Figures VII.C6-VII.C8). The major achievements of the OHO-hypothesis were the better predictions of the PHB degradation during the famine phase and of the OUR profile during both feast and famine phases. The different PHB degradation predicted by both hypotheses was due to the growth of OHO. This process predicted heterotrophic biomass growth using PHB. This additional consumption provided a better description of the PHB profile for OHO-hypothesis.

The most important difference between both hypotheses was observed in the OUR profiles (Figure VII.C8). During the feast phase, the oxygen consumption predicted by the OHO-hypothesis was higher than the one predicted by the PAO-hypothesis and closer to the experimental values. The difference between both models during the feast phase was that the oxygen consumption in the OHO-hypothesis was due to the simultaneous PHB storage and OHO growth while, in the PAO-hypothesis, the oxygen consumption was only linked to aerobic PHB storage. Both hypotheses did not consider PAO-growth when acetate was present. However, if PAO growth was considered when acetate was present, the OUR of the feast phase predicted by the PAO-hypothesis would be also lower than the experimental and both the P-release (feast phase) and the PHB degradation (famine phase) would be underestimated.

During the famine phase, the oxygen consumption predicted by the PAO-hypothesis model finished around minute 100, whereas the predicted by the OHO-hypothesis model described all the experimental oxygen consumption until minute 360. The reason for this discrepancy was that the kinetics of poly-P storage and PAO growth depend on P concentration, according to ASM2 model (Henze *et al.*, 2000). However, the kinetics of OHO growth (process 10) was predicted in spite of phosphorus absence, according to ASM3 model (Henze *et al.*, 2000).

In accordance with these results, the best description seemed to be provided by the OHO-hypothesis model. However, this observation should not be taken as a strong assertion. It has to be considered that for a more reliable description of the process, the contemplation of simultaneous growth and storage by both biomass fractions should be at least examined. However, this deepening was beyond the scope of this chapter which

aimed to understand the experimental profiles measured when acetate was aerobically consumed by a bio-P sludge.

On the other hand, this model predicted a high fraction of OHO, similar to the fraction of PAO. Probably, this was caused by the fact that the system was not nitrogen bubbled during the anaerobic phase when experiments were conducted. This facilitated OHO growth since there could be some oxygen in the feed phase and some oxygen could be transferred through the surface. In addition, some organic matter could be provided by means of the lysis processes, giving some additional substrate for OHO growth during aerobic phases. However, a rough estimation of the amount of oxygen transferred through the surface indicates that only about 3% of COD could be consumed aerobically. This is a low value which would not allow such a high OHO growth and may somehow contradict the OHO-hypothesis. Obviously, for a detailed model description of the processes occurring, more focusing and experimental data is needed.

VII.C.6 Extension of this chapter: the work of Pijuan *et al.*

This chapter describes the aerobic P-release, i.e. the observation that EBPR biomass can take up acetate under aerobic conditions linked to P release and glycogen degradation. After this observation some experiments were conducted by Pijuan *et al.* (2005a, b) to answer some of the questions that may arise in this chapter. These works represent an extension of the aerobic P release topic and contain extra valuable information such as Fluorescence *In-Situ* Hybridation (FISH) analyses. These analyses allow a qualitative assessment of amount of PAO present in the sludge.

First of all, the aim of Pijuan *et al.* (2005a) was to assess the response of an EBPR biomass in front of an organic substrate (acetate) under aerobic conditions, when this biomass contained different levels of PHA, polyphosphate and glycogen. Different experiments were performed in order to compare the standard reactor operation with the results obtained in batch experiments performed under aerobic conditions with sludge withdrawn at the end of the anaerobic period of the SBR (EAN experiment) and at the end of the aerobic period (EOX experiment). A higher P/C, Gly_{DEG}/Ac_{UPT} and Gly_{DEG}/PHA_F ratios were observed in the EOX experiment. These differences could be attributed to the fact that more polyP was present in the EOX experiment. These ratios suggest a higher PAO activity in the EOX experiment, although the ratio of PHA formed per acetate consumed did not change between both aerobic experiments.

On the other hand, Pijuan *et al.* (2005b) aimed to analyse the evolution of an EBPR community under permanent aerobic conditions. For this aim, biomass was withdrawn from a classical EBPR SBR system and aerated permanently. The shift to only-aerobic cycles was conducted after 90 days of SBR operation, when the reactor was working with an EBPR population in steady state. Once the operational conditions were shifted, the system was equally operated with 4 cycles per day, except for the anaerobic phase which became also aerobic. The OUR profile was obtained using the measured DO profile in the liquid phase of the reactor, which was continuously aerated with a steady flow and FISH analyses were performed during the whole experiment.

The permanent aerobic conditions were maintained for eleven days and net phosphorus removal was achieved during the first 4 days of operation. A progressive decrease in the P-uptake to P-release ratio was observed since the start up, with a lower P-uptake than P-release from the 7^{th} day of aerobic operation. It is remarkable that "*Candidatus* Accumulibacter phosphatis" was the predominant PAO in this study and its percentage did not change when the anaerobic/aerobic SBR was shifted to aerobic SBR. After 11 days of operation under aerobic conditions its percentage was the same as in the beginning.

A progressive decrease in the amount of glycogen in the biomass as well as in the ratios of glycogen degradation and formation was observed along the study. This fact suggests that PAO tended to deplete its internal glycogen, which in aerobic conditions would be less useful than in anaerobic conditions. In addition, PHB production ratio was maintained constant throughout the study, despite the decrease in glycogen degradation in the feast phase. Finally, the OUR profiles obtained suggested the occurrence of some processes (P-uptake, glycogen production and growth) during the feast phase which are generally attributed only to the famine phase.

Chapter VII.C CONCLUSIONS

In this study, a comparison between the behaviour of an EBPR sludge working under anaerobic/aerobic conditions and the behaviour of the same sludge with simultaneous presence of an electron donor (acetate) and a final electron acceptor (oxygen) was performed. The main conclusions obtained are:

- PHB storage from acetate by PAO observed in anaerobic conditions seems not to be affected by the oxygen presence. Under strictly aerobic conditions, PAO can uptake acetate obtaining energy from poly-P hydrolysis and reducing power from glycogen degradation.

- Part of the acetate consumed in aerobic conditions is stored as PHB linked to oxygen consumption.

- Two different hypotheses were formulated and simulated to describe this aerobic acetate consumption and PHB storage. The PAO-hypothesis considered that PAO store acetate as PHB linked to oxygen consumption, in addition to store acetate as PHB linked to P-release and glycogen degradation. The OHO-hypothesis considered that PAO store acetate as PHB linked to P-release and glycogen degradation, and that OHO are the only responsible for the additional acetate consumption and PHB storage.

- Assuming that PAO and OHO populations are well described by the modified ASM2 model and the ASM3 model respectively, the OHO-hypothesis describes better the experimental profiles. Nevertheless, none of both hypotheses can be totally rejected and it is also possible that its combination could describe better the experimental results. More research is needed in this field in order to clarify the experimental observations.

CHAPTER VIII

Summary and future perspectives

This thesis aimed to improve the current knowledge of wastewater biological organic matter and nutrient removal processes through the approach of modelling. These processes are the aerobic COD removal, nitrification and EBPR. There already exist some models in the literature of each process. Hence, a critical revision of these models was required. After that, a new model was developed in each chapter as an extension of the literature models. The models were extended so that they could be calibrated and validated with respirometric and titrimetric techniques.

VIII.1 Model identifiability

When modelling a process, some effort is necessary in examining the identifiability of this model with respect to the available output measurements for a reliable posterior utilisation of the model. Modelling should not be simplified to the estimation of model parameters through minimization algorithms with respect to experimental data. The lack of attention to the identifiability issues has probably caused the existing wide variability of the literature in the parameter estimation values (e.g. biomass yields).

“Modellers” need to realize that the assessment of the confidence intervals of their parameter estimates is as important as the estimation of the parameter value itself. Nowadays, mathematical tools are being developed in order to discriminate which of the model parameters are identifiable or not. A parameter can be identifiable as long as its variation has significant influence on one of the output signals and this output signal is measured with enough quantity and quality.

Chapter IV describes the methodology used in this thesis to deal with the identifiability issues with Andrews model for substrate inhibition as study case. This methodology is based on the Fisher Information Matrix (FIM) calculation. This matrix integrates the sensitivity of the measured outputs with the estimated parameters with the quantity and quality of the experimental data.

This methodology has very important strengths since the information provided for each of the output measurements is quantified in basis of quantity (amount of sampling points) and quality (sensitivity analysis). In this way, the information obtained with each sample point is calculated separately according to the importance of that output variable in the time instant when it was measured. For example, a measurement of nitrite in the nitrification process contains different amount of information depending if is done at the start, in the middle or at the end of the experiment. The sensitivity analysis is a very interesting tool in view of detecting parameter correlation problems. Moreover, the FIM is easily calculated and applicable once the model is developed.

However, the results obtained with on-line measurements are too optimistic when compared to measurements with lower frequency such as substrate or storage products. Each of the sampling points is used to corroborate the model, hence with on-line measurements (such as DO and pH) the sum of information is overestimated. The reason may be that the calculation of the measurement error weighting matrix (Q_K) for the experimental inputs used is too optimistic, despite the values obtained are in the range of similar works (e.g. Petersen, 2000).

FUTURE PERSPECTIVES

- The importance of confidence interval assessment must be stressed in all the modelling publications so that its calculation becomes more widespread. For this aim, the mathematical methodologies should be clearly reported and reviewers should demand their values in case they do not appear.

- The FIM methodology needs to be improved, mainly the Q_K estimation for on-line measurements, for a reliable estimation of confidence intervals.

VIII.2 Biological COD removal

This thesis has shown that the reference models in the field of biological nutrient removal field, Activated Sludge Models (ASM) are not suitable to describe short-term respirometric batch profiles. However, the application of these models in view of designing, monitoring and even for a macroscopic modelling of full-scale WWTP is not debated.

These two models were critically revised for its application with respirometric batch profiles. Hence, both models were fitted to four different respirometric batch profiles obtained with biomass from different WWTPs and some numerical inconsistencies were observed when using these models to interpret the results obtained.

On the one hand, ASM1 is a growth-based model where the biomass is considered to grow solely on the external substrate present. For instance, in experiments with considerable storage, ASM1 was not able to predict the tail observed due to the internal polymer consumption and obviously did not predict the storage product evolution in the cell since this compound was not considered.

On the other hand, ASM3 was developed in 1999 mainly to consider the storage phenomenon. It assumes that all the readily biodegradable organic substrates taken up under feast conditions are directly converted into stored material. These stored compounds become the carbon and energy source for growth purposes in the subsequent famine period. In ASM3, the decay processes are replaced with the endogenous processes. ASM3 could describe this second tail accurately, but non-mechanistic parameters were obtained. In addition, ASM3 is not able to predict the discontinuity in the growth rate of biomass observed experimentally between feast and famine phases. Secondly, ASM3 requires prediction of higher levels of internal storage polymers than measured to fit the oxygen consumption during feast and famine phases. From a practical identifiability point of view, Chapter V.A shows the difficulty to obtain reliable values of the parameters related to the ASM3-growth process because σ_H and K_{STO} are not identifiable, and high correlation exists between Y_{GSTO} and σ_H, and Y_{GSTO} and K_{STO}.

The parameter estimation values obtained in Chapter V.A seem to indicate that both ASM1 growth and ASM3 storage processes may occur at the same time. The main conclusion of Chapter V.A is that an alternative model taking into account simultaneous storage and growth processes should be proposed. For example, the growth yield (Y_H) obtained by fitting ASM1 to the short-term respirometric batch profiles is higher than the default one (0.67) and the storage yield (Y_{STO}) obtained by fitting ASM3 is lower than the default one (0.85). In addition, the introduction of this hypothesis would also help to improve the mechanistic meaning of the estimated parameters. There are some models in the literature which have adopted this approach such as van Aalst-van Leeuwen *et al.,* (1997); Krishna and Van Loosdrecht, (1999); Beccari *et al.,* (2002); van Loosdrecht and Heijnen, (2002) or Karahan Gül *et al.,*(2003).

Hence, a new model for biological COD removal including simultaneous storage and growth was developed in Chapter V.B based on the abovementioned models. This model is particularly focused on describing the natural conditions of a WWTP (i.e. slowly growing biomass under low and alternating F/M ratio with low PHB content). The elementary mass and reduction balances to obtain the corresponding stoichiometric coefficients and the deduction of the kinetics of each process is described in Chapter V.B. This model was based on a revision on previous models found in the literature, particularly following the research line of the Technical University of Delft. In addition, the model was developed to be calibrated using both respirometric and titrimetric data.

The major points of this model are:

A. IDENTIFIABILITY OF THE THREE YIELDS

If the simultaneous growth and storage is admitted, a new model with at least three processes with different rates and yields should be proposed: the substrate uptake for storage purposes, the substrate uptake for growth purposes and the growth on stored product. The model proposed solved this identifiability issue of the three necessary yields by linking their value to a unique parameter: the P/O ratio (ι), i.e. the mol of ATP for mol $NADH_2$ used in the oxidative phosphorylation as done in van Aalst-van Leeuven *et al.* (1997). This value can be calculated for pure cultures, but when dealing with mixed cultures it is not that easy. In any case, ι should not exceed the value of 3 due to thermodynamic considerations (Lehninger *et al.*, 1993).

B. DESCRIBING THE SUBSTRATE KINETICS IN THE FEAST PHASE

According to the research line of TUD, the kinetics of the feast phase strongly depends on the evolution of the growth rate with SRT. At low SRTs (i.e. high growth rate) negligible storage is observed since the growth rate is close to its maximum substrate uptake rate. On the other hand, at high SRTs (i.e. low growth rate) the substrate uptake rate of the biomass is higher than the the average growth rate. Consequently, the difference between substrate uptake (q_{MAX}) and substrate used for growth (σ_{MAX}) is diverted to formation of the storage polymers. Under these conditions, van Loosdrecht and Heijnen (2002) asserted that the q_{MAX} was slightly changing with SRT while σ_{MAX} is strongly affected by SRT variation. Hence, the ratio of PHB produced per acetate taken up can be considered constant since the storage becomes the dominant process under these conditions (around 0.67 g COD_{STO}/g COD_S). Based on these considerations, the model presented in this thesis considers that part of the substrate is used for growth and part for storage. f_{STO} is the fraction of the substrate flux diverted to the storage products (g COD_S/g COD_S). As discussed below, this value should be around 0.6-0.7 for WWTP with high SRT. However, this value should not be taken as universal, since it is influenced by many factors such as the alternating feed pattern or the plant SRT.

Hence, the kinetic modelling of the feast phase assuming no substrate limitations is shown on equations VIII.1 – VIII.3:

$$q_{MAX} = \frac{\sigma_{MAX,S}}{Y_{H,S}} + \frac{k_{STO}}{Y_{STO}} \qquad \text{(VIII.1)}$$

$$k_{STO} = f_{STO} \cdot q_{MAX} \cdot Y_{STO} \qquad \text{(VIII.2)}$$

$$\sigma_{MAX,S} = (1 - f_{STO}) \cdot q_{MAX} \cdot Y_{H,S} \qquad \text{(VIII.3)}$$

C. DESCRIBING PHB DEGRADATION KINETICS IN THE FAMINE PHASE

The description of the PHB degradation under famine conditions was stressed in the case of biomass with low PHB content. The typical surface saturation and multiple order kinetics used in other works were discarded because they could not describe correctly the experimental observations. These observations showed that there are at least two phenomena corresponding to a fast and a slow degradation rate of X_{STO} under famine conditions. A new expression is proposed which successfully describes this phenomenon.

$$f\left(\frac{X_{STO}}{X_H}\right) = \frac{\frac{X_{STO}}{X_H}}{K_{STO} + \frac{X_{STO}}{X_H}} \cdot \frac{\frac{X_{STO}}{X_H}}{f_{XSTO}^{REG}} \qquad \text{(VIII.4)}$$

The first part of this mathematical expression describes the surface-saturation type degradation kinetics of X_{STO} likewise ASM3 (Henze *et al.*, 2000). The second part assumes that the degradation of X_{STO} is regulated as function of the storage content of the cell, $f_{XSTO} = X_{STO}/X_H$ likewise Dircks *et al.* (2001). This means that when f_{XSTO} is high, the degradation of X_{STO} is faster, depending on the regulation constant of the cell, f_{XSTO}^{REG}. However, when f_{XSTO} is decreasing and approaching a minimum level in the biomass, the biomass starts to limit the degradation rate of X_{STO}.

D. INCLUDING DYNAMIC CO_2 SYSTEM FOR THE TITRIMETRIC DATA DESCRIPTION

In order to include the titrimetric data for the model calibration, the proton consuming/producing processes must be detected. Gernaey *et al.*, (2002a) identified the processes which mostly influenced the pH (i.e. substrate and ammonia uptake and CO_2 stripping). They calculated the effect of these processes on pH based on the chemical equilibriums of the substrate (weak acid) and ammonia (weak base). They used a simple ASM1 growth model. This thesis integrates the influence of the storage processes on pH, which is calculated in an analogous way as Gernaey *et al.*

As they used short-term experiments to calibrate their model, they assumed that under these conditions the CO_2 stripping rate could be considered constant. Hence, they predicted a constant acid addition which they called background proton production rate (BPPR). This may be the most controversial issue in their model, since this assumption is only valid under certain conditions, i.e. low oxygen transfer efficiency, high pH and short-term experiments (Pratt *et al.*, 2004; Sin, 2004). Later on, Sin (2004) from the same research group extended the ASM1 Gernaey's approach by integrating the physical and chemical equilibriums involved in the dynamic CO_2 system: the carbonic acid – carbonate equilibrium, aeration, carbon stripping processes.

This model is calibrated and validated in Chapter V.C and Chapter V.D with respirometric and titrimetric experiments from several different WWTPs. The results showed that this model is able to describe the behaviour of two different biomasses with very different storing capacities.

The model was first calibrated in Chapter V.C with OUR data obtained from batch experiments. The predictions of the calibrated model were also confirmed by independent PHB measurements, supporting the validity of the model. It was observed that some of the kinetic parameters could not be reliably identifiable with respirometric experiments. OED methodology was shown to be valuable in view of improving the parameter estimation accuracy, particularly for the identification of the second-order model developed in this study.

With respect to the parameter estimation values, the maximum growth rate of heterotrophs was estimated to be between 0.7 – 1.3 1/d for the sludge tested which is quite lower compared to the values reported in literature for the ASM models. The estimated yield coefficient for heterotrophic growth on acetate was around 0.58 g COD/g COD, lower than the values reported in literature for ASM models. It is believed that the proposed model gives a better prediction of the growth yield and the maximum growth rate of biomass in full-scale WWTPs since it accounts for the storage phenomenon. Finally, the estimated maximum substrate uptake rate of the biomass was much higher than the substrate usage rate at the maximum growth rate of the biomass.

In addition, it was observed that when two subsequent acetate pulses are added, the second peak is higher than the first. The model could describe this experimental observation if the growth on storage process was not inhibited by the external substrate concentration. However, this discrepancy may be due to the not modelled physiological adaptation of the biomass. In any case, further work on this topic is required.

The link between titrimetric data and the biological COD removal process was studied in Chapter V.D. It was shown that titrimetric measurements are a valuable tool for COD monitoring. For example, titrimetry allows an easy detection of the substrate depletion point and provides information about the process rate. This information is different than the one provided by the OUR measurement. However, these techniques are only significant if the substrate is a VFA or a dissociated compound as shown with some experiments with ethanol and methanol as substrate.

Moreover, titrimetric techniques should be also a quantification tool but it has been experimentally observed that the ratio of moles of protons added to moles of substrate taken up is lower than one (which is the theoretical one). Finally, titrimetric measurements were used for model calibration and resulted to be very useful since they provided complementary information and reduced the parameter confidence intervals.

FUTURE PERSPECTIVES

- The future work in this field should be addressed to the study of the storage processes with real wastewater with the different storage polymers involved. For instance, propionate represents a significant portion of VFA and it is mainly stored as polyhydroxyvalerate and poly-η-hydroxy-2methylvalerate. Hence, the effect of a certain fraction of propionate in the feed on the biomass growth and storage process should be studied.

- These experiments with different substrates should be also performed at different pHs to assess the link between pH and substrate uptake. Moreover, the quantification of the initial substrate uptake with the amount of acid added is an interesting topic to examine.

- ι is a key parameter in this model and a simple and reliable experimental estimation procedure should be found for a posterior use of the proposed model.

- The variability of the f_{STO} value on the plant conditions is also a very interesting issue to examine. This involves the effect of the plant characteristics on the storing capability of the bacteria present in that plant.

- Sin (2004) has examined the study of the simultaneous growth and storage process under anoxic conditions. This process must be studied and modelled with titrimetric and nitrate measurements.

- From a microbiological point of view the study of the causes of the second OUR peak being higher than the first one will provide extra information on the biomass internal mechanisms to divert substrate into growth and storage.

VIII.3 Nitrification

The nitrification (i.e. biological oxidation of ammonia to nitrate) is a two-step process with nitrite as intermediate. A new model for the nitrification process has been developed in this thesis based on other models found in the literature. The whole model development is described in Chapter VI.A. This description includes the elementary mass and reduction balances to obtain the corresponding stoichiometric coefficients and the deduction of the kinetics of each process. The main characteristics of the model are:

A. TWO STEPS

The model used in this thesis distinguishes between the two nitrification steps: nitritation and nitratation. Single-step models are only applicable when nitratation is not the limiting step and one-shouldered OUR profiles are obtained.

On the other hand, the two-step model can describe both cases, though some correlation problems may occur when nitritation is the limiting step.

B. DYNAMIC CO_2 SYSTEM

As it is thought to be calibrated with both OUR and HPR, it also includes the dynamic CO_2 system (i.e. the carbonic acid – carbonate equilibrium, aeration, carbon stripping processes). Moreover, the proton production/consumption rate of each process is quantified. As the protons are a nitritation product, HPR is a very useful technique to distinguish between the two process rates.

C. GAS PHASE AS CPFR

The gas phase is modelled as a CPFR because the description of the CO_2 concentration was very important in this thesis. The simpler hypothesis of gas phase as a CSTR had to be rejected because:

1. The amount of CO_2 in the gas inlet is very low (0.036 %) and for high CO_2 production levels and low aeration flows, the CO_2 concentration could not be considered constant in the gas phase.
2. The experiments of this thesis (except for those in the hybrid respirometer), were conduced under particularly low airflow conditions for an accurate OUR measurement.

D. ACCELERATION PHASE

All respirometric batch tests with ammonia as substrate showed an initial tail which could not be described with the start-up process. Apparently, the nitritation process was very slow just after the pulse addition and then it speeded up until it reached the maximum rate. This phenomenon was shown to be very significant since it lasted around 10 minutes. Smets (personal communication) named this phase as acceleration phase and maintained that it was due to the lack of reducing equivalents at the start of the pulse. This theory is possible since reducing equivalents are required to oxidize ammonia to hydroxylamine (the first reaction of the nitritation).This initial tail could not be described with a first order delay (start-up), since the start-up process describes convex shapes, whereas in the experimental OUR profiles the curvature changed from concave to convex. Then, a new expression for a proper fitting was searched. After some failed attempts an expression based on the Gaussian-like curve with only two unknown parameters was found to be successful [eq. VIII.5]. Moreover, this expression gathered the acceleration and start-up phenomenon.

$$e^{\frac{4(t4\eta)^2}{\cdots}} \qquad \text{(VIII.5)}$$

The two-step nitrification model is a very complex model with nine reactions and more than forty stoichiometric and kinetic parameters. Hence, its calibration would be very long if all the parameters had to be estimated. Moreover, from an identifiability point of view, not all the parameters could be reliably estimated using only short-term batch respirometric and titrimetric profiles and particular experiments would be required. Chapter VI.B examines each of the parameters of the model and decides which of them should be either calculated or assumed from the literature and which of them should be estimated. Most of the equilibrium constants were assumed from the literature except for pK1 which has a big influence on titrimetric data. This parameter is dependent on the ionic strength of the medium and in the experiments of this thesis; ionic strength was particularly high due to the feed concentration. Hence, pK1 needed was estimated.

The biomass growth yield could theoretically be assessed with a unique batch experiment, (i.e. knowing the initial substrate value and the total oxygen consumed). However, a sole experiment results in too much uncertainty on yield calculation. Small deviations in the total oxygen consumption imply high variations in the yield value. Hence a set of experiments measuring the oxygen consumption with different ammonium and nitrite loads was performed. In addition, the biomass growth yields for both populations should be calculated taking into account that part of the ammonia is directly incorporated in the biomass. For the populations used in this thesis, the yields were: Y_A = 0.21 g COD_X/g N and Y_N = 0.080 g COD_X/g N. The active fraction values were roughly approximated using the endogenous OUR value according to equation VIII.6, where f_i was assumed from the literature, OUR_{END} was measured and b_i were calculated from previous experiments (Jubany *et al.*, 2004). The obtained values were f_A=0.18 and f_N=0.07.

$$OUR_{END} = (1 - f_I) \cdot b_A \cdot X \cdot f_A + (1 - f_I) \cdot b_N \cdot X \cdot f_N \qquad \text{(VIII.6)}$$

As the experiments conducted in this thesis were generally performed with low airflow, the DO level in the respirometer decreased at values lower than 2 mg O_2/L and oxygen limitations were considered. This limitation is generally described using Monod-type kinetics with K_O as the oxygen affinity constant and many authors do not estimate the values of the affinity constants for nitritation and nitratation, but assume them from the literature. This assumption may be acceptable when working at high DO levels, but these constants should be calculated in experiments with low DO levels. Moreover, K_Os have recently gained a lot of importance, particularly in view of modelling tasks, since new alternatives to the classical BNR at low DO values have appeared.

After a critical review of different K_O estimation methods, a procedure which improves previous methodologies is proposed in Chapter VI.C. This procedure considers the oxygen surface transfer and the DO probe time response. It has been demonstrated that oxygen transfer from atmosphere should be taken into account when using open and stirred systems such as the one used in this work. Otherwise, the K_O values would be overestimated. To take into account this oxygen transfer, the volumetric oxygen transfer constant form atmosphere (k_La^{SUP}) was calculated by measuring the endogenous OUR value at different surface to volume ratios in the reactor. The DO probe time response was also estimated for a proper K_O estimation. Neglecting this response implied an underestimation of the K_O values because of the sharp experimental DO decrease which is faster than the time response of the probe.

The results obtained were K_{OA} = 0.74 ± 0.02 mg O_2/L and K_{ON} = 1.75 ± 0.01 mg O_2/L. As can be observed, the nitratation step is more influenced by oxygen limitations than the nitritation step (at 25 ºC). These K_O values are considerably higher than the default ones used in the classical ASM1, 0.4 (Henze *et al.*, 2000). The utilisation of 0.4 for both K_Os, could strongly influence the estimated values of σ_{MAX} and K_S from respirometric batch experiments.

As the nitrifying biomass is autotrophic, inorganic carbon is a substrate and its limitation should result in a decrease of the process rate. This limitation has often been omitted for modelling purposes since it is difficult to have a scenario with inorganic carbon limitations in real systems. However, the recent technology advances have brought new scenarios in biological nitrogen removal where these limitations should be considered. Chapter VI.D examined the TIC limitation through respirometric and titrimetric techniques. The evolution of the TIC is indirectly followed with titrimetry and the process rate is followed with both respirometry and titrimetry.

The nitrification process can be limited with a lack of inorganic carbon since at low TIC concentrations, the nitrification process rate decreases considerably. However, it seems that this limitation is stronger on the nitritation process than on the nitratation. In fact,

the range of TIC concentration where nitratation is limited is so low that it is difficult to reach in an aerobic bioreactor (where CO_2 is produced). It was experimentally observed that the nitritation limitation started at values lower than 3 mM TIC which is a much higher value than the one proposed by ASM2 (Henze *et al.*, 2000), i.e.K_{ALK} = 0.5 mmol HCO_3^-/L.

The values of the nitrification rate (measured as OUR) versus TIC concentration could be fitted to a classical Monod and Tessier kinetics. These fittings, though successfully described the experimental observations in the measured range, could be improved. A sigmoidal equation proposed by Wett and Rauch (2002) described successfully the experimental results.

The values of the nitratation rate (measured as OUR with nitrite addition) versus TIC concentration showed that this process is not influenced by the TIC concentration, even at very low TIC values. The values of the nitritation rate (measured as HPR) versus TIC concentration confirmed the observed TIC limitation. This limitation could be also described using either Monod or Tessier kinetics.

Once the model was developed, its identifiability was studied and the substrate limitations were quantified, it was successfully calibrated and validated with OUR and HPR experiments in the LFS respirometer in Chapter VI.E. The two-step model described accurately the experimental profiles obtained. The most important values obtained are σ_A= 1.52 1/d and σ_N = 1.22 1/d. These values were calculated with an estimation of the active fraction values using the endogenous OUR value. The value of the pK_1 obtained was lower than the default value for pure water (6.36). This is likely due to the huge ionic strength of the medium.

The possibility to include the CER measurement as an output variable for model calibrating was also examined and discarded. It was observed that minor changes in the pH were much more influent in the CER measurement than the CO_2 consumption linked to the nitrification. Thus, it can be concluded that CER measurement is useless for parameter estimation for a nitrification model.

In addition, parameter estimation was conducted using different output measurements such as OUR, HPR, ammonium or nitrite. The conclusion was that OUR and HPR contain enough information for a reliable description of the system without neither ammonia nor nitrite measurements, though the profile obtained was a single step. A huge correlation was observed between $\sigma_A \cdot f_A$ and K_{NH} and $\sigma_N \cdot f_N$ and $K_{NO,}$ respectively, even in the experiment with all the measurements, indicating that short-term batch experiments are not recommended for estimating the Monod affinity constants. Finally, the effect of pH on the nitrification rate was studied by measuring OUR_{MAX} at different pH set points. The results showed that the optimum pH was around 7.6, which is in agreement with the values found in the literature.

FUTURE PERSPECTIVES

- In general, the logical continuation of this work would be the extension of the two-step nitrification model to describe the rest of the processes involved in the biological nitrification removal processes such as denitrification.

- In the case of denitrification, this model should be calibrated using titrimetric measurements and, probably, nitrate measurements would be required for reliable parameter estimation.

- Moreover, the applicability of this model to the recent technology advances such as the SHARON® or the anammox® processes has to be tested. The oxygen and TIC limitation kinetics proposed on these processes should also be examined.

- As done with oxygen and carbon, the other nitrification inhibitions should be extensively studied and the effect on full-scale WWTP should be described. A lot of substrate and product inhibitions have been described in the literature (Anthonisen *et al.,* 1976) which could be quantified using both respirometric and titrimetric techniques. This work is currently part of the PhD thesis of Irene Jubany.

- From a microbiological point of view, a deeper study on the acceleration phase is necessary to confirm the reducing equivalent theory proposed in this thesis.

- Finally, a new method for a reliable estimation of the active fractions of both populations is required. Then, specific studies on a population could be performed. This work is currently part of the PhD thesis of Irene Jubany.

VIII.4 Enhanced Biological Phosphorus Removal

A new model was developed in the EPBR section as a modification of ASM2. The main modification was the inclusion of glycogen economy. This model was calibrated using the two most important VFA fractions: acetate and propionate. When fitted to experimental data, the model presented in this study gives a good prediction of the behaviour of the EBPR systems for either propionate or acetate as the sole carbon source and the parameter estimation values obtained are in agreement with the results in the literature.

PAOs demonstrated similar anaerobic VFA-uptake rates (mmol C/g VSS min) with acetate and with propionate. The major differences observed between both carbon sources were:

1. the amount of PHA produced per substrate COD unit taken up was higher for acetate.
2. more phosphate is released to produce the same amount of PHA with acetate (in mass basis).
3. the P-release per VFA taken up (in molar basis) for propionate (1.33) was very similar to the results obtained in the case of acetate (1.40).
4. less amount of reducing power is required to store propionate than acetate.

These observations agreed with the parameter values of the metabolic models found in the literature for acetate and propionate (Smolders *et al.*, 1995 and Oehmen *et al.*, 2005).

It was observed a remarkable second P-release possibly linked to PAO maintenance or to the peptone utilisation as carbon source. It was only detectable after the VFA substrate was exhausted but it probably occurred throughout the anaerobic period. A maintenance reaction is added in order to explain the second P-release detected in the experiments.

EBPR process is based on PAO enrichment from non-EBPR WWTP sludge. The experience accumulated in EEG-UAB says that this process can be very slow and not always successful since PAO are scarce in conventional WWTP sludge. Hence, one motivation of this thesis was to use the previously developed model to test new control strategies to improve the EBPR start-up process (Chapter VII.B). The start-up of an EBPR process in a SBR with biomass coming from a non-EBPR system was simulated during 30 days. This resulted in 120 cycles. The simulations performed in this work reveal that it is feasible to improve the start-up of this system by reducing the length of both the anaerobic phase and the aerobic phase so that they coincide with the depletion of VFA and orthophosphate, respectively.

Once VFA is depleted, the rest of the anaerobic phase can be considered useless in terms of PAO growth, since the main compounds only suffer small variations due to lysis

processes. On the other hand, once the orthophosphate is depleted, the rest of the aerobic phase is useless since only internal PHA pools are oxidised and the heterotrophic fraction is favoured to grow with the COD remaining in the medium and the aerobic conditions. According to the results of the simulations, if the anaerobic phase is reduced linked to VFA presence, 12 % of the start-up length could be omitted. On the other hand, if the aerobic phase was reduced linked to orthophosphate presence, 29 % of the start-up time would be ineffective for PAO growth and as such it could be omitted. However, these strategies have VFA and orthophosphate as input variable which may not be suitable for control purposes due to its measurement frequency. Hence, classical on-line measurements as pH and DO were used as input variables.

The linking between HPR and substrate uptake was experimentally demonstrated and modelled. As the substrate enters in the non-ionised form through the membrane, a proton is required. Hence, if an on-line VFA measurement is not available, the HPR can be used as an indicator of VFA depletion and, hence, as a measured variable for controlling the anaerobic phase length.

On the other hand, the link between OUR and orthophosphate depletion was also experimentally demonstrated and modelled. If an on-line orthophosphate measurement is not available, the OUR can be used as an indicator of its presence. Both the absolute OUR value and the OUR first derivative can be used as a measured value in the control strategy. However, if the absolute value is considered, the efficiency of the control strategy is not as higher as controlling the orthophosphate presence. The reason is that other processes as endogenous process have also a strong influence on OUR.

As a final conclusion, the best control strategy obtained is a control strategy including both the *P-control* and the *VFA-control* strategy. 120 EBPR cycles could be placed in 440 hours and then a reduction of 280 hours was accomplished. Hence, almost 40% could be considered useless. This was a significant improvement since, 219 cycles could be completed in the first 30 days of start-up.

Finally, a comparison between the behaviour of an EBPR sludge working under classical anaerobic/aerobic conditions and the behaviour of the same sludge with simultaneous presence of an electron donor (acetate) and a final electron acceptor (oxygen) was performed in Chapter VII.C.

The most significant conclusion obtained in Chapter VII.C is that PAO seem to take up acetate under aerobic conditions the same way as under aerobic conditions (i.e. linked to phosphorus release and glycogen degradation). Hence, PHB storage from acetate by PAO was not affected by the oxygen presence. Under strictly aerobic conditions, PAO could uptake acetate obtaining energy from poly-P hydrolysis and reducing power from glycogen degradation. In addition, the OUR profile was measured, and an important oxygen consumption was observed when acetate was present indicating that part of the acetate was consumed linked to oxygen consumption. Hence, two different ways for acetate uptake were observed in the same bio-P sludge.

Two different hypotheses were formulated and simulated to describe this aerobic acetate consumption and PHB storage. The PAO-hypothesis considered that PAO store acetate as PHB linked to oxygen consumption, in addition to store acetate as PHB linked to P-release and glycogen degradation. The OHO-hypothesis considered that PAO store acetate as PHB linked to P-release and glycogen degradation, and that OHO are the only responsible for the additional acetate consumption and PHB storage.

Assuming that PAO and OHO populations are well described by the modified ASM2 model of Chapter VII.A and the ASM3 model respectively, the OHO-hypothesis describes better the experimental profiles.

Nevertheless, none of both hypotheses can be totally rejected and it is also possible that its combination could describe better the experimental results. More research is needed in this field in order to clarify the experimental observations.

FUTURE PERSPECTIVES

- Future work in the EBPR field should address to understand PAO behaviour under conditions that differ from the classical anaerobic/aerobic conditions. This knowledge is essential for an optimal implementation of EBPR in WWTP.

- For instance, a deep examination of the aerobic P release process would help to establish the PAO behaviour when COD and oxygen coexist. Moreover, if PAO can remove some P aerobically it can certainly upgrade the operation of a conventional aerated WWTP.

- From a microbiological point of view, it would be very interesting to study the existing link between HPR and EBPR. This would require considering many processes that influence the pH: the substrate uptake, the ammonia consumption, the carbonate equilibriums and the equilibriums of the acid phosphoric should. This work is actually part of the MSc research of Marcos Marcelino.

- Finally, the control strategies presented in Chapter VII.B should be implemented and tested in a pilot-plant scale to confirm the success predicted by simulation.

REFERENCES

Ahn J., Daidou T., Tsuneda S. and Hirata A. (2002) Transformation of phosphorus and relevant intracellular compounds by phosphorus accumulating enrichment culture in the presence of both the electron acceptor and electron donor. Biotechnol. Bioeng. 79, 83-93.

Alleman J.E. (1984) Elevated nitrite occurrence in biological wastewater treatment system. Water Sci. Technol. 17:409–19.

American Public Health Association (APHA). (1995) Standard Methods for the Examination of Water and Wastewater, nineteenth ed. Washington, DC.

Anthonisen A.C., Loehr R.C., Prakasam T.B.S. and Srinath E.G. (1976) Inhibition of nitrification by ammonia and nitrous acid. J. Water Pollut. Control Fed. 48(5), 835-852.

Antoniou P., Hamilton J., Koopman B., Jain R., Holloway B., Lyberatos,G. and Svoronos S. (1990) Effect of temperature and pH on the effective maximum specific growth rate of nitrifying bacteria. Water Res. 24 (1), 97-101.

Arp D. , Sayavedra-Soto L.A., Hommes N.G. (2002) Molecular biology and biochemistry of ammonia oxidation by Nitrosomonas europaea. Arch. Microbiology 178, 250-255.

Arun V., Mino T. and Matsuo T. (1988) Biological mechanism of acetate uptake mediated by carbohydrate consumption in excess phosphorus removal systems. Water Res. 22, 565-570.

Aurola A., Beun J.J., Copp J., Morgenroth E., van Loosdrecht M.C.M. and Winkler S. (2000) Report of the work group meeting on Unbalanced Growth. Cost Action 624. Working Group 4. 6-7 April 2000. Delft.

Bae W., Baek S., Chung J., Lee Y. (2002) Optimal operational factors for nitrite accumulation in batch reactors. Biodegradation. 12, 359-366.

Baetens D. (2000) Enhanced biological phosphorus removal. Modelling and experimental design. Ph.D. Thesis. Ghent University.

Baeza J. (1999) Desarrollo e implementación de un sistema supervisor para la gestión y el control de EDAR. Ph. D. Thesis. Universitat Autònoma de Barcelona. (in Spanish).

Baeza J.A., Gabriel D., Lafuente J. (2002a) Improving the nitrogen removal efficiency o fan A^2/O based WWTP by using an on-line Knowledge Based Expert System. Water Res. 36, 2109-2123.

Baeza J.A., Gabriel D., Lafuente J. (2002b) In-line fase OUR measurements for monitoring and control of WWTP. Water Sci. Tech. 45(4-5), 19-28.

Baltes M., Scheider R., Sturm C. and Reuss M. (1994) Optimal experimental design for parameter estimation in unstructured growth models. Biotechnol. Prog. 10, 480-488.

Bandyopadhyay B., Humprey A.E. and Taguchi H. (1976) Dynamic measurement of the volumetric oxygen transfer coefficient in fermentation systems. Biotechnol. Bioeng. 9, 533-544.

Barnard J.L. (1984) Activated primary tanks for phosphate removal. Water SA 10:121-126.

Beavis A.D. and Lehninger M.L. (1986) The upper and lower limits of the mechanistic stoichiometry of mitochondrial oxidative phosphorylation. Stoichiometry of oxidative phosphorylation. European Journal of Biochemistry. 158, 315-322.

Beccari M., Dionisi D., Giuliani A., Majone M. and Ramadori R. (2002) Effect of different carbon sources on aerobic storage by activated sludge. Water Sci. Technol. 45(6), 157-168.

Beck M. B. (1987) Water quality modelling: a review of the analysis of uncertainty. Water Resour. Res. 23, 1393-1442.

Bernet, N., Dangcong, P., Delgenès, J. P., and Moletta, R. (2001) Nitrification at low oxygen concentration in biofilm reactor. J. Environ. Eng. 127(3), 266-271.

Beun J.J., Paletta F., van Loosdrecht M.C.M. and Heijnen J.J. (2000) Stoichiometry and kinetics of Poly-η-Hydroxybutyrate metabolism in aerobic, slow growing activated sludge cultures. Biotechnol. Bioeng. 67, 379-389.

Beun J.J., Dircks K., van Loosdrecht M.C.M. and Heijnen J.J. (2001) Poly-η-hydroxybutyrate metabolism in dynamically fed mixed microbial cultures. Water Res. 36, 1167-1180.

Bock E., Hoop H.P., Harms H. and Ahlers B. (1991) The biochemistry of nitrifying organisms. In: Shively J.M, Barton L.L. Editors. Variations in autotrophic life. New York: Academic Academic Press.

Bond P.L., Keller J. and Blackall L.L. (1999a) Bio-P and non-bio-P bacteria identification by a novel microbial approach. Water Sci. Technol. 39(6), 13-20.

Bond P., Keller J. and Blackall L.L. (1999b) Anaerobic Phosphate Release form Activated Sludge with Enhanced Biological Phosphours Removal. A possible Mechanism of Intracellular pH control. Biotechnol. Bioeng. 63, 507-515.

Brdjanovic D., Slamet A., van Loosdrecht M.C.M., Hooijmans C.M., Alaerts G.J. and Heijnen J.J. (1998) Impact of excessive aeration on biological phosphorus removal from wastewater. Water Res. 32, 200-208.

Brun R., Kuhni M., Siegrist H., Gujer W. and Reichert P. (2002) Practical identifiability of ASM2d parameters – systematic selection and tuning of parameter subsets. Water Res. 36(16), 4113-4127.

Burriel F., Lucena F., Arribas S., and Hernandez J. (1989) Química analítica cualitativa. Ed. Paraninfo. Madrid.

Byong-Hee J., Yasunori T. and Hajime U. (2000) Stimulating accumulation of nitrifying bacteria in porous carrier by addition of inorganic carbon in a continuous flow fluidized bed wastewater treatment reactor. J. Biosci. Bioeng. 89(4), 334-339.

Cai, W-J. and Y. Wang (1998) The chemistry, fluxes and sources of carbon dioxide in the estuarine waters of the Satilla and Altamaha Rivers, Georgia. Limnol. & Oceanogr. 43:657-668.

Carlsson H, Aspegren H. and Hilmer A. (1996) Interactions between wastewater quality and phosphorus release in the anaerobic reactor of the EBPR process. Water Res. 30, 1517-1527.

Carrera J. (2001) Eliminación biológica de nitrógeno en un efluente con alta carga. Ph. D. Thesis. Universitat Autònoma de Barcelona (in Spanish).

Carrera J., Baeza J.A., Vicent T. and Lafuente J. (2003) Biological nitrogen removal of high-strength ammonium industrial wastewater with two-sludge system. Water Res. 37, 4211-4221.

Carrera J., Jubany I., Carvallo L., Chamy R., Lafuente J. (2004a) Kinetic models for nitrification inhibition by ammonium and nitrite in a suspended and an immobilised biomass systems. Process Biochem. 39, 1159-1165.

Carrera J., Vicent T. and Lafuente J. (2004b) Effect of influent COD/N ratio on biological nitrogen removal (BNR) from high-strength ammonium industrial wastewater. Process Biochem. 39, 2035-2041.

Carucci A., Dionisi D., Majone M., Rolle E. and Smurra P. (2001) Aerobic storage by activated sludge on real wastewater. Water Res. 35, 3833-3844.

Cech J.S. and Hartman P. (1990) Glucose induced breakdown of enhanced biological phosphate removal. Environ. Technol. 11, 651-658.

Cech J.S. and Hartman P. (1993) Competition between polyphosphate and polysaccharide accumulating bacteria in enhanced biological phosphate removal systems. Water Res. 24, 1219-1225.

Chandran K. and Smets B.F. (2000) Single-step nitrification models erroneously describe batch ammonia oxidation profiles when nitrite oxidation becomes rate limiting. Biotechnol. Bioeng. 68(4), 396-406.

Chandran K. and Smets B.F. (2001) Estimating biomass yield coefficients for autotrophic ammonia and nitrite oxidation from batch respirograms. Water Res. 35(13), 3153-3156.

Chen Y., Trujillo M., Biggerstaff J., Ahmed G., Lamb B., Eremekdar F.G., McCue T. and Randall A.A. (2002) The Effects Of Propionic Versus Acetic Acid Content Of Domestic Sewage On Enhanced Biological Phosphorus Removal, Proceedings Water Environment Federation 75th Annual Conference and Exposition (WEFTEC) 2002, Research Symposium oral presentation, Sept 28 –Oct 2, 2002, Chicago, Illinois, USA (CD-Rom).

Chen Y., Randall A.A. and McCue T. (2004) The efficiency of enhanced biological phosphorus removal from real wastewater affected by different ratios of acetic to propionic acid. Water Res. 38(1), 27-36.

Chudoba P., Capdeville B. and Chudoba J. (1992) Explanation of biological meaning of the S0/X0 ratio in batch cultivation Water Sci. Technol. 26(3-4), 743-751.

Clark, C and Schmidt, E. (1967) Growth response of Nitrosomonas europaea to amino acids. J. Bacteriol. 93, 1302-1309.

Comeau Y., Hall K.J. and Oldham W.K. (1988) Determination of poly-hydroxybutyrate and poly-hydroxyvalerate in activated sludge by gas-liquid chromatography. Appl. Environ. Microbiol. 54, 2325-2327.

Copp J.B. and Murphy K.L. (1995) Estimation of the activated nitrifying biomass in activated sludge. Water Res. 29(8), 1855-1862.

Daims H., Nielsen P.H., Nielsen J.L., Juretschko S. and Wagner M. (2000) Novel *Nitrospira*-like bacteria as dominant nitrite-oxidizers in biofilms from wastewater treatment plants: diversity and in-situ physiology. Water Sci. Technol. 41, 85-90.

Daims H., Nielsen P.H., Nielsen J.L., Schleifer K.H. and Wagner M. (2001) In situ characterisation of *Nitrospira*-like nitrite-oxidizing bacteria active in wastewater treatment plants. Appl. Environ. Mircrobiol. 67(11), 5273–5284.

Dassanayake C.Y. and Irving R.L. (2001) An enhanced biological phosphorus removal (EBPR) control strategy for sequencing batch reactors (SBRs). Water Sci Technol. 45(3), 183-189.

Dircks K., Henze M., van Loosdrecht M.C.M., Mosbaek H. and Aspegren H. (2001) Storage and degradation of poly-η-hydroxybutyrate in activated sludge under aerobic conditions. Water Res. 35, 2277-2285.

Dochain D. and Vanrolleghem P.A. (2001) Dynamical modelling and estimation in wastewater treatment processes. IWA Publishing. London, UK.

Dworkin M. (2001) Prokaryotic life cycles in M.Dworkin *et al.*, eds, The Prokaryotes: an evolving electronic resource for the microbiological community, 3rd edition, release 3.7, November 2,2001, Springer,-Verlag, New York.

Edwards T.J., Maurer G., Newman J. and Prausnitz J.M. (1978) Vapor-liquid equilibria in multicomponent aqueous solutions of volatile weak electrolytes. AIChE Journal. 24, 966-976.

EPA (1993) Manual for Nitrogen Control. U.S. EPA Office Water, Washington, DC.

Ficara E., Cortelezzi P. and Rozzi A. (2003) Theory of pH-stat titration. Biotechnol. Bioeng. 82, 28-37.

Filipe C.D.M. and Daigger G.T. (1999) Evaluation of the capacity of Phosphorous-Accumulating Organisms to use nitrate and oxygen as final electron acceptors: a theoretical study on population dynamics. Water Environ. Res. 71, 1140-1150.

Filipe C.D.M., Daigger G.T. and Grady C.P.L. Jr. (2001a) Stoichiometry and kinetics of acetate uptake under conditions by an enriched culture of phosphorus-accumulating organisms at different pHs. Biotechnol. Bioeng. 76,32-43.

Filipe C.D.M., Daigger G.T. and Grady C.P.L. Jr. (2001b) A metabolic model for acetate uptake under anaerobic conditions by glycogen accumulating organisms: Stoichiometry, kinetics and the effects of pH. Biotechnol. Bioeng. 76:17-31.

Fleit E. (1995) Intracellular pH regulation in biological excess phosphorus removal systems. Water Res. 29(7), 1787-1792.

Frijlink M.J., Abee T., Laanbroek H.J., de Boer W. and Konings W.N. (1992) The bioenergetics of ammonia and hydroxylamine oxidation in *Nitrosomonas europaea* at acid and alkaline pH. Arch. Microbiol. 157, 194-199.

Fux C., Boehler M., Huber P., Bruner I. and Siegrist H. (2002) Biological treatment of ammonium-rich wastewater by partial nitratation and subsequent anaerobic oxidation (anammox) in a pilot plant. J. Biotechnol. 99, 295-306.

Fux C. and Siegrist H. (2004) Nitrogen removal from sludge digester liquids by nitrification/denitrification or partial nitritation/anammox: environmental and economical considerations. Water Sci. Technol. 50(10), 19-26.

Gabriel D. (2000) Monitoratge i modelització aplicats al control d'una EDAR pilot amb eliminació de nutrients. Ph.D. Thesis. Universitat Autònoma de Barcelona (in catalan)

Gapes D., Pratt S., Yuan Z. and Keller J. (2003) Online titrimetric and off-gas analysis for examining nitrification processes in wastewater treatment. Water Res. 37, 2678-2690.

Garrido J.M., van Benthum W.A.J., van Loosdrecht M.C.M. and Heijnen J.J. (1997) Influence of dissolved oxygen concentration on nitrite accumulation in a biofilm airlift suspension reactor. Biotechnol. Bioeng. 53(2), 168-178.

Gee C., Suidan M. and Pfeffer J. (1990a) Modeling of nitrification under substrate-inhibiting conditions. J. Environ. Eng. 116 (1), 18-31.

Gee C., Pfeffer J. and Suidan M. (1990b) Nitrosomonas and Nitrobacter interactions in biological nitrification. J. Environ. Eng. 116 (1), 4-17.

Gernaey K., Vanrolleghem P.A. and Verstraete W. (1998) On-line estimation of *Nitrosomonas* kinetic parameters in activated sludge samples using titration in-sensor-experiments. Water Res. 32, 71-80.

Gernaey K., Maffei D., Vanrolleghem P.A. and Verstraete W. (1999) A new pH-based procedure to model toxic effects on nitrifiers in activated sludge. J. Chem. Technol. Biotechnol. 74, 679-687.

Gernaey K., Petersen B., Nopens I., Comeau Y. and Vanrolleghem P.A. (2002a) Modelling aerobic carbon source degradation processes using titrimetric data and combined respirometric-titrmetric data: experimental data and model structure. Biotechnol. Bioeng. 79, 741-753.

Gernaey K., Petersen B., Dochain D. and Vanrolleghem P.A. (2002b) Modelling aerobic carbon source degradation processes using titrimetric data and combined respirometric-titrmetric data: structural and practical identifiability. Biotechnol. Bioeng. 79, 754-769.

Ginestet P., Audic J., Urbain V. and Block J. (1998) Estimation of nitrifying bacterial activities by measuring oxygen uptake in the presence of the metabolic inhibitors allylthiourea and azide. Appl. Env. Micr. 64(6), 2266-2268.

Grady C.P.L. Jr., Smets B.F. and Barbeau D.S. (1996) Variability in kinetic parameter estimates: a review of possible causes and proposed terminology. Water Res. 30, 742-748.

Grau P., Dohanyos M. and Chudoba J. (1975) Kinetics of multicomponent substrate removal by activated sludge. Water Res. 9, 637-642.

Grunditz C. and Dalhammar G. Development of nitrification inhibition assays using pure cultures of N*itrosomonas* and *Nitrobacter* Water Res. 35(2), 433-440.

Guisasola A., Baeza J.A., Carrera J., Casas C., Lafuente J. (2003) An off-line respirometric procedure to determine inhibition and toxicity of biodegradable compounds in biomass from an industrial WWTP. Water Sci. Technol. 48(11), 267-275.

Guisasola A., Pijuan M., Baeza J.A., Carrera J., Casas C., Lafuente J. (2004a). Aerobic phosphorus release linked to acetate uptake in bio-P sludge: process modelling using oxygen uptake rate. Biotechnol. Bioeng. 85, 722-733.

Guisasola A., Sin G., Carrera J., Baeza J.A. and Vanrolleghem P.A. (2004b) Limitations of ASM1 and ASM3: a comparison based on batch OUR profiles from different full-scale WWTP. In: Proceedings 4th IWA Word Water Congress and Exhibition. Marrakech (Morocco), 2004.

Guisasola A., Pijuan M., Baeza J.A., Carrera J. and Lafuente J. (2005a) Improving the start-up of an EBPR system using OUR to control the aerobic phase length: a simulation study. Proceedings of 2nd IWA Conference on Instrumentation, Control and Automation for Water and Wastewater Treatment and Transport System. Pusan (South Korea), 2005.

Guisasola A., Jubany I., Baeza J.A., Carrera J. and Lafuente J. (2005b) Respirometric estimation of the oxygen affinity constants for biological ammonium and nitrite oxidation. Journal of Chem. Technol. Biotechnol. 80(4), 388-39.

Gujer, W., Henze, M., Takahashi, M. and van Loosdrecht, M.C.M. (1999) Activated Sludge Model No. 3, Water Sci. Technol. 29 (1), 183-193.

Hagopian D.S. and Riley J.G. (1998) A closer look at the bacteriology of nitrification. Aquacultural Eng. 18(4), 223-244.

Haldane J.B.S. (1965) *Enzymes*. MIT Press. Cambridge MA.

Han K. and Levenspiel O. (1988) Extended Monod kinetics for substrate, product and cell inhibition. Biotechnol. Bioeng. 32, 430-437.

Hanada S. Sataoh H. and Mino T. (2002) Measurement of microorganisms with PHA production capability in activated sludge and its implication in Activated Sludge Model nº3. Water Sci. Technol. 45(6), 107-113.

Hao X., van Loosdrecht M.C.M., Meijer S.C.F. and Qian Y. (2001) Model-based evaluation of two BNR processes – UCT and A_2N. Water Res. 35, 2851-2860.

Heijnen J.J. (1999) Bioenergetics of microbial growth. In: Encyclopedia of bioprocess technology: fermentation, biocatalysis and bioseparation.Ed. Flickinger M.C. and Drew S.W. John Wiley & Sons Inc. 267-291.

Hellinga C., Schellen A.A.J.C., Mulder J.W., van Loosdrecht M.C.M. and Heijnen JJ. (1998) The SHARON process: An innovative method for nitrogen removal from ammonium-rich wastewater. Water Sci. Technol. 37(9), 135-142.

Hellinga C., Van Loosdrecht M.C.M., and Heijnen J.J. (1999) Model based design of a novel process for nitrogen removal form concentrated flows. Math. Comp. Model Dyn. 5, 351-371.

Henze M., Gujer W., Mino T. and van Loosdrecht M.C.M. (2000) Activated Sludge Models ASM1, ASM2, ASM2d and ASM3: Scientific and Technical Report nº9. IWA Task Group on Mathematical Modelling for Design and Operation of Biological Wastewater Treatment.

Hidalgo M.E. and Ayesa E. (2001) Numerical and graphical description of the information matrix in calibration experiments for state-space models. Water Res. 35, 3206-3214.

Holmberg A. (1982) On the practical identifiability of microbial growth models containing Michaelis-Menten nonlinearities. Math. Biosci. 62, 23-43.

Hood C.R. and Randall A.A. (2001) A biochemical hypothesis explaining the response of enhanced biological phosphorus removal biomass to organic substrates. Water Res. 35, 2758-2766.

Hunik J.H., Tramper J. and Wijffels R.H. (1994) A strategy to scale up nitrification processes with immobolized cells of *nitrosomonas europaea* and *nitrobacter agilis*. Bioprocess Eng. 11, 73-82.

Insel G., Orhon D. and Vanrolleghem P.A. (2003) Identification and modelling of aerobic hydrolysis mechanism -application of optimal experimental design, J. Chem. Technol. Biotechnol. 78(4), 437-445.

Janus H.M. and van der Roest H.F. (1997) Don't reject the idea of treating reject water. Water Sci. Technol. 35(10), 27-34.

Jeon C.O., Lee D.S., Lee M.W. and Park J.M. (2001) Enhanced Biological Phosphorus Removal in an Anaerobic-Aerobic Sequencing Batch Reactor: Effect of pH. Water Environ. Res. 73(3).

Jianlong W and Ning Y. (2004) Partial nitrification under limited dissolved oxygen conditions. Process Biochem. 39, 1223-1229.

Joshi J.B. and Sharma M.M (1979) A circulation cell model for bubble columns. Trans Inst Chem Eng. 54, 503-508.

Jubany I., Baeza J.A., Carrera J. and Lafuente J. (2004) Modelling biological nitrite oxidation including biomass growth and substrate inhibition using only oxygen uptake rate measurements. In: Proceedings 4th IWA Word Water Congress and Exhibition. Marrakech (Marocco), 2004.

Kantarci N., Borak F. and Ulgen K.O. (2005) Bubble column reactors (review). Proc. Biochem. 40, 2263-2283

Karahan-Gül Ö., van Loosdrecht M.C.M. and Orhon D. (2003) Modification of Activated Sludge nº3 considering direct growth on primary substrate. Water Sci. Technol. 47(11) 219-225.

Kathesis D. Diyamandoglu V. and Fillos J. (1998) Stripping and recovery of ammonia from centrate of anaerobically digested biosolids at elevated temperatures. Water Environ. Res. 70(2), 231-240.

Keesman K.J., Spanjers H. and van Straten G. (2000) Analysis of endogenous process behaviour in activated sludge. Biotechnol. Bioeng. 57, 155-163.

Knowles G., Downing A.L. and Barrett M.J. (1965) Determination of kinetic constants for nitrifying bacteria in mixed culture, with the aid of an electronic computer. J. Gen. Microbiol. 38, 263-278.

Koch G., Kühni M., Rieger L. and Siegrist H. (2000) Calibration and validation of an ASM3-based steady-state model for activated sludge systems—part II: : prediction of phosphorus removal Water Res. 35(9), 2246-2255.

Krishna C. and van Loosdrecht M.C.M. (1999) Substrate flux into storage and growth in relation to activated sludge modelling. Water Res. 33(14), 3149-3161.

Kuai L. and Verstraete W. (1998) Ammonium removal by the oxygen-limited auto-trophic nitrification-denitrification system. Appl. Environ. Microbiol. 64, 4500-4506.

Kuba T., Wachtmeister A., van Loosdrecht M.C.M., Heijnen J.J. (1996) Effect of nitrate on phosphorous release in biological phosphorous removal systems. Water Sci. Technol. 30(6), 263-269.

Laanbroek H.J. and Gerards S. (1993) Competition for limiting amounts of oxygen between nitrosomanas europaea and nitrobacteria winogradskyi grown in mixed continuous cultures. Arch. Microbiology. 159(6), 453 -459.

Lai E., Senkpiel S., Solley D. and Keller J. (2004) Nitrogen removal of high strength wastewater via nitritation/denitritation using a sequencing batch reactor. Water Sci. Technol. 82(10), 27-33.

Lavallée B., Lessard P. and Vanrolleghem P. (2005) Modeling the metabolic adaptations of the biomass under rapid growth and starvation conditions in the activated sludge process. J. Environ. Eng. Sci. *In press*.

Lehninger A.L., Nelson D.L. and Cox M.M. (1993) Principles of biochemistry. New York: Worth Publishers.

Lemos P.C., Viana C., Salgueiro E.N., Ramos A.M., Crespo J.P.S.G. and Reis M.A.M. (1998) Effect of carbon source on the formation of polyhydroxyalkanoates (PHA) by a phosphate-accumulating mixed culture. Enz. Microb. Technol. 22, 662-671.

Lemos P.C., Serafim L.S., Santos M.M., Reis M.A.M. and Santos H. (2003) Metabolic pathway for propionate utlization by phosphorus accumulating organisms in activated sludge: ^{13}C labelling and in vivo nuclear magnetic resonance. App Environ Microbiol 69, 241-251.

Levantesi C., Serafim L.S., Crocetti G.R., Lemos P.C., Rossetti S., Blackall L.L., Reis M.A.M. and Tandoi V. (2002) Analysis of the microbial community structure and function of a laboratory scale enhanced biological phosphorus removal reactor. Environ. Microbiol. 4, 559-569.

Liu C. and Zachara J.M. (2001) Uncertainties of Monod Kinetic Parameters Nonlinearly Estimated from Batch Experiments. Environ. Sci. Technol. 35(1), 133-141.

Liu W., Mino T., Matsuo T. and Nakamura K. (1996) Biological phosphorus removal processes. Effect of pH on anaerobic substrate metabolism. Water Sci. Technol. 34(1-2), 25-32.

Liu W., Nakamura K., Matsuo T. and Mino T. (1997) Internal energy based competition between polyphosphate and glycogen accumulating bacteria in biological phosphorus removal reactors. Effect of P/C feeding ratio. Water Res. 31(6), 1430-1480.

Liu Y., Geiger C. and Randall A.A. (2002) The role of poly-hydroxy-alkanoate form in determining the response of enhanced biological phosphorus removal biomass to volatile fatty acids. Water Environ. Res. 74, 57-67.

Luong J.H.T. (1987) Generalisation of Monod kinetics for analysis of growth data with substrate inhibiton. Biotechnol. Bioeng. 24, 242-248.

Majone M., Dircks K. and Beun J.J. (1999) Aerobic storage under dynamic conditions in activated sludge processes. The state of the art. Water Sci. Technol. 39(1), 61-73.

Manga J., Ferrer J., Garcia-Usach F., Seco A. (2001) A modification to the Activated Sludge Model No. 2 based on the competition between phosphorus-accumulating organisms and glycogen-accumulating organisms. Water Sci. Technol. 43(11), 161-171.

Marsili-Libelli S., Guerrizio S. ans Checchi N. (2003) Confidence regions of estimated parameters for ecological systems. Ecol. Model. 165, 127 - 146.

Massone A.G., Gernaey K., Bogaert H., Vanderhasselt A., Rozzi A. and Verstraete W. (1996) Biosensors for nitrogen control in wastewaters. Water Sci. Technol. 34(1-2), 213-220.

MATLAB. Optimization Toolbox. (1999). User's Guide. Version 2 (Release 11). The MathWorks. Natick, MA, USA.

Metcalf and Eddy (1991). Wastewater engineering: treatment, disposal and reuse. 3rd Ed. McGraw-Hill, Inc.

Mehra RK. (1974) Optimal input signals for parameter estimation in dynamic systems survey and new results. IEEE Transactions on Automatic Control. 19(6),753-768.

Meijer S.C.F., van Loosdrecht M. C. M. and Heijnen J.J. (2001) Metabolic modelling of full-scale biological nitrogen and phosphorus removing WWTP's. Water Res. 35(11), 2711-2723.

Meijer S. C. F., van Loosdrecht M. C. M. and Heijnen J. J. (2002) Modelling the start-up of a full-scale biological phosphorous and nitrogen removing WWTP. Water Res. 36(19), 4667-4682.

Meriç S., Tünay O & Ali San H. (2002) A new approach to modelling substrate inhibition. Env Technol. 23: 163-177.

Minkevich I.G. and Neubert N. (1985) Influence of carbon dioxide solubility on the accuray of measurements of carbon dioxide production rate by gas balance technique. Acta Biotechnol. 5, 137-143.

Mino T., Arun V., Tsuzuki Y. and Matsuo T. (1987) Effect of phosphorus accumulation on acetate metabolism in the biological phosphorus removal. In Ramadori R., editor. Biological phosphate removal from wastewaters (Advances in Water Pollution Control 4). Oxford: Pergamon Press. pp. 27-38.

Mino T, Satoh H. and Matsuo T. (1994) Metabolisms of different bacterial populations in enhanced biological phosphate removal processes. Water Sci. Technol. 29(7), 67-100.

Mino T., Liu W., Kurisu F. and Matsuo T. (1995) Modelling glycogen storage and denitrification capability of microorganisms in EBPR processes. Water Sci. Technol. 31(2), 25-34.

Munack A. and Posten C. (1989) Desing of optimal dynamical experiments for parameter estimation. In Proceedings of the American Control Conference AAC89; Pittsburgh, PA, 1989, 2011-2016.

Murnleitner E., Kuba T., van Loosdrecht M.C.M. and Heijnen J.J. (1997) An integrated metabolic model for the aerobic and denitrifying BPR. Biotechnol. Bioeng. 54(5), 434-450.

Musvoto E.V., Wentzel M.C., Loewenthal R.E. and Ekama G.A. (2000a) Integrated chemical-physical processes modelling Part I – Development of a kinetic based model for weak/acid base systems. Water Res. 34(6), 1857-1867.

Musvoto E.V., Wentzel M.C. and Ekama G.A. (2000b) Integrated chemical-physical processes modelling Part II – Simulating aeration treatment of anaerobic digester supernatants. Water Res. 34(6), 1868-1880.

Nelder J.A. and Mead R. (1964) A simplex method for function minimization. Computer Journal 7, 308-313.

Nowak O., Svardal K. and Schweighofer A. (1995) The dynamic behaviour of nitrifying activated sludge systems influenced by inhibiting wastewater compounds. Water Sci. Technol. 31(2), 115-124

Oehmen A., Zeng R., Yuan Z. and Keller J. (2005) Anaerobic metabolism of propionate by polyphosphate-accumulating organisms in enhanced biological phosphorus removal systems. Biotechnol. Bioeng. *In press*.

Olson G. and Newell B. (1999) Wastewater treatment systems. IWA publishing London (UK)

Omlin M. and Reichert P. (1999) A comparison of techniques for the estimation of model prediction uncertainty. Ecol. model. 115, 45-59.

Ossenbruggen P.J., Spanjers H. and Klapwijk, A. (1996) Assessment of a two-step nitrification model for activated sludge. Water Res. 30, 939-953.

Painter H.A. and Loveless J.E. (1983) Effect of temperature and pH value on the growth-rate constants of nitrifying bacteria in the activated-sludge process. Water Res. 17(3), 237-248.

Petersen B. (2000) Calibration, identifiability and optimal experimental design of activated sludge models. Ph.D. Thesis. Ghent University.

Petersen B., Gernaey K., Vanrolleghem P.A. (2001) Practical identifiability of model parameters by combined respirometric-titirimetric measurements. Water Sci. Technol. 43(7), 647-355.

Pereira H., Lemos P., Reis M., Crespo J., Carrondo M. and Santos H. (1996) Model for carbon metabolism in biological phosphorus removal processes based on in vivo C-NMR labeling experiments. Water Res. 30, 2128-2138.

Perez J., Montesinos J.L., Albiol J., Gòdia F. (2004) Nitrification by immobilised cells in a micro-ecological life support system using packed-bed bioreactors: an engineering study. J. Chem. Technol. Biotechnol. 79, 742-754.

Picioreanu C., van Loosdrecht M.C.M., Heijnen J.J. (1997). Modeling the effect of oxygen concentration on nitrite accumulation in a biofilm airlift suspension reactor. Water Sci. Technol. 36(1), 147-156.

Pijuan M., Saunders A.M., Guisasola A., Baeza J.A., Casas C. and Blackall, L.L. (2004a) Enhanced biological phosphorus removal in a sequencing batch reactor using propionate as the sole carbon source. Biotechnol. Bioeng. 85, 56-67.

Pijuan M., Baeza J.A., Casas C., Lafuente J. (2004b) Response of an EBPR population developed in a SBR with propionate to different carbon sources. Water Sci. Technol. 50(10), 131-138.

Pijuan M., Guisasola A., Baeza J.A., Carrera J., Casas C., Lafuente J. (2005) Aerobic phosphorus release linked to acetate uptake: influence of PAO intracellular storage compounds. Biochem. Eng. J. *In press.*

Pinsach J. (2003) Control del creixement en cultius discontinus alimentats. *E Coli* productora d'aldolases recombinants. Master of Sciences degree (in catalan).

Pollice A., Tandoi V. and Lestingi C. (2002) Influence of aeration and sludge retention time on ammonium axidation to nitrite and nitrate. Water Res. 36, 2541-2546.

Poughon L., Dussap C.D. and Gros J.B. (2001) Energy model and metabolic flux analysis for autotrophic nitrifiers. Biotechnol. Bioeng. 72(4), 416-433.

Pratt S., Yuan Z., Keller J. (2004) Modelling aerobic carbon oxidation and storage by integrating respirometric, titrimetric and off-gas CO2 measurements. Biotechnol. Bioeng. 88, 135-147.

Ramadori R., Rozzi A. and Tandoi V. (1980) An automated system for monitoring the kinetics of biological oxidation of ammonia. Water Res. 14, 1555-1557.

Randall C.W. and Chapin R.W. (1997) Acetic acid inhibition of biological phosphorus removal. Water Environ. Res. 69(5), 955-960.

Randall A.A. and Liu Y. (2002) Polyhydroxyalkanoates form potentially a key aspect of aerobic phosphorus uptake in enhanced biological phosphorus removal. Water Res. 36, 3473-3478.

Randall A.A., Chen Y., Liu H. and McCue T. (2003) Polyhydroxyalkanoate form and polyphosphate regulation: keys to biological phosphorus and glycogen transformations? Water Sci. Tecnhol. 47(11), 227–233.

Rieger L., Koch G., Kühni M., Gujer W. and Siegrist H. (2001) The eawag bio-p module for activated sludge model no. 3. Water Res. 35(16), 3887-3903.

Roels J.A. (1983) Energetics and Kinetics in Biotechnology. Elsevier Science Publishers, Amsterdam.

Royce P.N. and Thornmill N.F. (1991) Estimation of carbon dioxide concentrations in aerobic fermentations. AIChe J. 37, 1680-1686.

Ruiz G, Jeison D, Chamy R. (2003) Nitrification with high nitrite accumulation for the treatment of wastewater with high ammonia concentration. Water Res. 37, 1371-1377.

Sánchez O, Martí MC, Aspé E, Roeckel M. (2001) Nitrification rates in a saline medium at different dissolved oxygen concentrations. Biotechnol Lett. 23, 1597-1602.

Satoh H., Mino T. and Matsuo T. (1992) Uptake of organic substrates and accumulation of polyhydroxyalkanoates linked with glycolysis of intracellular carbohydrates under anaerobic conditions in the biological excess phosphate removal processes. Water Sci. Technol. 26(5-6), 933-942.

Schlegel H.G. and Bowien B. (1989) Autotrophic bacteria. Science Tech Publishers. Madison, Wi. USA.

Schmidt I., Sliekers O., Schmid M., Bock E., Fuerst J., Kuenen J.G., Jetten M. and Strous M. (2003) New concepts of microbial treatment processes for the nitrogen removal in wastewater. FEMS Microbiol. Rev. 27, 481-492.

Schuler, A. J. and Jenkins,D. (2002) Effects of pH on enhanced biological phosphorus removal metabolisms. Water Sci. Technol. 46(4-5), 171-178.

Schumpe A., Quicker G. and Deckwer W.D. (1982) Gas solubilities on microbial culture media. Adv. Biochem. Eng. 24, 1.

Serafim L.S., Lemos P.C. and Reis M.A.M. (2004) Change in the metabolism of PHA accumulation by activated sludge modifying opearating conditions. Water Sci. Technol. 46(1-2), 353-356.

Serralta J., Ferrer J., Borrás L. and Seco A. (2004) An extension of ASM2d including pH calculation. Water Res. 38, 4029-4038.

Seviour R.J., Mino T. and Onuki M. (2003) The microbiology of biological phosphorus removal in activated sludge systems. FEMS Microbiol. Rev. 27, 99-127.

Sheintuch M., Tartakovsky B., Narkis N. and Rebhun, M. (1995) Substrate inhibition and multiple states in a continuous nitrification process. Water Res. 29(3), 953-963.

Sin G., Malisse K. and Vanrolleghem P. (2003) An integrated sensor for the monitoring of aerobic and anoxic activated sludge activities in biological nitrogen removal plants. Water. Sci. Technol. 47(2), 141-148.

Sin G. (2004) Systematic calibration of activated sludge models. Ph. D. Thesis. Faculty of Agricultural and Applied Biological Sciences. Ghent University.

Sin G., Guisasola A., Baeza J., Carrera J. and Vanrolleghem P.A. (2005) A new approach for modelling simultaneous grwoth and storage processes for activated sludge systems under aerobic conditions. Biotechnol. Bioeng. *In press.*

Smolders G.J.F., van der Meij J., van Loosdrecht M.C.M. and Heijnen, J.J. (1994a) Model of the anaerobic metabolism of the biological phosphorus removal process: Stoichiometry and pH influence. Biotechnol. Bioeng. 42, 461-470.

Smolders G.J.F., van der Meij J., van Loosdrecht M.C.M. and Heijnen J.J. (1994b) Stoichiometric model of the aerobic metabolism of the biological phosphorus removal process. Biotechnol. Bioeng. 44, 837-848.

Smolders G.J.F., van der Meij J., van Loosdrecht M.C.M. and Heijnen, J.J. (1995) A structured metabolic model for anaerobic and aerobic stoichiometry and kinetics of the biological phosphorus removal process. Biotechnol. Bioeng. 47, 277-287.

Spanjers H. and Olson G. (1992) Modeling of the dissolves oxygen probe response in the improvement of the performance of a continuous respiration meter. Water Res. 26(7), 945-954.

Spanjers H., Vanrolleghem P.A., Olsson G. and Dold P.L. (1997) Respirometry in control of the activated sludge process: principles. Scientific and technical report, no7 IWA Publishing. London.

Sperándio M. and Paul E. (1997) Determination of carbon dioxide evolution rate using online gas analysis during dynamic biodegradation experiments. Biotechnol. Bioeng. 53(3), 243-252.

Stephanopoulos G. (1990) Chemical process control: an introduction to theory and practice. Ed. Prentice/Hall International Inc.

Stumm W. and Morgan J.J. (1996) Aquatic chemistry: chemical equilibria and rates in natural waters. 3rd ed. John Wiley & Sons, Inc.

Suzuki I., Dular V. and Kwok S.C. (1974) Ammonia or ammonium ion as substrate for oxidation by *Nitrosomonas europaea* cells and extracts. J. Bacteriol. 120, 556-558.

Third K., Newland M. and Cord-Ruwisch R. (2003) The effect of dissolved oxygen on PHB accumulation in activated sludge cultures. Biotechnol. Bioeng. 82(2), 238-250.

Thomas M., Wright P., Blackall L.L., Urbain V. and Keller J. (2002) Optimisation of Noosa BNR plant to improve performance and reduce operating costs. Third IWA World Water Congress, Melbourne, Australia, 7-12 April, 2002.

Torrijos M., Carrera J. and Lafuente J. (2004) Improving the biological nitrogen renoval process in pharmaceutical wastewater treatment plants: a case study. Environ. Technol. 25, 423-431.

Trambouze P., van Landeghem H., Wauquier J.P. (1988) Chemical reactors: design/ engineering/ operation. Éditions Technip. Paris.

Ubisi M.F., Jood T.W., Wentzel M.C. and Ekama G.A. (1997) Activated sludge mixed liquor heterotrophic biomass. Water SA. 23(3), 239-248.

Van Aalst-van Leeuwen M.A., Pot M.A, van Loosdrecht M.C.M. and Heijnen J.J. (1997) Kinetic modelling of poly/η-hydroxybutyrate) production and consumption by *Paracoccus pantotrophus* under dynamic substrate supply. Biotechnol. Bioeng. 55(5), 773-782.

van Donguen U., Jetten M.S.M. and van Loosdrecht M.C.M. (2001) The SHARON®-Anamox® process for the treatment of high ammonium wastewater. Water Sci. Technol. 44(1), 153-160.

van Loosdrecht M.C.M., Pot M.A. and Heijnen J.J. (1997) Importance of bacterial storage polymers in bioprocesses. Water Sci. Technol. 35(1), 41-47.

van Loosdrecht M.C.M. and Jetten M.S.M. (1998) Microbial conversions in nitrogen removal. Water Sci. Technol. 38(1), 1-7.

van Loosdrecht M.C.M. and Henze M. (1999) Maintenance, endogenous respiration, lysis, decay and predation. Water Sci. Technol. 39(1), 107-117.

van Loosdrecht M.C.M. and Heijnen J.J (2002) Modelling of activated sludge processes with structured biomass. Water Sci. Technol. 45(6), 12-23.

van Veldhuizen H.M., van Loosdrecht M.C.M. and Heijnen J.J. (1999) Modelling biological phosphorus and nitrogen removal in a full scale activated sludge process. Water Res. 33, 3459-3468.

Vanrolleghem P.A., Kong Z., Rombouts G. and Verstraete W. (1994) An on-line respirographic biosensor for the characterization of load and toxicity of wastewaters. J. Chem. Technol. Biotechnol. 59, 321-333.

Vanrolleghem P.A., Van Daele M. and Dochain D. (1995) Practical identifiability of a biokinetic model of activated sludge respiration. Water Res. 29, 2561-2570.

Vanrolleghem P.A and Spanjers H. (1998a) A hybrid respirometric method for more reliable assessment of activated sludge model parameter. Water Sci. Technol. 37(12), 237-246.

Vanrolleghem P.A., Gernaey K., Coen F.0., Petersen B., De Clerq B. and Ottoy J.P. (1998b) Limitations of short-term experiments designed for identification of activated sludge biodegradation models by fast dynamic phenomena. In: Proceedings 7th IFAC Conference on Computer Applications in Biotechnology. Osaka. Japan. May 31-June 4. 1998.

Vanrolleghem P., Sin G. and Gernaey K. (2004) Transient response of aerobic and anoxic activated sludge activities to sudden concentration changes. Biotechnol. Bioeng. 86(3), 277-290.

Versyck K., Claes J.E, and Van Impe J.F. (1997) Practical identification od unstructured growth kinetics by application of Optimal Experimental Design. Biotechnol. Prog. 13, 524-531.

Villaverde S., García-Encina P. and Fernandez-Polanco F. (1996) Influence of pH over nitrifying biofilm activity in submerged biofilters. Water Res. 31(5), 1180-1186.

Wallace W. and Nicholas D.J.D. (1968) Properties of some reductase enzymes in the nitrifying bacteria and their relationship to the oxidase systems. Biochem. J. 109, 763-773.

Walter E. and Pronzato L. (1999) Identification of parametric models from experimental data. Springer Verlag, Heidelberg.

Watson S.T., Bock E., Harms H., Koops H.P. and Hooper A.B. (1989) In: Bergey's manual of systematic bacteriology. Staley J.T., Bryant M.P., Pfenning N. and Holt J.G. Ed: Williams & Wilkins. Baltimore. USA. 3(20), 1807-1835.

Weijers S.R., Kok J.J., Preisig H.A., Buunen A. and Bouda T.W.M. (1996) Parameter identifiability in the IAWQ model No. 1 for modelling activated sludge plants for enhanced nitrogen removal. Computers Chem. Eng. 20, 1455-1460.

Weijers S.R. and Vanrolleghem P.A. (1997) A procedure for selecting best identifiable parameters in calibrating activated sludge model no.1 to full-scale plants. Water Sci. Technol. 36(5), 69-79.

Wentzel M.C., Ekama G.A., Dold P.A. and Marais G.R. (1990) Biological excess phosphorous removal - Steady state process design. Water SA. 16(1).

Wentzel M.C., Lötter L.H., Ekama G.A., Lowenthal R.E. and Marais G.v.R. (1991) Evaluation of biochemical models for biological excess phosphorus removal – a biochemical model. Water Sci. Technol. 23, 567-576.

Wett B. and Rauch W. (2002) The role of inorganic carbon limitation in biological removal of extremely ammonia concentrated wastewater. Water Res. 37, 1100-1110.

Weon S.Y., Lee S.I., Koopman B. (2004) Effect of temperature and dissolved oxygen on biological nitrification at high ammonia concentrations. Environ. Technol. 25, 1211-1219.

Wiessmann U. (1994). Biological nitrogen removal form wastewater. Adv. Biochem. Eng. 51, 113-154.

Wyffels S., Boeckx P., Pynaert K., Verstraete W. and van Cleemput O. (2003). Sustained nitrite accumulation in a membrane-assisted bioreactor (MBR) for the treatment of ammonium-rich wastewater. J. Chem. Technol. Biotechnol. 78, 412-419.

Yagci N., Artan N., Ubay Çokgör E., Randall C.W. and Orhon D. (2003) Metabolic model for acetate uptake by a mixed culture of phosphate- and glycogen-accumulating organisms under anaerobic conditions. Biotechnol. Bioeng. 84(3), 359-373.

Zeng R.J., Saunders, A.M., Yuan Z., Blackall L.L. and Keller J. (2003) Identification and comparison of aerobic and denitrifying polyphosphate-accumulating organisms. Biotechnol. Bioeng. 83, 140-148.

ACRONYMS AND NOMENCLATURE

ACRONYMS

AOB: Ammonium Oxidising Biomass
ASM1: Activated Sludge Model nº1
ASM2: Activated Sludge Model nº2
ASM2d: Activated Sludge Model nº2d
ASM3: Activated Sludge Model nº3
ATP: Adenosine-Triphosphate
ATU: Allyl-thiourea
AWMC: Advanced Wastewater Management Center
BPPR: Background Proton Production Rate
CER: Carbon Evolution Rate
COD: Chemical Oxygen Demand
CPFR: Continuous Plug Flow Reactor
CPR: Carbon Production Rate
CPR_{END}: Carbon Production Rate under endogenous conditions
CSTR: Continuous Stirred Tank Reactor
CTR: Carbon Transfer Rate
DO: Dissolved Oxygen
EBPR: Enhanced Biological Phosphorus Removal
F/M ratio: Feed to microorganisms ratio
FIM: Fisher Information Matrix
FISH: Fluorescence In-Situ Hybridisation
GAO: Glycogen Accumulating Organisms
HP: Hydrogen Production
HPR: Hydrogen Production Rate
HRT: Hydraulic Residence Time
IWA: International Water Association
LFS: continuously aerated bioreactor without liquid inputs or outputs where the oxygen is measured in the liquid phase
LSS: bioreactor without liquid/gas inputs or outputs where the oxygen is measured in the liquid phase
NOB: Nitrite Oxidising Biomass
OED: Optimal Experimental Design
OHO: Ordinary Heterotrophic Organisms
OTR: Oxygen Transfer Rate
OUR: Oxygen Uptake Rate
OUR_{END}: Endogenous OUR
OUR_{EX}: Exogenous OUR
PAO: Phosphate Accumulating Organisms
PH2MV: Poly-η-hydroxy-2methylvalerate
PHA: polyhydroxyalkanoates
PHB: poly-η-hydroxybutyrate
pH^{SS}: pH in steady state
PHV: polyhydroxyvalerate
PHV: Poly-η-hydroxyvalerate
polyP: Polyphosphate
RQ: Respiratory Quotient
S/X ratio: Substrate to biomasss
SRT: Sludge Residence Time
SSE: Sum of Squared Errors
TIC: Total Inorganic Carbon
TSS: Total Suspended Solids
VFA: Volatile Fatty Acid
VSS: Volatile Suspended Solids
WWTP: Wastewater Treatment Plants

MODEL PARAMETERS

A: flowing area
b_A: AOB decay rate
b_{GLY}: Glycogen lysis rate
b_H: heterotrophic decay rate
b_N: NOB decay rate
b_{PAO}: PAO decay rate
b_{PHA}: PHA lysis rate
b_{PP}: PolyP lysis rate
b_{STO}: X_{STO} respiration rate
$CH_{1.5}O_{1.5}$: PHB
$CH_{1.6}O_{0.4}$: PHV
$CH_{10/6}O_{5/6}$: glycogen
CH_2O: acetate
$CH_2O_{2/3}$: propionate
$CH_{5/3}O_{1/3}$: PH2MV
f_{PHB}: ratio of PHB in the cell (i.e. X_{PHB}/X_H)
f_{PHB}^{MAX}: maximum X_{PHB}/X_H ratio
f_{PHB}^{MIN}: minimum X_{PHB}/X_H ratio
f_{STO}: fraction of flux diverted to storage
f_{XI}: fraction of inerts products from lysis
f_{XS}: fraction of biodegradable products from lysis
f_{XSTO}: X_{STO}/X_H ratio
H: Henry's law constant
i_{CSS}: number of carbon atoms in the substrate
$i_{NB:}$ nitrogen content of the biomass (mass basis)
$i_{PB:}$ phosphorus content of the biomass (mass basis)
J: weighed sum of squared errors between model outputs and the measured outputs
K_1: constant for the kinetic description of PHB degradation
K_2: constant for the kinetic description of PHB degradation
k_3: ammonium-ammonia forward equilibrium rate constant
k_4: nitrous acid forward equilibrium rate constant
K_{ALK}: Alkalinity affinity constant for nitrifiers
K_{GLY}: Affinity constant for the ratio X_{GLY}/X_{PAO}
k_H: hydrolysis maximum rate
K_I : Inhibition constant for Andrews model
K_{IPP}: Kinetic constant for the X_{PP} storage process
k_La: global oxygen transfer coefficient
k_La_{CO2}: global carbon dioxide transfer coefficient
k_La_{NH3}: global ammonia dioxide transfer coefficient
k_La_{O2}: global oxygen dioxide transfer coefficient
K_{MAX}: Maximum X_{PP}/X_{PAO} ratio
$K_{NH4,A}$: AOB ammonium affinity constant
$K_{NH4,N}$: NOB ammonium affinity constant
K_{NO}: nitrite affinity constant
K_O: heterotrophic/ PAO oxygen affinity constant
K_{OA}: AOB oxygen affinity constant
K_{ON}: NOB oxygen affinity constant
K_{PHA_P}: Affinity constant for X_{PHA}/X_{PAO} in X_{PP} storage process
K_{PP}: Affinity constant for the ratio X_{PP}/X_{PAO}
K_{PS}: Orthophosphate affinity constant
K_S: substrate affinity constant
K_{STO}: affinity constant for the fraction of storage product
k_{STO}: maximum storage rate
m_{ATP}: maintenance coefficient
N: number of measurements

pK_1: carbonic acid- bicarbonate equilibrium constant
pK_2: bicarbonate- carbonate equilibrium constant
pK_3: ammonium-ammonia equilibrium constant
pK_4: nitrous acid equilibrium constant
Q: gas flow
q_{GLY} : maximum glycogen storage rate
Q_k: weighting matrix for parameter estimation
q_{MANT}: maximum maintenance rate
q_{MAX}: maximum substrate uptake rate
q_{PHA}: maximum PHA storage rate (EBPR model)
q_{PP}: maximum X_{PP} storage rate
R: ideal gases constant
S_{CO2}^{*}: CO_2 saturation concentration
S_{CO2}: dissolved carbon dioxide
S_{CO2}^{SS}: CO_2 concentration in steady state
S_{HCO3}: dissolved bicarbonate concentration
S_{HCO3}^{SS}: HCO_3^- concentration in steady state
S_{HP}: hydrogen proton concentration
S_{NH4}: N-ammonium concentration
S_O: dissolved oxygen concentration
S_{PO4}: P-orthophosphate concentration
S_S: external substrate
S_{VFA}: VFA concentration
u: input (*u:* vector of inputs)
v: flow velocity
V_G: Volume of the gas phase
V_L: Volume of the gas phase
V_T:total volume
X_{GLY}: Glycogen concentration
X_{GLY}^{MAX} : Maximum X_{GLY}/X_{PAO} ratio
X_H: heterotrophic biomass
X_{PAO}: PAO concentration
X_{PHA}: PHA concentration
X_{PP}: PolyP concentration
X_S: Slowly biodegradable products
X_{STO}: storage products
y: model outputs
Y_A: g COD_X formed/ g $N\text{-}NH_4^+$ oxidised
Y_{GLY1}: g COD_{GLY} degraded /g COD_{PHA} produced
Y_{GLY3}: g COD_{GLY} produced for g COD_{PHA} used
$Y_{H,S}$: heterotrophic growth yield on external substrate
$Y_{H,STO}$: heterotrophic growth on storage products
y_M: measured outputs
Y_N: g COD_X formed/ g $N\text{-}NO_2^-$ oxidised
Y_{PAO}: PAO growth yield
Y_{PHA}: g COD_{PHA} oxidised/ g P taken up
Y_{PO}: g P released /g COD_{PHA} produced
Y_{STO}: heterotrophic storage yield
Y_{VFA}: g COD_{VFA} taken up /g COD_{PHA} produced
$Y_\chi(t)$: output sensitivity function
ζ]#dissociation factor for ammonia
ι] mol of ATP for mol $NADH_2$ used in the oxidative phosphorylathion
κ_G: gas hold-up
ν_A: degree of reduction of acetate
ν_G: degree of reduction of glycogen
ν_P: degree of reduction of PHA
ν_S: degree of reduction of the substrate

ν_{STO}: degree of reduction of the storage product
ν_X: degree of reduction of the biomass
$\sigma_{H,STO}$: maximum growth rate on storage products
$\sigma_{H:}$ maximum heterotrophic growth rate
$\sigma_{MAX,A:}$ maximum AOB growth rate
$\sigma_{MAX,N:}$ maximum NOB growth rate
σ_{MAX}: maximum growth rate
σ_{PAO} : maximum PAO growth rate
χ]#parameter
ϑ: time constant (start-up)
φ]#dissociation factor for a weak acid

Albert Guisasola Canudas

PERSONAL DATA

Birth date: 04.09.1978
Birthplace: Mataró (Barcelona)
Address: C/ Esteve Albert 73 1er 1era 08304 Mataró (Barcelona)
Telf: (93) 5363951 – (93) 5811879
e-mail: Albert.Guisasola@uab.es
Fax: (93) 5812013

EDUCATION

2001-Present: Ph. D. student in the Environmental Engineering Group of Universitat Autònoma de Barcelona

Title: "Modelling biological organic matter and nutrient removal processes from wastewater using respirometric and titrimetric techniques"

02/2003: Master of Science Degree in Environmental Technology.

Title: "La respirometria LFS com a eina per a la caracterització dels processos d'eliminació biològica de nutrients en aigües residuals"
(LFS respirometry as a tool for the characterisation of wastewater biological nutrient removal processes).

02/2001: Chemical Engineer degree in Universitat Autònoma de Barcelona.

LANGUAGE and COMPUTER SKILLS

- LANGUAGES :
  - Catalan and Spanish (native speaker).
  - English (fluent)

- COMPUTER:
  - Microsoft Office environment (advanced level)
  - MATLAB 6.5 (advanced level)
  - PLC programming (Siemens S7) (advanced level)
  - Sigmaplot 8.0 (advanced level)
  - Visual Basic 6.0 (advanced level)
  - Autocad R14 (medium level)
  - Photoshop 7.0 (medium level)
  - FORTRAN (medium level)

TEACHING

- "Simulació i optimització de processos químics" (Simulation and optimisation of chemical processes). 2004-2005.
  Chemical Engineering degree (Universitat Autònoma de Barcelona)
  Practice (15 hours)

- "Fundamentos y aplicaciones de la respirometria LFS" (LFS respirometry: Fundamentals and applications), 21/01/05
  Seminar in Universitat Rovira i Virgili.
  Theory and lab practice (6 hours)

- "Tractament biologic d'aigües residuals" (Biological wastewater treatment systems) , 1/02/05
  Ph. D. course on in Universitat de Girona
  Theory (4 hours)

- "Enginyeria Ambiental II". (Environmental Engineering II), 2003-2004
  Environmental Sciences degree (Universitat Autònoma de Barcelona)
  Practice (15 hours)

- "Introducció a la programació en Visual Basic 6.0" (Fundamentals of Visual Basic 6.0) , 2003-2004
  Optative course (Universitat Autònoma de Barcelona)
  Theory and practice (15 hours)

ACCEPTED PUBLICATIONS

Referred international journals

Guisasola A., Baeza J.A., Carrera J., Casas C., Lafuente J. (2003) An off-line respirometric procedure to determine inhibition and toxicity of biodegradable compounds in biomass from an industrial WWTP. *Water Sci. Techno*l. 48(11), 267-275.

Guisasola A., Pijuan M., Baeza J.A., Carrera J., Casas C., Lafuente J. (2004). Aerobic phosphorus release linked to acetate uptake in bio-P sludge: process modelling using oxygen uptake rate. *Biotechnol. Bioeng*. 85, 722-733.

Guisasola A., Jubany I., Baeza J.A., Carrera J. and Lafuente J. (2005) Respirometric estimation of the oxygen affinity constants for biological ammonium and nitrite oxidation. *Journal of Chem. Technol. Biotechnol*. 80(4), 388-39.

Pijuan M., Saunders A.M., *Guisasola A.*, Baeza J.A., Casas C. and Blackall, L.L. (2004) Enhanced biological phosphorus removal in a sequencing batch reactor using propionate as the sole carbon source. *Biotechnol. Bioeng*. 85, 56-67.

Pijuan M., *Guisasola A.*, Baeza J.A., Carrera J., Casas C. and Lafuente J. (2005) Aerobic phosphorus release linked to acetate uptake: influence of PAO intracellular storage compounds. *Biochem. Engin J.* (in press)

Sin G., *Guisasola A.*, Baeza J., Carrera J. and Vanrolleghem P.A. (2005). A new approach for modelling simultaneous grwoth and storage processes for activated sludge systems under aerobic conditions. *Biotechnol. Bioeng.* (accepted)

National journals

Guisasola A., Baeza J.A., Carrera J. and Lafuente J. (2002) Descripción y implementación de las técnicas respirométricas. *Tecnología del Agua*. 224, 32-39.

Guisasola A., Baeza J.A., Carrera J. and Lafuente J. (2002) Respirometría con aireación continua (LFS): parámetros operacionales básicos para el funcionamiento óptimo. *Ingeniería Química*. 414, 151-162.

CONFERENCES

International conferences

Guisasola A., Baeza J.A., Carrera J., Casas C. and Lafuente J. (2002) An off-line respirometric procedure to determine inhibition and toxicity of biodegradable compounds in biomass from an industrial WWTP. *5th Conference on Small Wastewater Treatment Processes. Istanbul. Sept. 2002*. (Oral presentation)

Guisasola A., Sin G., Baeza J.A., Carrera J. and Vanrolleghem P.A. (2004) Limitations of ASM1 and ASM3: a comparison based on batch OUR profiles from different full-scale WWTP *IWA 2004 World Water Congress and exhibition. Marrakech.* (Oral presentation)

Guisasola A., Pijuan M., Baeza J.A., Carrera J. and Lafuente J. (2005). Improving the start-up of an EBPR system using OUR to control the aerobic phase length: a simulation study. *ICA 2005* (Oral presentation)

Guisasola A., Pijuan M., Baeza J.A., Carrera J., Casas C.and Lafuente J. (2005) Simulation of a novel strategy for improving a biological phosphorus removal system start-up ESCAPE 2005. (Poster presentation)

Suárez-Ojeda M.E., *Guisasola A.*, Fabregat A., Stüber F., Fortuny A., Baeza J., Carrera J. and Font J. (2005) Catalytic wet air oxidation plus biological treatment to deal with industrial wastewater. 7th World Congress of Chemical Engineering.Glasgow 2005 (Poster presentation)

Guisasola A., Baeza J.A., Carrera J. and Lafuente J. (2004) Improving biological WWTP operation through respirometric techniques. 9th Mediterranean Congress on Chemical Engineering. Barcelona 2002. (Poster presentation)

National conferences

Pijuan M., *Guisasola A.*, Baeza J.A., Carrera J., Casas C. and Lafuente J. (2004) Aerobic phosphorous release linked to acetate uptake: influence of PAO intracellular storage compounds**.** *BIOTEC 2004. Oviedo* (Oral presentation)

Torrijos M., Carrera J., Guisasola A. and Lafuente J. (2002) Análisis de los parámetros clave para el proceso de eliminación biológica de nitrógeno en plantas de tratamiento de aguas residuales de la industria farmaceútica. *BIOTEC 2002.* (Oral presentation)